Acta Universitatis Tamperensis 2103

LEO SYRJÄNEN

Protozoan and Metazoan Carbonic Anhydrases

Potential target enzymes for anti-parasitic drug development

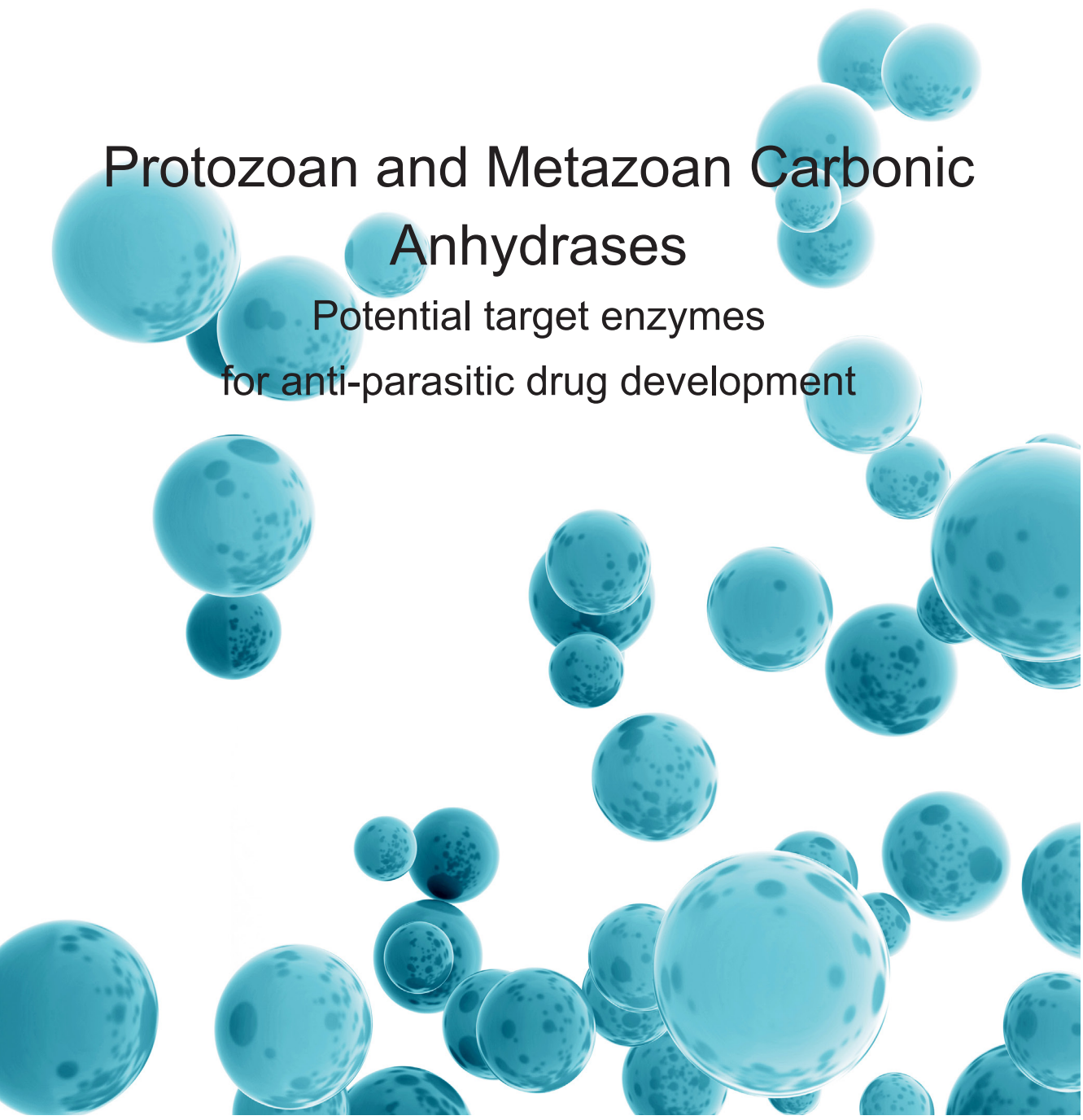

LEO SYRJÄNEN

Protozoan and Metazoan Carbonic Anhydrases

Potential target enzymes for anti-parasitic drug development

ACADEMIC DISSERTATION
To be presented, with the permission of
the Board of the School of Medicine of the University of Tampere,
for public discussion in the small auditorium of building M,
Pirkanmaa Hospital District, Teiskontie 35, Tampere,
on 6 November 2015, at 12 o'clock.

UNIVERSITY OF TAMPERE

LEO SYRJÄNEN

Protozoan and Metazoan Carbonic Anhydrases

Potential target enzymes for anti-parasitic drug development

Acta Universitatis Tamperensis 2103
Tampere University Press
Tampere 2015

UNIVERSITY OF TAMPERE

ACADEMIC DISSERTATION
University of Tampere, School of Medicine
University of Tampere, BioMediTech
Finland

Supervised by
Professor Seppo Parkkila
University of Tampere
Finland

Reviewed by
Professor Matti Karp
Tampere University of Technology
Finland
Associate Professor Marc Ilies
Temple University School of Pharmacy
USA

The originality of this thesis has been checked using the Turnitin OriginalityCheck service in accordance with the quality management system of the University of Tampere.

Cover design by
Mikko Reinikka

Distributor:
verkkokauppa@juvenesprint.fi
https://verkkokauppa.juvenes.fi

Acta Universitatis Tamperensis 2103
ISBN 978-951-44-9932-6 (print)
ISSN-L 1455-1616
ISSN 1455-1616

Acta Electronica Universitatis Tamperensis 1597
ISBN 978-951-44-9933-3 (pdf)
ISSN 1456-954X
http://tampub.uta.fi

Suomen Yliopistopaino Oy – Juvenes Print
Tampere 2015

Table of Contents

List of original communications

This thesis is based on the following original communications, which are referred to in the text by their Roman numerals (I-IV)

I. **Syrjänen L**, Tolvanen M, Hilvo M, Olatubosun A, Innocenti A, Scozzafava A, Leppiniemi J, Niederhauser B, Hytönen VP, Gorr TA, Parkkila S, Supuran CT. "Characterization of the first beta-class carbonic anhydrase from an arthropod (Drosophila melanogaster) and phylogenetic analysis of beta-class carbonic anhydrases in invertebrates". BMC Biochemistry, 11: 28. 2010.

II. **Syrjänen L***, Tolvanen ME*, Hilvo M, Vullo D, Carta F, Supuran CT, Parkkila S. Characterization, bioinformatic analysis and dithiocarbamate inhibition studies of two new α-carbonic anhydrases, CAH1 and CAH2, from the fruit fly Drosophila melanogaster. Bioorganic & Medicinal Chemistry, 21:1516-21. 2013.

III. **Syrjänen L**, Vermelho AB, Rodrigues Ide A, Corte-Real S, Salonen T, Pan P, Vullo D, Parkkila S, Capasso C, Supuran CT. Cloning, characterization, and inhibition studies of a β-carbonic anhydrase from Leishmania donovani chagasi, the protozoan parasite responsible for leishmaniasis. Journal of Medicinal Chemistry, 56:7372-81. 2013.

IV. **Syrjänen L***, Valanne S*, Kuuslahti M, Tuomela T, Sriram A, Sanz A, Jacobs HT, Rämet M, Parkkila S. β carbonic anhydrase is required for female fertility in *Drosophila melanogaster*. Front Zool, 12:19. 2015.

* equal contribution

Abbreviations

BSA	bovine serum albumin
CA	carbonic anhydrase
CAI	carbonic anhydrase inhibitor
DKO	double knock-out
DNA	Deoxyribonucleic acid
DLS	dynamic light scattering
DmBCA	*Drosophila melanogaster* β-CA
E. coli	*Escherichia coli*
GFP	green fluorescent protein
hCA	human carbonic anhydrase
LdcBCA	*Leishmania donovani chagasi* β-CA
MIC	minimum inhibitory concentration
Mif	Mifepristone
PBS	phosphate-buffered saline
PBT	phosphate-buffered saline containing 0.3% Triton X-100
PFA	paraformaldehyde
PCR	polymerase chain reaction
RNA	ribonucleic acid
RNAi	RNA interference
qRT-PCR	quantitative real-time polymerase chain reaction
SDS-PAGE	sodium dodecyl sulphate - polyacrylamide gel electrophoresis
Sf	*Spodoptera frugiperda* (fall armyworm)

Tiivistelmä

Hiilihappoanhydraasit (carbonic anhydrase, CA) ovat entsyymejä, jotka katalysoivat käänteistä veden ja hiilidioksidin muuttumista bikarbonaatiksi ja protoniksi. Nämä entsyymit osallistuvat eliöissä muun muassa happo-emästasapainon säätelyyn, erilaisiin biosynteettisiin prosesseihin sekä hiilidioksidin ja bikarbonaatin kuljetukseen. Reaktion yleisluontoisuudesta johtuen nämä entsyymit esiintyvät laajalti luonnossa. Hiilihappoanhydraasit jaotellaan kuuteen luokkaan: α, β, γ, δ, ζ ja η. ζ-luokkaa löytyy vain meren piilevistä, δ-luokkaa piilevistä ja meren fytoplanktoneista. α-, β- ja γ-CA:t sen sijaan ovat laajalti levinneitä eri lajeihin. Aiemmin on ajateltu, että α-CA:t ovat laajimmin levinnyt CA-luokka. Näitä entsyymeitä on myös tutkittu eniten johtuen ainakin osittain siitä syystä, että kaikki ihmisen CA:t ovat α-luokkaa. Hiljattain löydetty kuudes CA-entsyymiperhe, η-CA:t, näyttää esiintyvän malariaa aiheuttavissa *Plasmodium* -suvun parasiiteissa.

Tämän väitöskirjatutkimuksen keskeisimpänä tarkoituksena oli selvittää β-CA -entsyymien ilmentymistä ja merkitystä eläimissä (*Animalia, Metazoa*), tarkemmin määriteltynä selkärangattomissa eläimissä. Pääasiallisena mallieläimenä tutkimuksissa käytettiin banaanikärpästä (*Drosophila melanogaster*), joka on laajalti käytetty malliorganismi. Banaanikärpäsen β-CA entsyymi tuotettiin rekombinanttiproteiinina ja sen solunsisäinen sijainti selvitettiin hyönteissoluissa. Lisäksi määritettiin entsyymin katalyyttiset ominaisuudet. β-CA -entsyymin merkityksen selvittämiseksi entsyymiä koodaava geeni hiljennettiin, ja selvitettiin tämän vaikutusta banaanikärpäsessä. Väitöskirjatyössä karakterisoitiin myös kaksi banaanikärpäsen α-CA:ta. Banaanikärpäsen β-CA:n lisäksi karakterisoitiin leishmaniaasia aiheuttavan yksisoluisen *Leishmania* -alkueläimen (alkueläimet, *Protozoa*) β-CA, ja tutkittiin CA-inhibiittoreiden vaikutusta eläviin *Leishmania* parasiitteihin.

Tutkimuksissa selvisi, että todennäköisesti kaikista selkärangattomista eläimistä löytyy ainakin yksi β-CA. Entsyymin esiintyminen selkäjänteisissä on epäselvää. Tulosten perusteella β-CA entsyymiä koodaava geeni on muuttunut inaktiiviseksi ja hävinnyt evoluution aikana ennen selkärankaisten kehittymistä. Tutkimuksissa selvisi, että banaanikärpäsen β-CA on korkean aktiivisuuden omaava mitokondriaalinen, dimeerinen entsyymi. Sitä koodaavan geenin hiljentyminen ei vaikuta banaanikärpäsen elinkykyyn, mutta aiheuttaa naaraissa täydellisen hedelmättömyyden. Näin ollen entsyymi on oleellinen banaanikärpäsen

lisääntymisen kannalta. Ongelma liittynee ainakin osittain ns. border solujen hidastuneeseen vaeltamiseen eli migraatioon. Koska entsyymi on mitokondriaalinen, testattiin myös geenin hiljennyksen vaikutusta mitokondrioiden hengitysketjun toimintaan. Näissä kokeissa ei kuitenkaan havaittu tilastollisesti merkitsevää eroa verrattuna kontrollimitokondrioihin. β-CA:n merkitystä korostaa lisäksi se, että *Leishmania* -parasiiteille tehdyissä kokeissa β-CA-spesifisimmillä inhibiittoreilla saatiin aikaan merkittävä väheneminen parasiittien kasvussa ja eräällä tioli-yhdisteellä lisäksi palautumattomia eliön kuolemaan johtavia solunsisäisiä muutoksia. Kaikkien entsyymien kohdalla tehtiin katalyyttiset määritykset ja testattiin useita erilaisia inhibiittoreita entsyymejä vastaan. Kaikilla entsyymeillä oli korkea katalyyttinen aktiivisuus ja niiden inhibitioprofiili poikkesi selvästi ihmisen entsyymeistä.

Yhteenvetona voidaan todeta, että β-CA:t näyttävät olevan selkärangattomille eläimille ja alkueläimille tärkeitä entsyymejä. Näitä vastaan kehitetyillä inhibiittoreilla voitaisiin muun muassa rajoittaa erilaisten trooppisten tautien leviämistä ja mahdollisesti myös parantaa erilaisia, lähinnä parasiittien aiheuttamia tauteja. Inhibiittoreiden mahdollisuudet eivät rajoitu pelkästään ihmislääketieteeseen, vaan sovelluskohteita löytyy myös mm. eläinlääketieteen ja kasvinsuojelun aloilta.

Abstract

Carbonic anhydrases (CAs) are enzymes that catalyze the reversible hydration of carbon dioxide to bicarbonate and proton. These enzymes are involved in many processes in living organisms, including acid-base regulation, a variety of biosynthetic processes and carbon dioxide and bicarbonate transport. Due to the general nature of the reaction, the enzymes are widely found in nature. CAs are divided into six groups: α, β, γ, δ, ζ and η. ζ-class is only found in marine diatoms, δ-class in diatoms and marine phytoplankton. α-, β-, and γ-CAs on the other hand, are widely distributed. Previously, it was thought that the α-CAs are the most widely spread CA group. These enzymes have also been studied the most due at least in part to the fact that all human CAs are α-class. A recently discovered novel CA-group, namely η-CAs, are found in malaria causing *Plasmodium* parasites.

The aim of this study was primarily to study β-CA enzymes from animals (*Animalia, Metazoa*), more specifically invertebrate animals. The main model organism in the studies was fruit fly (*Drosophila melanogaster*), which is a widely used model organism. The *Drosophila* β-CA was produced as a recombinant protein and its intracellular localization was investigated. In addition, the catalytic properties of the enzyme were determined. The significance of β-CA enzyme to fruit fly was studied by silencing the gene encoding the enzyme, and the effect of this on the fruit fly phenotype was examined. Two *Drosophila* α-CAs were also characterized during the studies involved in this thesis. In addition to studying *Drosophila*, a β-CA from *Leishmania*, a unicellular protozoan (*Protozoa*) parasite causing leishmaniasis, was characterized and the effect of various inhibitors was tested against living parasites.

The studies showed that at least one β-CA can be probably found from all invertebrate animals. The presence of β-CAs in chordates is unclear. It seems that some organisms have lost the *β-CA* gene during evolution. In vertebrate animals, including humans, the enzyme is not found. Studies revealed that the fruit fly β-CA is a highly active dimeric mitochondrial enzyme. Silencing of the corresponding gene does not affect the viability of the fruit fly, but causes complete infertility in females. Thus, the enzyme is essential for reproduction of *D. melanogaster*. It seems that the functional defect in reproduction is at least partly due to slow migration of so called border cells. Since the enzyme is mitochondrial, the effect of gene silencing on mitochondrial respiratory chain was also studied. In these experiments

however, statistically significant difference compared to the control mitochondria was not found. The importance of β-CAs is further highlighted by inhibition studies that revealed that some CA inhibitors inhibited the growth of *Leishmania* parasites *in vivo*. In addition, one of the thiol CA-inhibitors caused irreversible intracellular changes that led to the death of the parasite. Catalytic assays were performed with all the studied enzymes and a number of different inhibitors were tested against them. All of the enzymes had high catalytic activity and the inhibitor profile was clearly different from human enzymes.

In summary, it can be concluded that invertebrate and protozoan β-CAs seem to be important enzymes for physiology. Inhibitors against these enzymes could be used, for example, to limit the spread of tropical diseases, and possibly to cure various, mainly parasitic, diseases. The possibilities of inhibitors are not limited to human medicine, but the applications can also be found in both veterinary medicine and agriculture.

1. Introduction

Carbonic anhydrases (CAs, EC 4.2.1.1) are ubiquitous metalloenzymes that catalyze the reversible hydration reaction of carbon dioxide according to the following equation: $CO_2 + H_2O \leftrightarrow HCO_3^- + H^+$ (Sly & Hu, 1995). CAs are generally zinc-containing metalloenzymes. However, other metal cofactors are also used, such as Cd^{2+} in ζ-CAs (Lane et al., 2005; Xu, Feng, Jeffrey, Shi, & Morel, 2008) and iron (γ-CAs from anaerobic *Archaea* (Macauley et al., 2009; Tripp, Bell, Cruz, Krebs, & Ferry, 2004)). The reaction catalyzed by CAs is essential in the regulation of acid-base balance in organisms. In addition, these enzymes help to remove carbon dioxide out of tissues, participate in gluconeogenesis and ureagenesis, and are involved in many other physiological processes as well (Sly & Hu, 1995).

To date, six different classes of CAs have been identified: α, β, γ, δ, ζ and η (Zimmerman & Ferry, 2008; Del Prete et al., 2014). The ζ-CAs are found only in marine diatoms, and the δ-CAs in diatoms and other marine phytoplankton. The three major classes (α, β and γ) are widely distributed. Previously it was thought that α-CAs are most widely appearing group of CAs. α-CAs are also the most studied CA-group, probably mainly due to the fact that all human CAs belong to the α-CAs. α-CAs are also involved in many pathological states. A recently discovered novel class of CAs, the η-CAs, is found in malaria causing *Plasmodium* parasites (Del Prete et al., 2014). The β-CAs are found in most species belonging to the *Archaea* and *Bacteria* domains and probably all species of plants and fungi among *Eukarya* (Hewett-Emmett, 2000).

β-CAs differ from other CA groups in many respects. While α-CAs are typically found as monomers and γ-CAs as trimers, β-CAs are found in many oligomerization states. Crystal structures of dimeric, tetrameric and even octameric β-CAs have been reported in the literature (Kimber & Pai, 2000; Smith, Cosper, Stalhandske, Scott, & Ferry, 2000; Strop, Smith, Iverson, Ferry, & Rees, 2001). Secondly, the zinc atom in the active site is coordinated by one histidine and two cysteine residues instead of three histidine residues present in α-, γ- and δ-CAs (Cox et al., 2000). Also, the amino acid sequences are completely different. Despite these differences, all of these enzyme groups catalyze the same chemical reaction. CAs generally show fast enzyme kinetics. Human CA II is considered as one of the fastest enzymes characterized, for example. However, notable differences in kinetics exist between different CAs.

Using bioinformatics searches we found that β-CA sequence is present in a genome of common fruit fly (*D. melanogaster*). However, the enzyme was not characterized nor was any other β-CA from any animal species. Therefore, it was unclear if this putative enzyme is functional. Previously it was thought that animal CAs are all α-CAs, which made this study even more interesting. Since this enzyme was found in a *Drosophila* species, we further hypothesized that it can be found also in other invertebrate animal species, many of which cause diseases (e.g. *Schistosoma* parasites) or act as disease vectors (e.g. malaria mosquito *Anopheles gambiae* and yellow fever mosquito *Aedes Aegypti*). Presuming that β-CAs are relevant for these animals, it could be anticipated that specific inhibitors could be used to cure and to restrict the spread of these diseases.

During this study it became evident that *D. melanogaster* does indeed possess a β-CA. One aim of this study was to characterize this enzyme. *D. melanogaster* β-CAs subcellular localization was examined using GFP (Green Fluorescent Protein). The enzyme´s oligomeric state was examined using dynamic light scattering and gel filtration. In addition to β-CA, two *D. melanogaster* α-CAs were also characterized. After the basic properties of *D. melanogaster* β-CA were clarified, next logical step was to find out by RNA interference if disruption of this enzyme activity causes a visible phenotype. To further assess the significance of the β-CA enzyme as a potential anti-parasitic drug target, a representative enzyme was characterized from the protozoan *Leishmania* parasite. Kinetic properties of all of the enzymes were investigated and a series of CA-inhibitors were tested against all these biochemical targets. Some inhibitors were also tested *in vivo* against living *Leishmania* parasites, revealing an ability to control the growth process of the parasite.

2. Review of the literature

2.1 Roles of carbonic anhydrases

2.1.1 General aspects

Carbon dioxide and bicarbonate constitute the main buffer system for pH regulation in all living cells. Two other commonly recognized buffer systems *in vivo* are phosphate and ammonia buffers. Carbon dioxide easily diffuses through biological membranes and is moderately soluble in water. On the contrary, bicarbonate is highly soluble but diffuses relatively poorly through membranes. The reversible hydration of carbon dioxide to bicarbonate and proton ($CO_2 + H_2O \leftrightarrow HCO_3^- + H^+$) occurs at slow rate even without a catalyst. However, the presence of CA enzymes enables this reaction to occur at sufficiently high rate required by the metabolism of living cell (Guyton AC, 2006).

Besides the importance of CAs as a part of pH regulation, in a more global perspective, the most important function of CAs is related to carbon fixation in plants. In photosynthesis, plants, photosynthetic cyanobacteria and phytoplankton are able to trap carbon dioxide from air and subsequently concentrate and fix it to organic carbon compounds. CA activity is implicated in diffusion of CO_2 into and across chloroplasts, and provides a supply of CO_2 to ribulose 1,5-phosphate carboxylase/oxygenase in chloroplasts or carboxysomes (Majeau & Coleman, 1996). CAs are also suggested to play a role in retention and recycling of CO_2 released from plant mitochondria (Zabaleta, Martin, & Braun, 2012).

In addition to their role in pH regulation and carbon fixation, CAs participate in many other physiological processes, such as gluconeogenesis, production of body fluids, transport of CO_2 and HCO_3^- and bone resorption in vertebrates (Sly & Hu, 1995). The involvement of CAs in the physiology of tetrapods is most obvious in the kidneys and respiratory system where CAs are involved in regulation of acid-base balance as a means of respiratory or metabolic compensation.

Most likely invertebrate CAs participate in the same processes as in other animal species. Some processes have been studied more extensively. For example, CAs have been linked to anion transport in mosquito midgut pH regulation

(Linser, Smith, Seron, & Neira Oviedo, 2009) and invertebrate CAs are known to participate in biomineralization of corals (Mass, Drake, Peters, Jiang, & Falkowski, 2014).

2.1.2 Catalytic mechanism

Carbonic anhydrases are metalloenzymes that catalyze the reversible hydration reaction of carbon dioxide according to the following equation: $CO_2 + H_2O \leftrightarrow HCO_3^- + H^+$. Because of the close structural homology of the α- and β-CA active sites, the catalytic mechanism of both follow a similar metal-hydroxide mechanism (Kimber & Pai, 2000).

In principle, the catalytic step involves a reaction between zinc- (or other metal cofactor) bound OH^- and CO_2. This reaction yields a coordinated HCO_3^- ion which is subsequently replaced from zinc-ion with an H_2O molecule. This is shown in equation 1, where E indicates enzyme. The regeneration of OH^- involves a transfer of H^+ from the zinc-bound H_2O molecule to the solvent, which is shown in equation 2 (Supuran, 2004).

$$(1)\quad EZn\text{-}OH^- + CO_2 \leftrightarrow EZn\text{-}HCO_3^- \overset{H_2O}{\leftrightarrow} EZn\text{-}H_2O + HCO^-$$

$$(2)\quad EZn\text{-}H_2O \leftrightarrow EZn\text{-}OH^- + H^+$$

The active form of the CA enzyme has a hydroxide ion bound to the Zn^{2+} ($EZn\text{-}OH^-$). This strong nucleophile, pre-oriented by Thr-199 residue, attacks the CO_2 molecule, which leads to the formation of HCO_3^-, coordinated to the Zn^{2+} ion. The HCO_3^- ion is subsequently replaced by an H_2O molecule and diffuses out of the active site. This leads to the formation of the acid form of the enzyme, where H_2O is coordinated to the Zn^{2+} ion (Equation 1). In this form the enzyme is inactive. To regenerate the basic, active form of the enzyme ($EZn\text{-}OH^-$) a proton must be transferred from the active site to the surrounding solution (Supuran, 2004).

The rate-limiting step in the reaction is the proton transfer reaction (Equation 2). In α-isozymes possessing high catalytic activity, this step is assisted by a histidine residue (His 64) located at the rim of the active site (Supuran, 2004).

β-CAs possess a highly conserved dyad comprising aspartate and arginine residues that seem to be crucial for the catalytic mechanism since mutation of these residues severely reduces the catalytic activity of the enzyme (Smith, Ingram-Smith, & Ferry, 2002). The aspartate makes a hydrogen bond with the Zn^{2+} coordinated water molecule, activating it for nucleophilic attack of the CO_2 molecule (Schlicker et al., 2009), similar to the Thr-199 residue in α-CAs.

2.1.3 Inhibition and drug design

CA inhibition was studied immediately after enzyme discovery. Since CAs are involved in many physiological and pathophysiological processes, CA-inhibition has relevance in medicine (Chegwidden WR, 2000). Inhibition of CAs has been exploited in pharmacology as glaucoma medication, anticancer agents and also anti-infectives. Sulfonamides and their isosteres sulfamates and sulfamides constitute the main class of CA-inhibitors (CAIs). The molecules bind to the metal ion in the enzyme active site, displacing the H_2O/OH^-. Dithiocarbamates share the same mechanism of action. Phenols, sulfocoumarins, polyamines and some carboxylates bind to the zinc-coordinated water molecule, which is possibly relevant for their inhibitory action. There are also prodrugs (coumarins and five or six-membered lactones) that bind in a hydrolyzed form to the entrance of the active site cavity, thereby affecting the catalysis (McKenna & Supuran, 2014). The design of new isoform-selective inhibitors requires determination of three dimensional structures of other CA classes, including invertebrate β-CAs as the basis for selectivity and ultimately parasite/human selective toxicity.

2.2 Carbonic anhydrase families

Six different classes of CAs have been identified: α, β, γ, δ, ζ and η (Zimmerman & Ferry, 2008; Del Prete et al., 2014). α-CAs are typically found as monomers and γ-CAs as trimers. On the other hand, β-CAs are found in many oligomerization states. Figure 1 shows example structures of the major CA families α, β, γ. Active sites are highlighted by sphere representation of the metal atom and stick representation of the metal binding amino acid residues. Different CA classes are described more closely below.

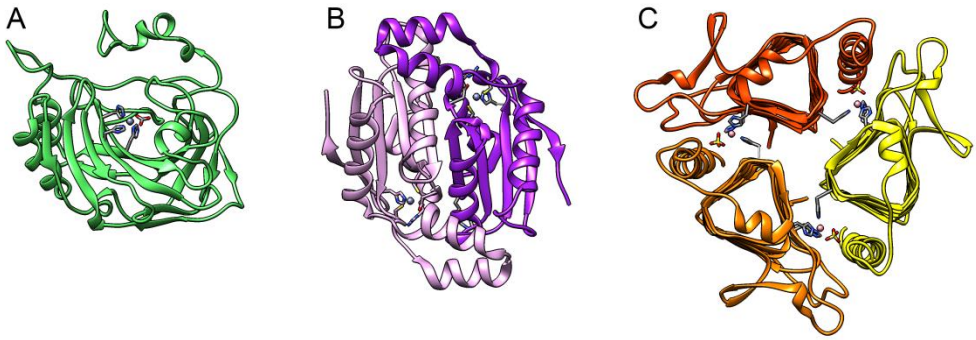

Figure 1. **Examples of structures of the major CA classes α, β and γ**. 3D structures are retrieved from PDB and visualization has been made with Chimera. Catalytic metal ion and metal-binding amino acid side chains are shown in detail. **A**, α-CA: human CA I, PDB 1hcb (Kumar & Kannan, 1994); **B**, β-CA: "cab-type" dimer from the archaeon Methanobacterium thermoautotrophicum, chains A and B of PDB 1g5c (Strop et al., 2001); **C**, γ-CA from the archaeon Methanosarcina thermophila, chain A of PDB 1qrf (Iverson, Alber, Kisker, Ferry, & Rees, 2000), tripled by crystallographic symmetry operations to give the biological form of a trimeric enzyme. Image courtesy of Dr. Martti Tolvanen.

2.2.1 α-CA family

α-CAs have been previously considered to be the CA-class with the widest distribution. α-CAs are also the most studied CAs, mostly because of the fact that all human CAs are α-CAs. Indeed, in animals, α-CAs exist as numerous isoforms. For example, 15 and 16 α-CAs have been described in primates including humans, and non-primate mammals, respectively (Fabre, Reiter, Becuwe-Linka, Genty, & Rumeau, 2007; Sly & Hu, 1995). In humans there are 12 catalytically active α-CAs and three acatalytic forms, denominated carbonic anhydrase related proteins (CARPs). In humans, there are five cytosolic enzymes (I, II, III, VII and XIII), two mitochondrial (VA and VB), one secreted (VI) and four membrane bound forms (IV, IX, XII and XIV). CARPs include CAs VIII, X and XI (Lehtonen et al., 2004; Sly & Hu, 1995). The α class is missing from *Archaea* (M. Tolvanen, unpublished observation) but is widely present in *Bacteria* and *Eukarya*, with the exception of *Fungi*, in which only filamentous ascomycetes have α-CAs (Elleuche & Poggeler, 2009b). To date, CA II has been reported to be the isozyme with the highest catalytic efficiency of all CAs, with a k_{cat}/K_m = 1.5 × 10^8 m^{-1} s^{-1} (Innocenti, Leewattanapasuk, Muhlschlegel, Mastrolorenzo, & Supuran, 2009).

The 15 human α-CAs participate in various physiological functions. It has to be noted that different CAs are expressed in different tissues. Table 1 summarizes the major functions and sites of expression of human CAs.

Table 1. Major functions and sites of expression of human CAs.

Isozyme	Functions	Major site of expression	Selected references
CA I	Gas exchange and ion transport	Red blood cells and GI tract	(Sly, Hewett-Emmett, Whyte, Yu, & Tashian, 1983)
CA II	Bone resorption, secretion of cerebrospinal fluid, production of aqueous humor, urine acidification, gas exchange	Almost all cells	(Sly et al., 1983)
CA III	Antioxidative agent	Muscle and adipose tissue	(Kim et al., 2004)
CA IV	Bicarbonate reabsorption, pH regulation	GI tract, pancreas, eye, colon, kidney, endothelium, salivary glands, heart muscle	(Fleming, Crouch, Ruzicka, & Sly, 1993)
CA VA	Biosynthetic reactions, detoxification of ammonia	liver	(Fujikawa-Adachi, Nishimori, Taguchi, & Onishi, 1999; Shah et al., 2013)
CA VB	Biosynthetic reactions, detoxification of ammonia	Heart and skeletal muscle, pancreas, kidney, salivary glands, spinal cord	(Fujikawa-Adachi et al., 1999; Shah et al., 2013)
CA VI	Protection of teeth, taste function	Tears and milk, nasal, lacrimal, von Ebner's and mammary glands, major constituent of saliva	(Patrikainen, Pan, Kulesskaya, Voikar, & Parkkila, 2014)
CA VII	Neuronal excitation(speculative)	Colon, liver, muscle, central nervous system	(Ruusuvuori et al., 2004; Sly & Hu, 1995)
CA VIII (CARP8)	Motor coordination	Purkinje cells in cerebellum	(Aspatwar, Tolvanen, & Parkkila, 2013)
CA IX	pH regulation, cell proliferation and adhesion, tumorigenic processes	Several cancers, healthy GI tract	(Hilvo et al., 2008)
CA X (CARP10)	Unknown	Central nervous system	(Aspatwar et al., 2013)
CA XI (CARP11)	Unknown	Central nervous system	(Aspatwar et al., 2013)
CA XII	pH regulation, tumorigenic processess	Colon, kidney, prostate, intestine, lymphocytes, breast, lung, eye, male excurrent ducts, reproductive epithelia. Also several cancers.	(Ivanov et al., 2001)
CA XIII	Unknown	thymus, small intestine, spleen, prostate, ovary, colon and testis.	(Lehtonen et al., 2004)
CA XIV	Acidification of urine, participation in neuronal transmission	Central nervous system, liver, heart, skeletal muscle colon, small intestine, kidney, urinary bladder	(Shah et al., 2005; Whittington et al., 2004)

α-CAs are monomeric enzymes. There are many defined structures available for α-CAs, and they have revealed that the active site is approximately 15 Å of width and

depth, accessible to solvent (Krishnamurthy et al., 2008). The Zn^{2+} ion at the base of the active site is in a distorted tetrahedral coordination by three histidine amino acid residues (for example His 94, His 96 and His 119 in CA II) and a water molecule (or hydroxide ion) (Stams & Christianson, 2000). Additionally, His64 has been shown to facilitate the catalysis (McKenna & Supuran, 2014). Crystallographic, catalytic and inhibition studies have shown that similar active site structures and kinetic properties are shared between α-CAs from mammals and other vertebrates, prokaryotes, sponges, corals and nematodes (Boone, Pinard, McKenna, & Silverman, 2014). Of course, differences are found related to kinetic properties and inhibition profiles.

2.2.2 β-CA family

β-CAs represent another CA family containing a Zn^{2+} ion in the active site. β-CAs are found in fungi, bacteria, archaea, algae, plants (Hewett-Emmett, 2000), and in light of current knowledge, metazoans (animals). First β-CA was discovered in 1939 by Arthur Neish (Neish, 1939). In 1990, it was identified as a chloroplastic CA in spinach (*Spinacea oleracea*) (Burnell, Gibbs, & Mason, 1990). Many putative β-CAs from photosynthetic organisms, bacteria, archaea and yeasts have been reported since then. *Escherichia coli* β-CA CynT was the first reported bacterial β-CA (Guilloton, Korte, Lamblin, Fuchs, & Anderson, 1992). Thereafter, β-CAs from many pathogenic bacteria have been characterized (Supuran, 2011). In 2009, the first animal β-CA from a nematode *Caenorhabditis elegans* was reported (Fasseas, Tsikou, Flemetakis, & Katinakis, 2009).

Important differences were found between the β-CAs and other CA groups, even if they catalyze the same reaction. First of all, the Zn^{2+} ion in the active site of β-CAs is coordinated by two cysteines and one histidine instead of the three histidines found in α- and γ-CAs active sites (Cox et al., 2000). Secondly, β-CAs possess a unique α/β -fold that promotes association with the formation of dimers. Thus, β-CAs are found in many oligomerization states instead of being monomers like α-CAs or trimers like γ-CAs. Crystal structures of dimeric, tetrameric and octameric β-CAs have been reported (Kimber & Pai, 2000; Smith et al., 2000; Strop et al., 2001). The monomer components of a dimer bind to each other tightly, usually by non-covalent interactions or in some cases, via a short polypeptide linker. The latter case is called a "pseudo-dimer" (Rowlett, 2014). Tetramers and octamers are formed when dimers form dimer-of-dimers and dimer-of-dimer-of-dimers, respectively. Thus far the most frequently seen

quaternary structure in β-CAs is a tetramer. However, dimer seems to be the fundamental structural unit in β-CAs.

Altogether, the physiological roles of β-CAs are not well known. In some organisms β-CA often serves as a supportive factor for other enzymes that utilize or dispose carbon dioxide or bicarbonate. Examples of these kind of enzymes are ribulose-1,5-bisphosphate carboxylase (or Rubisco), urease, cyanase and carboxylases that are associated with fatty acid biosynthesis. It has been shown that Rubisco and β-CA are transcriptionally linked in *Pisum sativum*. When plants are transferred from a high carbon dioxide environment to one with lower, atmospheric, pressure of carbon dioxide, the expression levels increase (Majeau & Coleman, 1996). On the other hand, up to 99% suppression of chloroplastic β-CA expression in tobacco (*Nicotiana tabacum*) did not have any significant impact on carbon assimilation (Majeau, Arnoldo, & Coleman, 1994).

β-CAs have also been shown to be important for normal growth in certain bacteria and yeasts. β-CA is an important component of the carboxysome that is the carbon dioxide concentrating structure in cyanobacteria. If this β-CA is mutated, it yields a phenotype that requires high carbon dioxide concentrations for normal growth in *Synechococcus* (Fukuzawa, Suzuki, Komukai, & Miyachi, 1992). In addition, it has been determined to be essential for normal growth in *Corynebacterium glutamicum* (Mitsuhashi, Ohnishi, Hayashi, & Ikeda, 2004)*, E. coli* (Merlin, Masters, McAteer, & Coulson, 2003) and *Saccharomyces cerevisiae* (Clark, Rowlett, Coleman, & Klessig, 2004; Gotz, Gnann, & Zimmermann, 1999) under normal aerobic concentrations and atmospheric pressures of carbon dioxide. Complementation with catalytically active α- or β-CA restored the ability to grow in a normal way under atmospheric carbon dioxide concentrations, when β-CA activity was blocked with site-directed mutagenesis in *S. cerevisiae* (Clark et al., 2004). In β-CA deficient *Streptococcus pneumoniae*, supplementation with unsaturated fatty acids restored normal growth under low carbon dioxide concentrations (Burghout et al., 2010). This latter finding supports the fact that β-CA (at least in this organism) facilitates the activity of bicarbonate-dependent carboxylases that are required in fatty acid synthesis, for example. Additionally, studies in mice have shown that gastric mucosal inflammation was markedly reduced when *Helicobacter pylori* were devoid of β-CA as compared to control bacteria expressing β-CA (Bury-Mone et al., 2008).

Interestingly, a mitochondrial β-CA has been shown to be important in the sexual reproduction in filamentous ascomycete *Sordaria macrospore* (Elleuche & Poggeler, 2009a). In the presence of a mutant of the normal β-CA, *cas2,* vegetative growth, fruiting-body development, and ascospore germination were affected, and the double mutant strain *cas1/2* was completely sterile. *cas2* was shown to be mitochondrial while the other two β-CAs of *S. macrospore, cas1* and *cas3*, were

cytoplasmic. Defects caused by the lack of *cas2* could be partially compensated by elevated carbon dioxide levels in addition to overexpression of *cas1*, *cas3*, or a non-mitochondrial *cas2* variant. It was depicted that there may be a functional connection between β-CAs and adenylyl cyclase. In this way, cAMP signaling would be affected.

The physiological functions of animal β-CAs are not known. RNAi suppression of β-CA activity did not reveal any visible phenotype in *C. elegans* (Fasseas et al., 2009).

2.2.3 γ-CA family

γ-class CAs were first reported in 1994 (Alber & Ferry, 1994). γ-CAs are of ancient origin and orthologs are present in *Archaea, Bacteria* and plants (Parisi et al., 2004; Zimmerman & Ferry, 2008). γ-CAs differ from the other CA-classes in that the enzymes are found in trimers instead of being monomers (like α-CAs) or dimers/tetramers/octamers like β-CAs. Interestingly γ-CAs can contain iron *in vivo*, as identified in anaerobic *Archaea* (Macauley et al., 2009).

2.2.4 δ- and ζ-CA families

ζ- and δ-CAs have the narrowest distribution among different CA classes in nature. ζ-CAs are present in marine diatoms and δ-CAs in diatoms and other marine phytoplankton (Supuran, 2008). ζ-CAs can use cadmium as an alternative metal cofactor, which make them exceptional CAs (Lane et al., 2005; Xu et al., 2008). The first δ-CA was characterized from *Thalassiosira weissflogii* and was later found to be present in a broader range of eukaryotic phytoplankton (McGinn & Morel, 2008). There are no three-dimensional structures of δ-CA available at this moment, but X-ray absorption spectroscopy has shown that the catalytic Zn^{2+} ion has three histidine ligands, similar to α and γ classes (Cox et al., 2000).

2.2.5 New proposed class of η-CAs

Recently, a new class of CAs, η-CAs, was proposed to exist in malaria causing *Plasmodium* species (Del Prete et al., 2014). These CAs have been previously

thought to be α-CAs. The proposal of the new CA-class was based on results from sequence alignment and phylogenetic analysis.

2.3 Invertebrate CAs

Almost all previous studies concerning invertebrate CAs have dealt with α-CAs, which have been reported, for example, in *C. elegans* (Fasseas, Tsikou, Flemetakis, & Katinakis, 2011), *A. aegypti* (Corena et al., 2002), *Ostertagia ostertagi* (DeRosa, Chirgwin, Williams, & Klei, 2008) and *Riftia pachyptila* (De Cian, Andersen, Bailly, & Lallier, 2003). α-CAs from protozoan parasites *Trypanosoma cruzi* (Pan et al., 2013) and *Plasmodium falciparum* (Krungkrai, Suraveratum, Rochanakij, & Krungkrai, 2001) have also been published.

In 2009, Fasseas and coworkers published a study in which two β-CAs were characterized from *C. elegans* (Fasseas et al., 2009). One of the enzymes was shown to be active. RNA interference studies were also performed in this study but they failed to reveal any visible phenotype. This study was published only one year after our first observations on *D. melanogaster* β-CA, and only few additional articles have been reported on this topic during the recent years. Thus, there is extremely limited information in the literature about invertebrate β-CAs.

2.4 Classification of organisms

Organisms are typically divided into three domains: *Bacteria*, *Archaea* and *Eukarya*. The lattermost is further divided into four kingdoms: *Fungi*, *Animalia*, *Protista* and *Plantae*. Animals, or *Animalia* (*Metazoa*), are further divided into many subgroups. Figure 2 shows that actually only a minority of animals fall into the category of vertebrates (*Vertebrata*). Other animals are considered as invertebrates and account for 97% of all animal species, according to some estimates. *Fungi* are eukaryotic organisms that include yeasts and molds, as well as mushrooms. *Plantae* include multicellular green plants. The kingdom *Protista* includes unicellular, eukaryotic micro-organisms. These include animal-like protozoans.

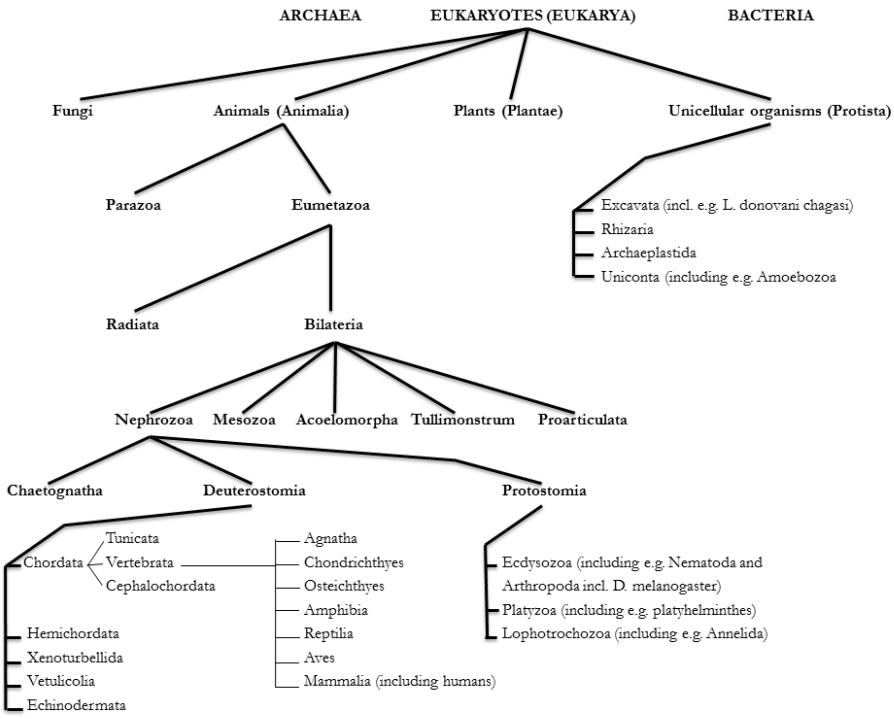

Figure 2. Classification of organisms with emphasis on animal species (*Animalia*). A majority of subgroups have been omitted for clarity. *D. melanogaster*, the major model organism used in our studies, belongs to the Phylum *Arthropoda*. *L. donovani chagasi* belongs to the kingdom of *Protista* and is not usually considered an animal.

2.5 Model organisms used in the studies

2.5.1 Drosophila melanogaster

The fruit fly, or *D. melanogaster* (Greek for dark-bellied dew lover), is a *Dipteran* invertebrate species that has been used as a model organism in scientific research for over a century. Early studies on *D. melanogaster* were performed by Thomas Hunt Morgan and his students in Columbia University. These studies led to great discoveries, such as sex-linked inheritance and that ionizing radiation causes mutations in genes (Stephenson & Metcalfe, 2013). *D. melanogaster* was also the first major complex organism to have its genome sequenced (Adams et al., 2000). Its

genome encodes for a little more than 14,000 genes on four chromosomes, three of them carrying the bulk of the genome (Reiter, Potocki, Chien, Gribskov, & Bier, 2001). One of the major advantages in using *D. melanogaster* as a model organism is its rapid life cycle. A single fertile mating pair can produce hundreds of genetically identical offspring within only 10 to 12 days at 25ºC (Pandey & Nichols, 2011). Moreover, flies can be multiplied quite easily even in room temperature with food that can be easily made in the laboratory. Additionally, invertebrate fruit flies do not raise as many ethical concerns as vertebrate model organisms. *D. melanogaster* has been used extensively in scientific research and can be used as a model organism in pesticide research, for example.

The complete *D. melanogaster* genome is available and has made the study of *Drosophila* genes relatively easy (Adams et al., 2000). Many genetic tools have also been developed (Rubin & Lewis, 2000). One such method is called RNA interference (RNAi), in which a gene can be inactivated in a controlled manner. A genome-wide collection of RNAi fly lines are publicly available (Dietzl, Chen, Schnorrer, Su, Barinova, Fellner, Gasser, Kinsey, Oppel, Scheiblauer, Couto, Marra, Keleman, & Dickson, 2007). The expression of RNAi constructs can be strictly controlled both temporally and spatially with the UAS-GAL4 (Upstream activating sequence) system that was originally adapted from yeast (Brand & Perrimon, 1993b).

Reproductive system in D. melanogaster

The reproductive system of *D. melanogaster* is illustrated in Figure 3, and is composed of ovaries, oviducts, seminal receptacle, spermathecas, parovaries (accessory glands), uterus and vulva. The eggs are developed in the ovaries. Eggs move through the lateral oviduct into the common oviduct where fertilization takes place. Male sperm is not necessarily used immediately but can be stored by female in organs called the seminal receptacle and paired spermatheca. Sperm can be stored by the female *Drosophila* for about two weeks (Bloch Qazi, , Heifetz & Holfner, 2003).

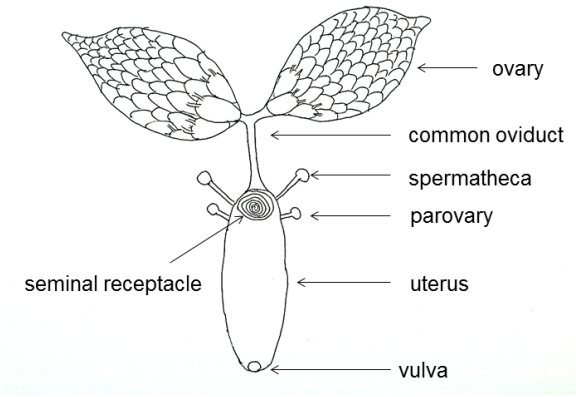

Figure 3. Overview of *D. melanogaster* female reproductive tract.

6.5.1.1 Egg-chamber development in D. melanogaster

Egg-chamber development (see Figure 4) in the *D. melanogaster* ovary begins in a structure called the germarium (Bastock & St Johnston, 2008; Montell, 2003). At the anterior end, specialized somatic follicle cells make a niche that supports the germline stem cells. These divide to produce a cystoblast and a daughter stem cell that remains in the niche. The cystoblast subsequently undergoes four rounds of cell division to yield 16 germline cells, which remain connected to one another as a result of incomplete cell cleavages. Out of these 16 germline cells, one differentiates into the oocyte and subsequently enters meiosis, while the other 15 become nurse cells. After this event, follicle cells encircle the 16-cell cyst and the oocyte travels into the most posterior position. At this point, the developing egg chamber buds off the germarium and stage 1 is reached.

Stages 2–7 involve polyploidization of the nurse cells, mitotic division of the follicle cells and increase of the size of the egg chamber as a whole. At the same time when the egg-chamber is developing and pushed forward, new egg-chambers bud off from the germarium. Egg chambers remain connected to each other by stalk cells which makes the entity resemble a string of pearls. During this development, a specialized pair of follicle cells, called polar cells, differentiates at both ends of the egg chamber. They stop dividing soon after they become fully differentiated, whereas the rest of the follicle cells continue to divide until stage 6. At stage 8, the oocyte begins to accumulate yolk. At stage 9, the majority of the follicle cells change their shape from cuboidal to columnar and accumulate in the posterior half of the egg chamber. At this point, they are directly contacting the oocyte. Some cells remain in the anterior part and form a layer of cells that covers the nurse cells. At the same time, the anterior pair of polar cells (left-hand side in

the Figure 4) recruits 4–8 neighbouring follicle cells to form the so called border-cell cluster. The outer border cells detach themselves from the epithelium, become invasive and deliver the polar cells across the center of the egg chamber to the border of the oocyte and nurse-cells. At stage 10, the oocyte occupies half of the egg-chamber. The function of nurse cells is to nourish the oocyte. Finally, the nurse cells undergo apoptosis and the follicle cells produce the eggshell. Stage 14 designates a mature egg (not shown in figure).

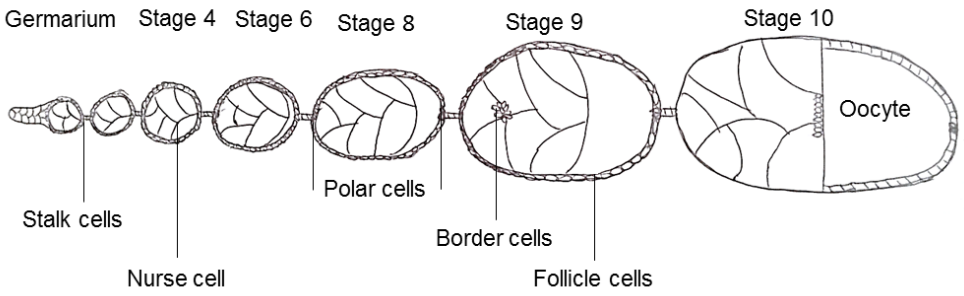

Figure 4. Egg-chamber development in *D. melanogaster* ovary.

6.5.1.2 Border cell migration in the ovary of D. melanogaster

Border cells have a special role during *D. melanogaster* oogenesis, which involves an invasive and directed cell migration. Border cells are a commonly used model system for the study of collective cell migration during *Drosophila* oogenesis (Montell, 2003; Rorth, 2009). *Drosophila* eggs mature in structures called egg chambers, which are composed of 16 interconnected germ-line cells that are encapsulated by a monolayer of somatic follicle cells (Bastock & St Johnston, 2008). One of the 16 germ-line cells differentiates as the oocyte, while the other 15 become nurse cells that aid oocyte in the maturation process. The somatic follicle cells undergo a complex developmental and morphogenetic program which is tightly linked to germ line development. Ultimately, this leads to the formation of the egg shell (Wu, Tanwar, & Raftery, 2008). During stage 8 of oogenesis the border cells are specified at the anterior pole of the follicular epithelium and start to express the C/EBP transcription factor. During stages 9 and 10, the border cells detach from the follicular epithelium and migrate as a cluster toward the oocyte. At stage 10B, the border cell cluster has reached the anterior face of the oocyte and subsequently migrates laterally to its final anterodorsal position. This process involves several signaling pathways as well as extensive remodeling of cell adhesion

properties and of the cytoskeleton (Bastock & St Johnston, 2008; Montell, 2003; Rorth, 2009).

The border cells are involved in formation of the eggshell by forming a structure called the micropyle. Micropyle contains a pore through which the sperm enters the oocyte at fertilization. If border cells are absent, or if their migration fails, the micropyle is deformed and lacks a pore (Montell, Rorth, & Spradling, 1992). Therefore, females with disrupted border-cell migration cannot be fertilized and are sterile.

2.5.2 *Leishmania donovani chagasi*

L. donovani chagasi is a subspecies of *L. donovani*. *Leishmania* parasites are unicellular protozoan organisms that cause a vector-borne tropical disease called leishmaniasis. The parasites are transmitted to the mammalian host organism, such as humans, by an infected sand fly. Disease is different depending on the *Leishmania* strain causing the infection. For example, *L. major* remains mainly in the skin, while some others, such as *L. donovani chagasi*, infect visceral organs. Leishmaniasis is associated with a wide range of clinical manifestations from self-healing cutaneous lesions to fatal visceral infections. Visceral leishmaniasis accounts for 20 000 – 40 000 deaths every year (McCall, Zhang, & Matlashewski, 2013).

2.6 Why is studying invertebrate CAs important?

According to the results from our studies, mammals do not possess β-CAs, but these enzymes are widespread throughout the tree of life. This makes them exciting new targets for anti-parasitic drug development. Among invertebrates, there are various organisms that cause or transmit diseases, most of which are causing problems in tropical countries. These invertebrates include malaria mosquito *Anopheles*, yellow fever mosquito *Aedes*, filariasis vector *Culex*, *Ancylostoma* hookworms, *Brugia* filarial nematodes, blood fluke *Schistosoma mansoni* and liver fluke *Schistosoma sinensis*. These invertebrate β-CAs most likely have a three dimensional structure that is different from β-CAs studied so far, and significantly different from α-CAs. Because of this, specific inhibitors against these β-CA enzymes could be designed with minimal effects on human CAs and normal bacterial flora. Applications can also be found in veterinary medicine and agriculture.

3. Aims of the study

When the project started, there were no reports about invertebrate β-CAs. Because mammals clearly possess only α-CAs, I became excited about the hypothesis that these enzymes could provide novel possibilities for anti-parasitic drug development.

The specific aims of my research were:

1) To verify that β-CAs are present in invertebrates and characterize a β-CA enzyme from a commonly used invertebrate model organism, fruit fly *D. melanogaster*. (I)
2) To characterize α-CAs (CAH1 and CAH2) from *D. melanogaster*. (II)
3) To characterize a β-CA from a parasitic organism, namely protozoan *L. donovani chagasi*. (III)
4) To investigate the biological function of β-CA in *D. melanogaster* (IV) and to study the effect of β-CA inhibition in *L. donovani chagasi in vivo* (III).

4. Materials and methods

4.1 Production of recombinant invertebrate carbonic anhydrases

Production of recombinant invertebrate carbonic anhydrases, namely *D. melanogaster* β-CA (named DmBCA), two *D. melanogaster* α-CAs (CAH1 and CAH2) and *L. donovani chagasi* β-CAs (LdcBCA) is described below. All primers used in the construction of recombinant enzymes are listed in Table 2.

Table 2. PCR primers used in recombinant protein production.

Primer	Enzyme	Sequence
F1	DmBCA	5´-ATGGAGCGTATTTTGAGGGGAATC-3´
F2	DmBCA	5´-GGCCAGATCTATGGAGCGTATTTTGAGGGGA-3´
F3	LdcBCA	5´-ATGTCGCTGTGCAGCTGCGGC-3´
F4	LdcBCA	5´-CGCGAATTCATGTCGCTGTGCAGCTGCGGC-3´
F5	CAH1	5´-ATGAGCCACCACTGGGGATACACC-3´
F6	CAH1	5´-CGCGGATCCAGCCACCACTGGGGATACACC-3´
F7	CAH2	5´-ATGAGGAGGTGTCGCAACACCCCG-3´
F8	CAH2	5´-CGCGGATCCTACGAGGGCAGACATGGACCC-3´
F9	DmBCA	5´-TCGCTGGTGCCCCGTGGTTCCGTGAG CAAGGGCGAGGAGCTG-3´
F10	DmBCA	5´-GACAAGGGAGCAAATGGTCAA-3´ (qPCR)
R1	DmBCA	5´- CTACGAATAGAATCTTCTGACCTC-3
R2	DmBCA	5´- GCCCTCGAGTTAATGGTGGTGATGGTGG TGGGAACCACGGGGCACCAGCGAATAGAATCTTCTGACCTC-3´
R3	LdcBCA	5´-CTACAGCTGCCCGTAGCGCCA-3´
R4	LdcBCA	5´-GCCCTCGAGTTAATGGTGGTGATGGTGGTGG GAACCACGGGGCACCAGCAGCTGCCCGTAGCGCCAGAA-3´
R5	CAH1	5´-TTAGTGGCCCCCGATCTCGCGCAG-3´
R6	CAH1	5´-CCGCTCGAGTTAGTGGCCCCCGATCTCGCG-3´
R7	CAH2	5´-TTAAAAACCCCGGAAAATGGAGGT-3´
R8	CAH2	5´-CCGCTCGAGTTAGTAGTTCTTGTACAAGGT-3´-
R9	DmBCA	5´ - CACGGAACCACGGGGCACCAGCGAATAGAATCTTCTGACCTC - 3´
R10	DmBCA	5´-CCGCTCGAGTTATTTGTATAGTTCATCCAT-3´
R11	DmBCA	5´-TCTACTGTCCATGCAGGTGAAGAA-3´ (qPCR)

4.1.1 Production of D. melanogaster and L. donovani chagasi β-CA enzymes

Construction of recombinant baculoviruses for D. melanogaster β-CA

Two constructs were engineered to study functional aspects of DmBCA. The first construct contained a C-terminal histidine tag for protein purification. The second contained a GFP (Green Fluorescent Protein) sequence fused to the C-terminus of DmBCA for detection of the recombinant protein with confocal microscopy. BglII and XhoI restriction sites and a thrombin cleavage site (for histidine tag removal) were added into both constructs.

Total RNA extracted from *D. melanogaster* S2 cells (TRIzol® reagent and protocol, Invitrogen) was precipitated using sodium acetate at a final concentration of 100 mM and 100% ethanol. The solution was centrifuged at 13,000xg for 15 min at +4°C. The RNA sample was washed once with 70% ethanol and recentrifuged. The sample was evaporated at room temperature and suspended in sterile water. Precipitated RNA was transcribed into cDNA using a First strand cDNA Synthesis Kit #K1612 (Fermentas) according to the manufacturer's instructions.

The *DmBCA* gene was identified and amplified from cDNA by PCR using PhusionTM Hot Start High Fidelity DNA Polymerase (Finnzymes, Espoo, Finland). Sequence-specific primers were ordered from Sigma-Aldrich (St. Louis, MO). The forward primer was F1, and the reverse primer was R1. PCR was performed in a PTC 2000 thermal cycler (MJ Research, Waltham, MA), and the program consisted of a single 98°C denaturation step for 30 s, followed by 33 cycles of denaturation at 98°C for 10 s, annealing at 53°C for 15 s and extension at 72°C for 25 s. A final extension was performed at 72°C for 5 min. The PCR product band was separated from the gel and dissolved using Illustra™ GFX PCR DNA and GEL Band Purification Kit (GE Healthcare Life Sciences, Buckinghamshire, UK).

In the next step the *DmBCA* gene construct with a C-terminal polyhistidine tag of six histidines was constructed and cloned into the pFastBac1TM vector. The forward primer used in the initial amplification of the *DmBCA* gene was F2, and the reverse primer was R2. The latter primer contains nucleotide repeats to create the polyhistidine tag. The PCR program was as follows: 98°C for 60 s; then 35 cycles of 98°C for 10 s, 66°C for 15 s, and 72°C for 60 s; and finally 72°C for 5 min. The PCR product was run on an agarose gel, and the obtained band was purified.

The recombinant baculoviruses encoding the DmBCA recombinant protein was generated with the Bac-To-Bac® Baculovirus expression system (Invitrogen, Carlsbad, CA) according to the manufacturer´s instructions. pFastBacTM1 plasmid (Invitrogen) and the PCR product were digested at +37°C overnight with BamHI and XhoI restriction enzymes (New England Biolabs). The digested plasmid and DmBCA-polyhistidine construct were purified and ligated overnight at +4°C using T4 DNA ligase (New England Biolabs). The ligated product was transformed into TOP10 bacteria (Invitrogen). Overnight cultures (8 ml) were made from these colonies, and plasmids were purified using a QIAprep Spin Miniprep Kit™ (Qiagen, Hilden, Germany). Sequencing was performed to check the validity of the DmBCA-GFP construct. In the sequencing, the purified plasmid was used as a template. The sequencing was carried out using ABI PRISM Big Dye Terminator Cycle Sequencing Ready Reactions Kit version 3.1 (Applied Biosystems). The sequencing was performed in both directions using F1 and R1 primers described above. 1μL of purified plasmid was mixed with 4 μl of Big Dye mix, 4 μL of ddH2O and 1 μL of 1.6 μM primer. The reactions were performed in a PTC 2000 thermal cycler (MJ Research, Waltham, MA) according to the manufacturer's instructions. The products were purified by ethanol precipitation, resuspended in HiDi formamide (Applied Biosystems) and denatured according to the manufacturer's instructions. The sequencing was performed using an ABI PRISM Genetic Analyser instrument 9100 (Applied Biosystems).

The expression cassettes were transferred from the donor vector (pFastBac1) to the baculovirus genome by site-directed transposition. This was made by transforming DH10Bac cells that contain the baculovirus shuttle vector (bacmid) and helper plasmid that produces the proteins needed for the transposition, with the donor vector. Transformation was performed as follows: a streak of DH10Bac bacteria was suspended in 100μl of 100mM $CaCl_2$ and incubated on ice for 15min. After this, approximately 100ng of plasmid was added to the suspension, and the cells were incubated on ice for 30min. Heat shock was performed at 37ºC for 2min after which 450μl of SOC medium (Invitrogen) was added. The cells were grown at 37ºC for four hours in an orbital shaker. After this, the cells were centrifuged at 6000g (20ºC, 1min), resuspended to 100μl of SOC medium and spread on Luria-Bertani (LB) plates which were prepared according to the Bac-To-Bac® instructions. Recombinant bacmid selection and transfection of the insect cells were carried out according to the manufacturer´s instructions (Invitrogen).

Construction of recombinant baculoviruses for L. donovani chagasi β-CA

Total RNA of *L. donovani chagasi* homogenate was isolated using RNAeasy® Mini Kit (Qiagen) according to manufacturer´s instructions. However, 800µl of RLT-buffer was used instead of 600µl. DNAase treatment was performed after the isolation. The RNA was converted to cDNA using First Strand cDNA Synthesis Kit #K1612 (Fermentas) according to manufacturer´s instructions. The *β-CA* gene was retrieved from NCBI protein databases using Blast, http://blast.ncbi.nlm.nih.gov/Blast.cgi. In the primer design the sequence from *L. infantum* was used since *L. donovani* sequence was not available at the time of primer design. The full length *β-CA* gene was identified and amplified from cDNA by PCR using PhusionTM Hot Start High Fidelity DNA Polymerase (Finnzymes, Espoo, Finland). Sequence-specific primers were ordered from Sigma-Aldrich (St. Louis, MO). The forward primer was F3, and the reverse primer was R3. PCR was performed in a PTC 2000 thermal cycler (MJ Research, Waltham, MA), and the program consisted of a single 98°C denaturation step for 3 min, followed by 35 cycles of denaturation at 98°C for 10 s, annealing at 73°C for 30 s and extension at 72°C for 30 s. A final extension was performed at 72°C for 10 min. The PCR product band was separated from the gel and dissolved in the same manner as with DmBCA. Validity of the PCR product was verified by sequencing as described earlier, using primers F3 and R3.

For recombinant protein production the *LdcBCA* gene was constructed and cloned into the pFastBac1TM vector. The forward primer used in the initial amplification of the *β-CA* gene was F4, and the reverse primer was R4. The latter primer contains nucleotide repeats to create the C-terminal polyhistidine tag of six histidines. In addition, the forward primer contained the restriction site for EcoRI and the reverse primer for XhoI. The reverse primer also contained the nucleotide sequence encoding thrombin cleavage site. The PCR program was as follows: 98°C for 3 min; then 35 cycles of 98°C for 10 s, 62°C for 15 s, and 72°C for 30 s, and finally 72°C for 10 min.

The PCR product was run on an agarose gel, and the obtained band was purified. pFastBacTM1 plasmid (Invitrogen) and the PCR product were digested at +37°C overnight with EcoRI and XhoI restriction enzymes (New England Biolabs). The ligation and generation of recombinant baculoviruses were made in the same manner as described above for DmBCA.

Production and purification of recombinant D. melanogaster and L. donovani chagasi β-CA enzymes

The DmBCA producing Sf9 insect cells were grown in HyQ SFX-Insect serum-free cell culture medium (HyClone, Logan, UT) in an orbital shaker at 27°C (125 rpm) for three days after infection. Protein purification was performed after centrifugation (5000 x g, 20°C, 8 min) from the supernatant. Purification was performed using the Probond™ Purification System (Invitrogen) under native binding conditions, with wash and elution buffers made according to the manufacturer's instructions. The purification procedure per 500 ml of insect cell medium was as follows: 1 l of native binding buffer and 25 ml of the nickel-chelating resin were added to the medium, and the His-tagged protein was then allowed to bind to the resin on a magnetic stirrer at 25°C for 3 h. The resin was washed with 100 + 30 ml of washing buffer (Invitrogen). The protein was then eluted with elution buffer (50 mM NaH_2PO_4, 500 mM NaCl, 250 mM imidazole, pH 8.0).

The purified recombinant protein was transferred to a buffer of 50 mM Tris-HCl, pH 7.5, using an Amicon Ultracel™ - 10k centrifugal filter device (Millipore) according to the manufacturer's instructions. To remove the His tag, the recombinant protein was treated with 60 µl of resin-coupled thrombin (Thrombin CleanCleave KIT™, Sigma) per 1 mg of protein with gentle shaking at 25°C for 1 h, according to the manufacturer's instructions. Protein concentration was determined using the DC Protein Assay™ (Bio-Rad) with three different dilutions. Purified recombinant DmBCA proteins were analyzed using 10% sodium dodecyl sulfate polyacrylamide gel electrophoresis (SDS-PAGE) under reducing conditions. The gels were stained using the Colloidal Blue Staining Kit™ (Invitrogen).

The production and purification of LdcBCA was made from most parts in the same way than with DmBCA. Instead of Probond™ Purification System (Invitrogen), Protino® Ni-NTA Agarose (Macherey-Nagel) was used. The purification procedure per 400 ml of insect cell medium was as follows: 3 L of native binding buffer (50 mM NaH_2PO_4, 500 mM NaCl, pH 8.0) and 8 mL of the nickel-chelating agarose were added to the medium, and the His-tagged protein was then allowed to bind to the resin on a magnetic stirrer at 25°C for 3 h. The resin was washed with 40 + 20 mL of washing buffer (50 mM NaH_2PO_4, 500 mM NaCl, 20 mM imidazole pH 8.0). The protein was then eluted with elution buffer (50 mM NaH_2PO_4, 500 mM NaCl, 250 mM imidazole, pH 8.0). The purified recombinant protein was transferred to a buffer of 10 mM HEPES, pH 7.5, using an Vivaspin® Turbo 15 centrifugal filter device (Sartorius-Stedim) according to the manufacturer's instructions. During the purification the protein was tightly attached to the filter membrane after the His-tag removal. Because of this

unwanted property of the protein, we decided to use the uncleaved β-CA protein (containing polyhistidine tag) in the kinetic measurements.

4.1.2 Production of recombinant α-CAs using BL-21 cells

CAH1- and CAH2-GST-fusion protein constructs were designed for enzyme production in BL21(DE3)pLysS Competent Cells (Promega), and purification. Both constructs included BamHI and XhoI restriction sites. Total RNA extracted from *D. melanogaster* S2 cells was precipitated, purified and transcribed as described earlier. The cDNA obtained from total RNA was copied with PCR using Phusion™ Hot Start High Fidelity DNA Polymerase (Finnzymes, Espoo, Finland). For PCR, sequence specific primers for *CAH1* were ordered from Sigma-Aldrich. The forward primer was F5 and the reverse primer was R5. PCR was performed with PTC 2000 thermal cycler (MJ Research, Waltham, MA). The program consisted of a single 98 ºC denaturation step for 30 s, followed by 33 cycles of denaturation at 98 ºC for 10 s, annealing at 60 ºC for 15 s and extension at 72 ºC for 25 s, followed by a final extension at 72 ºC for 5 min. The band was separated from the gel and dissolved using Illustra™ GFX™ PCR DNA and GEL Band Purification Kit (GE Healthcare Life Sciences, Buckinghamshire, UK).

The obtained PCR product was used as a template in the next PCR reaction in which the forward primer was F6 and the reverse primer was R6. The PCR program used was identical to the one described above, except that annealing temperature was 70 ºC. pGEX-4T1 vector (Amersham Biosciences) and *CAH1* gene were digested overnight at +37 ºC. pGEX plasmid was run into gel and purified. pGEX-4T1 and *CAH1* were ligated at +4 ºC overnight using T4 DNA ligase (New England Biolabs). The Ligated pGEX-4T1 plasmid was transformed into BL-21(DE3)pLys Competent Cells (Promega) according to the manufacturer's instructions. Sequencing was performed to confirm the validity of product. Sequencing was made in the same way described with DmBCA but with F5 and R5 primers. Amino acids 1–269 were included in the construct (full length protein). The cloning of the *CAH2* gene was done exactly in the same way as with *CAH1*, except for the following parts. In the first PCR reaction the forward primer was F7 and the reverse primer was R7. The PCR program used was: a single 98 ºC denaturation step for 30 s, followed by 33 cycles of denaturation at 98 ºC for 10 s, annealing at 65 ºC for 15 s and extension at 72 ºC for 40 s, followed by a final extension at 72 ºC for 5 min. In the next PCR reaction the forward primer was F8 and the reverse primer was R8. Amino acids 30–286 were included. The proposed signal sequence and membrane anchor region were excluded from the construct.

Production and purification of recombinant CAH1 and CAH2 enzymes

For production of CAH1 and CAH2 proteins, *E. coli* bacteria were cultured in LB medium (5 ml) in the presence of ampicillin overnight. After 18 h, the culture media were diluted 100-fold and was grown at +37ºC until optical density at 600 nm was between 0.6 and 0.8. The expression of *CAH1* and *CAH2* were induced by 1 mM isopropyl β-D-thiogalactoside (IPTG) and the culturing was continued for an additional 3 h. After this, the bacterial cells were harvested by centrifugation. The purification protocol for 500 ml culture of bacterial cells was as follows: the bacterial cell pellet was lysed in 1x PBS containing 80 mg of lysozyme. The solution was incubated for 15 min on ice after which 20 µl (200 U) of DNAse was added. The solution was again incubated on ice for 15 min. The supernatant was gathered by centrifugation at 12 900 g for 15 min at +4 C. 530 µl of glutathione sepharose slurry (GST Bulk Kit, GE Healthcare) was added to the supernatant. The solution was incubated in gentle shaking for 30 min at room temperature. For separation of the glutathione sepharose beads, the solution was transferred to a column containing filter paper at the bottom. The column was washed four times with 1 ml of PBS. 20 µl (20 U) of thrombin (GE Healthcare) was added to 700 µl of PBS. The beads were gathered from column with this solution and incubated with gentle shaking for 1 h at room temperature. The solution was transferred to a column and the buffer containing the purified protein was collected followed by additional washes with 1400 µl of PBS. The fractions were analyzed by SDS–PAGE under reducing conditions using 10% acrylamide gels.

4.1.3 Studying subcellular localization of D. melanogaster β-CA enzyme

To construct the DmBCA-GFP recombinant protein, the sequences of *DmBCA* and *GFP* were first amplified separately using sequence specific primers, and the constructs were then combined using PCR reactions whose F9 and R9 primer sequences partly overlapped. This allowed the ends of the PCR products to recognize and bind each other. The forward primer used for *DmBCA* amplification was F2, and the reverse primer was R9. Part of the sequence was designed to recognize the thrombin site and part of the *GFP* PCR product, while the other half recognized the *DmBCA* PCR product. Original *DmBCA* gene product obtained from cDNA was used as a template.

The forward primer used for GFP amplification was F9, and the reverse primer was R10. Part of the sequence in the F9 primer was designed to recognize the thrombin site and part of the *DmBCA* PCR product, while the other half

recognized the *GFP* PCR product. For *GFP*, the pEGFP-N1™ Vector (Clontech) was used as a template, and the PCR program was as follows: 98°C for 2 min; then 33 cycles of 98°C for 10 s, 55°C for 15 s, and 72°C for 30 s; and finally 72°C for 7 min.

Both PCR products were run on agarose gel, purified and used as templates in the next PCR reaction. The PCR program was as follows: 98°C for 2 min; then 33 cycles of 98°C for 10 s, 55°C for 15 s and 72°C for 40 s; and finally 72°C for 8 min. The forward primer used in this PCR was F2, and the reverse primer was R10. The extra sequence overlaps at the 3' end of *DmBCA* and at the 5' end of the *GFP* allowed these PCR products to anneal with each other. Otherwise, the construct and recombinant baculovirus were generated essentially in the same way as the DmBCA-polyhistidine construct described above.

100 µl of Sf9 insect cells (2 million cells/ml) were infected with 10 µl of baculovirus stock. The cells were kept at +27C° in incubator for three days in Lab-Tek™ Chamber Slide™ System™ plates (Nunc). After this the medium was removed, and the cells were incubated in 600 µl of medium containing 100 nM Mitotracker Red CMXros™ (Invitrogen) at +27°C for 20 minutes. The cells were washed three times with 600 µl of medium and kept at +27°C in an incubator for an additional two hours. The cells were then washed with PBS, fixed with 4% paraformaldehyde for five minutes and then washed again with PBS. The cells were mounted in VectaShield® Mounting Medium (Vector Laboratories), covered with cover slips and analyzed using a confocal scanning laser microscope (Perkin Elmer-Cetus/Wallac UltraView LCI system™) with two different wavelengths: 488 nm for GFP detection and 579 nm for MitoTracker™. Image acquisition was performed with an Andor iXon™ DV885 EMCCD camera and the Andor iQ™ software (Andor).

Predictions of subcellular localization were performed usingTargetP v1.1 (http://www.cbs.dtu.dk/services/TargetP/), Secretome 2.0 (http://www.cbs.dtu.dk/services/SecretomeP/), WolF PSORT, (http://wolfpsort.org/) and MitoProt II v. 1.101 (http://ihg2.helmholtz-muenchen.de/ihg/mitoprot.html). Predictions of subcellular localization were made in collaboration with Dr. Martti Tolvanen.

4.1.4 Dynamic light scattering and gel filtration analysis

To find out the oligomerization state of *D. melanogaster* β-CA, a dynamic light scattering (DLS) and analytical gel filtration were performed. In DLS analysis, the hydrodynamic diameters were determined in temperature range 4 ºC to 37 ºC. The molecular weight of the enzyme was estimated from these values using globular

protein standard curve. Analytical gel filtration was used to support results from DLS. The studies were conducted in Dr. Vesa Hytönen´s laboratory, BioMediTech, University of Tampere, Finland. A detailed methodology can be found in (I).

4.2 Biological function of D. melanogaster β-CA

4.2.1 Generation of CAHβ knock-down flies

Two different *β-CA* RNAi lines were obtained from Vienna *Drosophila* RNAi Center (VDRC) from GD and KK collections with the following IDs: #100233 (called henceforth as *β-CA RNAi¹)* and #38612 (called henceforth as *β-CA RNAi²)* (Dietzl, Chen, Schnorrer, Su, Barinova, Fellner, Gasser, Kinsey, Oppel, Scheiblauer, Couto, Marra, Keleman, & Dickson, 2007). These stocks overexpress a dsRNA hairpin construct, which is specific for *β-CA* gene under *upstream activation sequence* (*UAS*) control. When these flies are crossed over with a GAL4 activator protein expressing line, *β-CA* gene is subsequently silenced in the tissue where GAL4 protein is expressed (Brand & Perrimon, 1993). For ubiquitous RNAi-mediated silencing, *CAHβ* RNAi lines were crossed over *Actin-GAL4* line or a Mifepristone-inducible *Geneswitch-tub5-GAL4* line (Fernandez-Ayala et al., 2009).

4.2.2 Survival and fertility studies with D. melanogaster

To study the effect of the *β-CA* gene knockdown to the survival rate of *D. melanogaster* flies, the *β-CA RNAi¹* and *β-CA RNAi²* lines were crossed over *GS-tub-GAL4*. *β-CA RNAi¹/ GS-tub-GAL4* flies and *β-CA RNAi²/ GS-tub-GAL4* flies were collected and grown in food vials containing 400 μM Mifepristone (Mif, RU-486) for 15 days. Flies from the same crosses were collected and used as controls by growing them in food vials without Mif. The number of dead flies was counted daily.

To study the fertility of D. melanogaster β-CA knockdown flies, the *β-CA RNAi1/GS-tub-GAL4* and *β-CA RNAi2/GS-tub-GAL4* eclosed flies were collected and placed at +29ºC in normal food (control) or food containing 400 μM Mif (*β-CA* RNAi induced) for six days. *w1118* control flies were kept in the same

conditions. Thereafter the flies were mated with flies from the same cross or with *w1118* control flies, in different combinations. Fertility was followed up to 15 days.

Additionally, the possible reversibility of fly fertility was studied by providing normal food to the previously mentioned flies after 6 days. The flies were put into new vials daily to find out when their fertility was restored.

4.2.3 Examination of D. melanogaster ovaries

One to two-day old female *β-CA RNAi1/GS-tub-GAL4* and *β-CA RNAi2/GS-tub-GAL4* F1 flies were placed at +29ºC in normal food (control) or food containing 400 μM Mifepristone *β-CA* RNAi induced) for six days. Flies were moved to fresh food with or without Mif every two days. On fourth day, male *Oregon R* flies were added to induce the egg production of the females. On the 6th day, the knock down and control females were anesthetized on a CO_2 pad and the ovaries were dissected using a pair of forceps.

The dissected ovaries were transferred in 0.5 ml tubes containing phosphate-buffered saline (PBS), fixed using 4% paraformaldehyde (PFA) for 20 min at +4ºC and rinsed 2x with PBS containing 0.3% Triton X-100 (PBT). Ovaries were washed 2x 15 min in PBT containing 0.5% bovine serum albumin (BSA), incubated overnight with the DCAD2 primary antibody (Developmental Studies Hybridoma Bank, Iowa, USA, 1:20) in PBT-BSA, rinsed 2x with PBT and washed again 2 x 15 min in PBT-BSA. Incubation with the secondary Goat anti-rat antibody (AlexaFluor 488 conjugate, Life Technologies, 1:1000) in PBT-BSA was carried out for 2h at RT. Ovaries were rinsed again 2x in PBT and washed 3x 15 min in PBT. DAPI (final conc. 1 μg/ml, Sigma) was added to the second last wash. After the final wash, ovaries were placed in 70% glycerol for at least 30 min at +4ºC, and then transferred in Vectashield Mounting medium (Vector Laboratories).

Prior to microscopy, the ovaries were placed on microscope slides. The egg chambers were separated using a needle and the samples mounted and sealed using cover slips and nail varnish. Ovaries were examined and imaged using the Zeiss LSM 780 confocal microscope with 20x objective. Images were snap-shots of the focal plane of each developing oocyte where border cells are visible.

4.2.4 qRT-PCR

β-CA RNAi lines were crossed over the *GS-tub-GAL4* line and the eclosed F1 generation progeny was grown for 6 days at +29ºC in food with 400 μM Mif (knockdown flies) or without Mif (control flies). The flies were transferred into

new vials once during the period. RNA extractions were made as triplicates: for each line, 3 x 3-5 females and males were used. RNA extraction was done using TRI Reagent® Solution (Ambion), according to manufacturer´s instructions. The purity and amount of purified RNA were measured using NanoDrop 1000 (Thermo Scientific).

qRT-PCR was performed from the abovementioned extracted total RNAs to quantify the level of gene silencing. Also *GS-tub-GAL4* were tested in qRT-PCR to test the possible leakiness of the tubulin driver. PCR reactions were performed in MicroAmp optical 96-well reaction plates using a SYBR-Green PCR master mix kit (Applied Biosystems) according to the manufacturer's instructions. Primers for qRT-PCR were designed using Primer Express Software v2.0 (Applied Biosystems). Forward primer (F1) used in the reaction was 5´-GACAAGGGAGCAAATGGTCAA-3´ and reverse primer (R1) was 5´-TCTACTGTCCATGCAGGTGAAGAA-3´. The reaction was carried out in ABI PRISM 7000 Detection System (Applied Biosystems). The data were analyzed with ABI PRISM 7000 SDS software and normalized to the *RPL32* housekeeping gene. Forward primer (F2) used for *RPL32* was 5´-GGTTACGGATCGAACAAGCG-3´ and reverse primer (R2) was 5´-TTCTGCATGAGCAGGACCTC-3´. The final results were expressed as the N-fold difference in the gene expression between the knock-down and control samples as described in (Pfaffl, 2001).

4.2.5 Measurement of mitochondrial oxygen consumption by High-resolution respirometry

Studies were made to measure mitochondrial oxygen consumption by High-resolution respirometry. Whole fly homogenates from twenty *β-CA RNAi1/GS-tub-GAL4* and *β-CA RNAi2/GS-tub-GAL4,* grown with or without Mif for six days, were used for these measurements. Studies were carried out at research group of Dr. Alberto Sanz. Detailed description of methodology can be found in (IV).

4.3 Bioinformatic studies

Bioinformatic studies of *D. melanogaster* were performed by Dr. Martti Tolvanen, University of Turku, Finland. Bioinformatic studies related to *L. donovani chagasi* were performed by Dr. Clemente Capasso, Istituto di Biochimica delle Proteine−CNR, Napoli, Italy. Sequences were retrieved from NCBI protein database and other databases. Sequence alignments were performed to study the conservation of active residues and other key residues. Furthermore, phylogenetic

trees were constructed to show the evolutionary distances between CAs from different organisms. Detailed methodology for bioinformatics of *D. melanogaster* CA sequences can be found in (I) and (II). Methodology related to bioinformatics of *L. donovani chagasi* can be found in (III).

4.4 Catalytic activity and inhibition studies

Kinetic measurements in I, II and III have been made by professor Claudiu Supuran´s research group (University of Florence, Italy).

An Applied Photophysics stopped-flow instrument was used to assay the CA-catalyzed CO_2 hydration activity. Phenol red at a concentration of 0.2 mM was used as an indicator, working at the absorbance maximum of 557 nm, with 10 – 20 mM HEPES (pH 7.5) or Tris (pH 8.3) as buffers and 20 mM Na_2SO_4 or 20 mM $NaClO_4$, following the initial rates of the CA-catalyzed CO_2 hydration reaction for a period of 10 – 100 s. The CO_2 concentrations ranged from 1.7 to 17 mM for the determination of kinetic parameters and inhibition constants. For each inhibitor at least six traces of the initial 5-10% of the reaction were used to determine the initial velocity. The uncatalyzed rates were determined in the same manner and subtracted from the total observed rates. Stock solutions of inhibitors (100 mM) were prepared in distilled-deionized water, and dilutions up to 0.01 μM were made thereafter with distilled-deionized water. Inhibitor and enzyme solutions were preincubated together for 15 min at room temperature prior to the assay to allow for the formation of the enzyme-inhibitor complex. The inhibition constants were obtained by non-linear least-squares methods using PRISM 3, whereas the kinetic parameters for the uninhibited enzymes were obtained from Lineweaver-Burk plots, each representing the mean of at least three different determinations.

In vivo anti-leishmanial studies were performed by Dr. Alane Beatriz Vermelho´s research group (University of Rio de Janeiro, Brazil). In these studies, some thiol CA-inhibitors were tested against promastigote forms of two *Leishmania* species, *L. chagasi* and *L. amazonensis*. Minimum inhibitory concentrations and anti-leishmanial activity were determined. Ultrastructural analysis was performed with transmission electron microscopy. Detailed experimental procedures can be found in III.

5. Results

5.1 Production and purification of recombinant α- and β-CAs

The relative molecular masses of the purified recombinant proteins were estimated from the SDS-PAGE (Figure 5). DmBCA appeared as 28 and 27 kDa polypeptide bands before and after thrombin treatment, respectively. According to DLS analysis, average molecular weight of DmBCA was 48.9 kDa which was based on hydrodynamic diameters obtained. In analytical gel filtration the molecular weight estimate was 38.1 kDa. However, it was found that gel filtration seems to underestimate the molecular weight of CAs. Based on these studies it was concluded that DmBCA is a dimer.

In case of LdcBCA the molecular mass of the enzyme was around 35 kDa before the removal of the polyhistidine tag. SDS-PAGE showed that LdcCA appeared as three distinct bands. Therefore, an electrophoretically separated protein sample was analysed by mass spectrophotometry in the Protein Chemistry Unit of the University of Helsinki and subsequently the proteins were identified. All three bands proved to represent LdcCA.

In the cases of CAH1 and CAH2, the molecular masses were approximately 30 and 28 kDa before and after the removal of the GST purification tags, respectively.

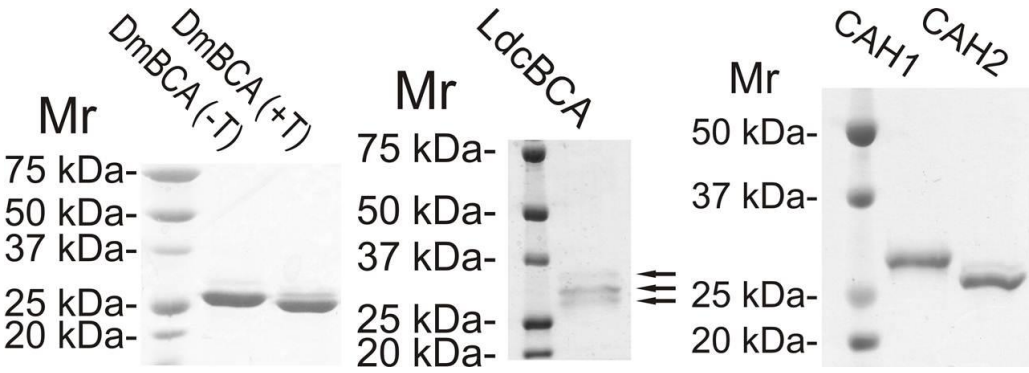

Figure 5. **SDS-PAGE results from protein purifications.** DmBCA = *D. melanogaster* β-CA, LdcBCA = *L. donovani chagasi* β-CA, CAH1 = *D. melanogaster* CAH1, CAH2 = *D. melanogaster* CAH2. Mr = relative molecular mass, +T = after thrombin treatment, -T = no thrombin treatment.

5.2 Subcellular localization of D. melanogaster β-CA

38 complete animal β-CA sequences were analyzed for subcellular targeting with TargetP. 22 sequences were predicted to be mitochondrial with low reliability. Most of the remaining sequences were predicted to be cytoplasmic, again with low reliability. The results from WolF PSORT, Secretome 2.0 and MitoProt II v. 1.101 also supported the fact that DmBCA is probably a mitochondrial enzyme, with a possibility for non-classical secretion (without a signal peptide) suggested by Secretome 2.0. A mitochondrial targeting N-terminal signal sequence was also predicted. Length of the signal sequence varied from 14 in MitoProt to 49 in TargetP. Based on these findings made with the prediction tools, a DmBCA-GFP construct was designed to study the subcellular localization of the protein in Sf9 cells.

According to the experiments on DmBCA-GFP fusion protein, DmBCA is a mitochondrial protein, supporting the bioinformatic predictions. Figure 6A shows the DmBCA-GFP recombinant protein in Sf9 insect cells. The positive signal was located in intracellular granular structures. Fig. 6B shows the same cells labeled with a mitochondrial marker, MitoTracker Red CMXros™. In panel C, the previous images have been combined, showing the colocalization of DmBCA-GFP and MitoTracker Red CMXros™ in mitochondria.

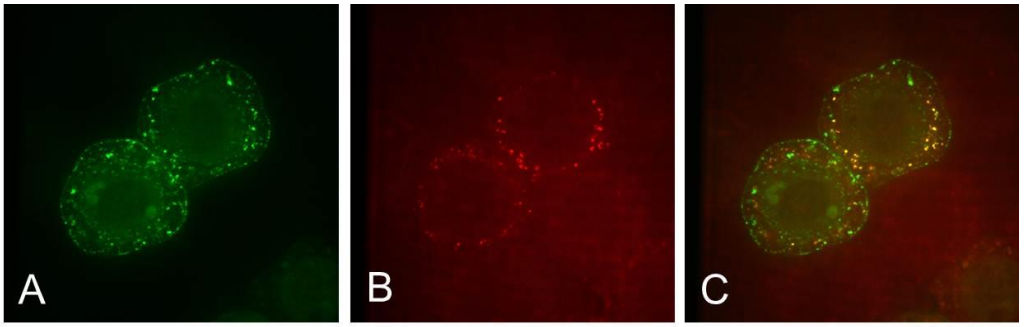

Figure 6. Double immunofluorescence staining of DmBCA-GFP and mitochondria in Sf9 cells. Green fluorescent signal indicates the localization of DmBCA fusion protein (A), red color labels the mitochondria (B), yellow color in panel C indicates colocalization of these labels.

5.3 Bioinformatic studies on α- and β-CAs

β-CAs were found in all complete non-chordate animal genomes. Multiple sequence alignment of all animal β-CAs showed perfect conservation of the known active site motifs CxDxR and HxxC and several other key residues. The phylogenetic tree indicated that the duplication of *β-CA* genes in nematodes is specific for the nematode lineage. Other invertebrates seemed to encode for one β-CA. No β-CA sequences existed in vertebrate genomes, but the possible existence in chordates remained somewhat unclear. All of the complete β-CA sequences were classified as β-CA domains of type "BCA_CladeB" in the NCBI Conserved Domain Database. Because all plant β-CAs were also classified as BCA_CladeB domains, animal β-CAs can well be said to represent "plant-type β-CAs".

β-CA expression levels in 17 adult and 8 larval *D. melanogaster* tissues can be found in FlyAtlas (http://flyatlas.org/atlas.cgi?name=CG11967-RA). The highest upregulated values in adult are found in spermatheca (female), fat body, and heart. In larval tissues (third instar) downregulated or average expression levels are seen for all tissues. A time-course study published in FlyBase (http://flybase.org/reports/FBgn0037646.html) shows upregulated expression of DmBCA in early larval stages and late in metamorphosis, but downregulated levels in embryonal, late larval, early metamorphosis, and adult stages. This may indicate relevant roles for β-CA enzyme.

In total, there are one β-CA, nine α-CAs, and as many as five CARPs in *D. melanogaster* genome (Ortutay, Olatubosun, Parkkila, Vihinen, & Tolvanen, 2010). The phylogenetic analysis indicated that CAH1 and the mammalian cytoplasmic isozymes share a common ancestor, whereas CAH2 has descended from the same common ancestor as the mammalian extracellular isozymes. Sequence identities suggested that CAH1 is the more strongly conserved of the two analyzed *Drosophila* CA isozymes. The predicted localizations conform with the phylogenetic results in that CAH1 is expressed in the cytoplasm, and CAH2 is an extracellular, membrane-attached isozyme. Based on high-throughput expression studies reported in Fly-Base, *CAH1* has the highest expression levels and widest expression pattern of all CA isozymes in *D. melanogaster*. *CAH1* expression is highest in the salivary gland, midgut and hindgut in both larva and adult, and in larval trachea. Slightly lower (but still very high) levels are observed in adult head, eye, brain, and thoracic-abdominal ganglion, and larval central nervous system. Out of all measured tissues, *CAH1* expression is low or absent only in the ovary, testis, and male accessory gland. During development, *CAH1* transcription is high or very high from late embryo to white prepupae (12 h) and again high from late pupa to all of the adult forms, being low only in early embryo (up to 16 h) and in mid-metamorphosis. *CAH2* has very high or high expression in the larval hindgut and trachea, and in adult salivary gland, midgut and Malpighian tubules. Contrary to *CAH1, CAH2* has a low or no expression in nerve tissues or reproductive tissues. In developmental time course there is a notable peak at hatching, with very high expression from 18 to 20 h embryo to larva L2. Interestingly, *CAH2* is also upregulated in the adult fly eye.

5.4 Kinetic properties of studied α- and β-CAs

All of the studied enzymes were shown to be highly active (Table 3). k_{cat} and k_{cat}/K_m values were compared to two common human α-CAs CA I and II.

Table 3. **Catalytic activities of the studied enzymes and their inhibition constants against acetazolamide. hCA I and II were used for comparison.**

enzyme	k_{cat} (s^{-1})	k_{cat}/K_m ($M^{-1}s^{-1}$)	K_I (acetazolamide) (nM)
hCAI	2.00×10^5	5.00×10^7	250
hCAII	1.40×10^6	1.50×10^8	12
DmBCA	9.5×10^5	1.1×10^8	49
LdcBCA	9.35×10^5	5.9×10^7	91.7
CAH1	6.4×10^5	1.2×10^8	106
CAH2	6.0×10^5	1.0×10^8	78

5.5 Biological function of β-CAs

5.5.1 Ubiquitous silencing of β-CA causes lethality in Drosophila during development

Crossing two independent *β-CA* RNAi lines *β-CA RNAi¹* and *β-CA RNAi²*, over ubiquitous *ActGAL4 / CyOy+* flies did not produce any viable progeny of the right phenotype, which indicates that silencing of *β-CA* is lethal during fly development. In order to analyze the significance of *β-CA* expression for adult *Drosophila* flies, the inducible *GeneSwitch-tubulin-GAL4 (GS-tub-GAL4)* driver line was used for *β-CA* silencing. The Gene Switch system allows selective expression of the hairpin construct in adults after addition of the inducing agent, Mif, in the fly food. At first, the efficacy of gene silencing in *β-CA RNAi¹* and *β-CA RNAi²* flies crossed over *GS-tub-GAL4* and following addition of Mif, was analyzed using qRT-PCR. Both RNAi lines showed effective silencing as shown in Figure 7. In *β-CA RNAi¹* males the level of gene expression was 35±6% from that of control males without Mif induction, and in females 69±16% when compared to control females without induction. With *β-CA RNAi² / GS-tub-GAL4* flies the values were 39±8% and 65±4%. These data indicated that Mif induced RNAi can be used to analyze the importance of *β-CA* expression in adult flies, and the gene silencing was more efficient in male flies.

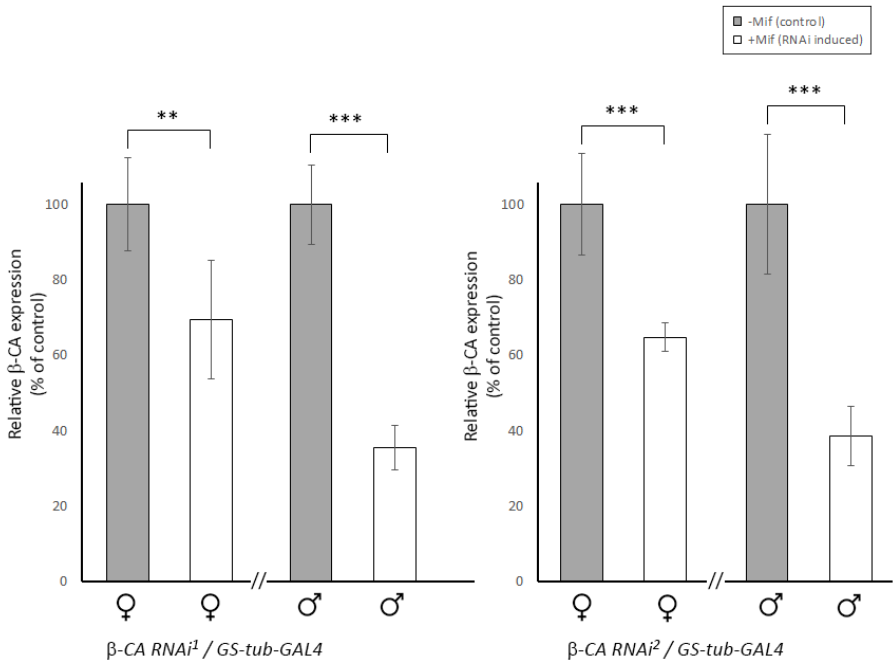

Figure 7. β-CA gene expression level is reduced in RNAi knockdown flies (+Mif) compared to control flies (-Mif). *β-CA* RNAi lines were crossed over the *GS-tub-GAL4* line and the eclosed F1 generation progeny was grown for 6 days at +29ºC in food with Mif (knockdown flies, +Mif) or without Mif (control flies, -Mif). Total RNA was extracted from 3 x 3-5 females and males of the lines indicated. Results are shown as % of expression of the control lines, which were normalized to 100% each. ** = $p < 0.01$, *** = $p < 0.001$.

5.5.2 D. melanogaster survival and fertility studies

To evaluate whether β-CA expression is required for survival of adult flies, *β-CA* RNAi flies were crossed over *GS-tub-GAL4* flies and the progeny was monitored for survival after introduction to a Mif-containing diet. After 15 days follow-up, there were no statistically significant differences between β-CA knockdown flies and controls: 90% of β-CA *RNAi¹ / GS-tub-GAL4* F1 progeny flies were alive, while the percentage of live flies was 96% in the control group. From *β-CA RNAi² / GS-tub-GAL4* group the values were 92% and 93%, respectively (Figure 7). Thus, *β-CA* expression is not required for viability of the flies.

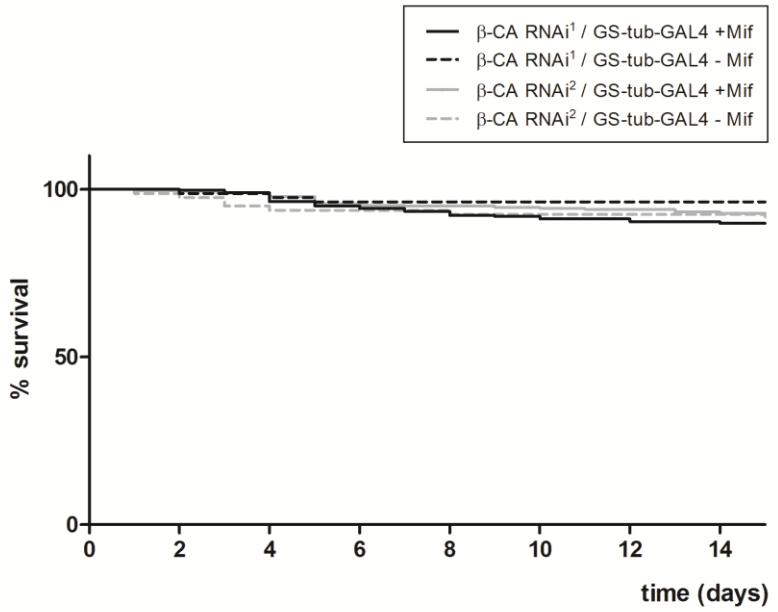

Figure 8. Fly survival is not impaired upon knockdown of β-CA expression. *β-CA RNAi*^{1} and *β-CA RNAi*^{2} lines were crossed over *GS-tub-GAL4*. *β-CA RNAi*^{1}*/ GS-tub-GAL4* flies (n = 385) and *β-CA RNAi*^{2}*/ GS-tub-GAL4* flies (n = 504) were collected and grown in food vials containing 400 µM Mif for 15 days. Flies from the same crosses were collected and used as controls by growing them in food vials without Mif (n = 81 and n = 80, respectively). The number of dead flies was recorded daily.

In fertility studies it was noted that the egg laying capacity of *β-CA* RNAi females was severely reduced. For example, in one experiment performed, 50 female knock-down flies were kept together with 30 wild type males, and flies did not lay a single egg in four days. On the other hand, larvae and adult flies were found in all other cross combinations (Table 4), namely combinations that did not include *β-CA* RNAi females. In vials containing wild type females and β-CA RNAi males, adult flies eclosed. This result implicated that β-CA has an essential function for female fertility in *Drosophila*. However, fertility of female flies was restored already on the second day after transferring the flies into normal food. Thus, the effect of β-CA knockdown on fertility was reversible.

Table 4. Fly fertility is severely reduced in crosses where β-CA is knocked down in females. Both *β-CA RNAi[1]/ GS-tub-GAL4* and *β-CA RNAi[2]/ GS-tub-GAL4* flies were used in the studies, with identical results. + = tens or hundreds found daily, (+) = 0-5 found daily, - = none found.

Cross		Eggs		Larvae		Pupae		Adult flies	
female	male	normal food	400μM Mif	normal food	400μM Mif	normal food	400μM Mif	normal food	400μM Mif
wildtype	wildtype	+	+	+	+	+	+	+	+
RNAi	wildtype	+	(+)	+	-	+	-	+	-
wildtype	RNAi	+	+	+	+	+	+	+	+
RNAi	RNAi	+	(+)	+	-	+	-	+	-

5.5.3 Examination of the D. melanogaster ovaries

After discovering that silencing of *β-CA* causes female sterility by almost completely abolishing the egg laying capacity, we hypothesized that *β-CA* knockdown might cause a functional defect in the ovaries. To study this hypothesis, we exposed the one to two-day old *β-CA RNAi[1]/GS-tub-GAL4* and *β-CA RNAi[2]/GS-tub-GAL4* female flies to a Mif-containing diet in order to silence *β-CA* expression. Flies from the same crosses without Mif were used as controls. At day four, flies were exposed to males to facilitate egg production and after 6 days, ovaries from *β-CA RNAi/GS-tub-GAL4* knockdown and control flies were dissected.

Ovaries were immunostained with DCAD2 antibody and observed under Carl Zeiss LSM 780 confocal microscope. DCAD2 antibody stains DE-cadherin in border cells. These, in turn, are a group of somatic cells that migrate at stage 9 during *Drosophila* oogenesis. Border cells arise and detach from the monolayer follicular epithelium, and subsequently invade and migrate between the nurse cells towards the oocyte. Representative images of developing oocytes in *β-CA* knockdown (+Mif) and control (-Mif) ovaries are shown in Figure 9. The results clearly indicate that border cell migration was delayed in *β-CA* knockdown cells compared to controls. At stage 10, border cells reached the edge of the developing oocyte in controls, but in the knockdown ovaries the border cells were still on their

way, located between the nurse cells. Although stronger in the *β-CA RNAi*^{1} line, the phenotype was visible with both RNAi lines. We conclude that silencing *β-CA* expression in *Drosophila* females causes delayed border cell migration during oogenesis, which contributes to the sterility of the female *β-CA* knockdown flies.

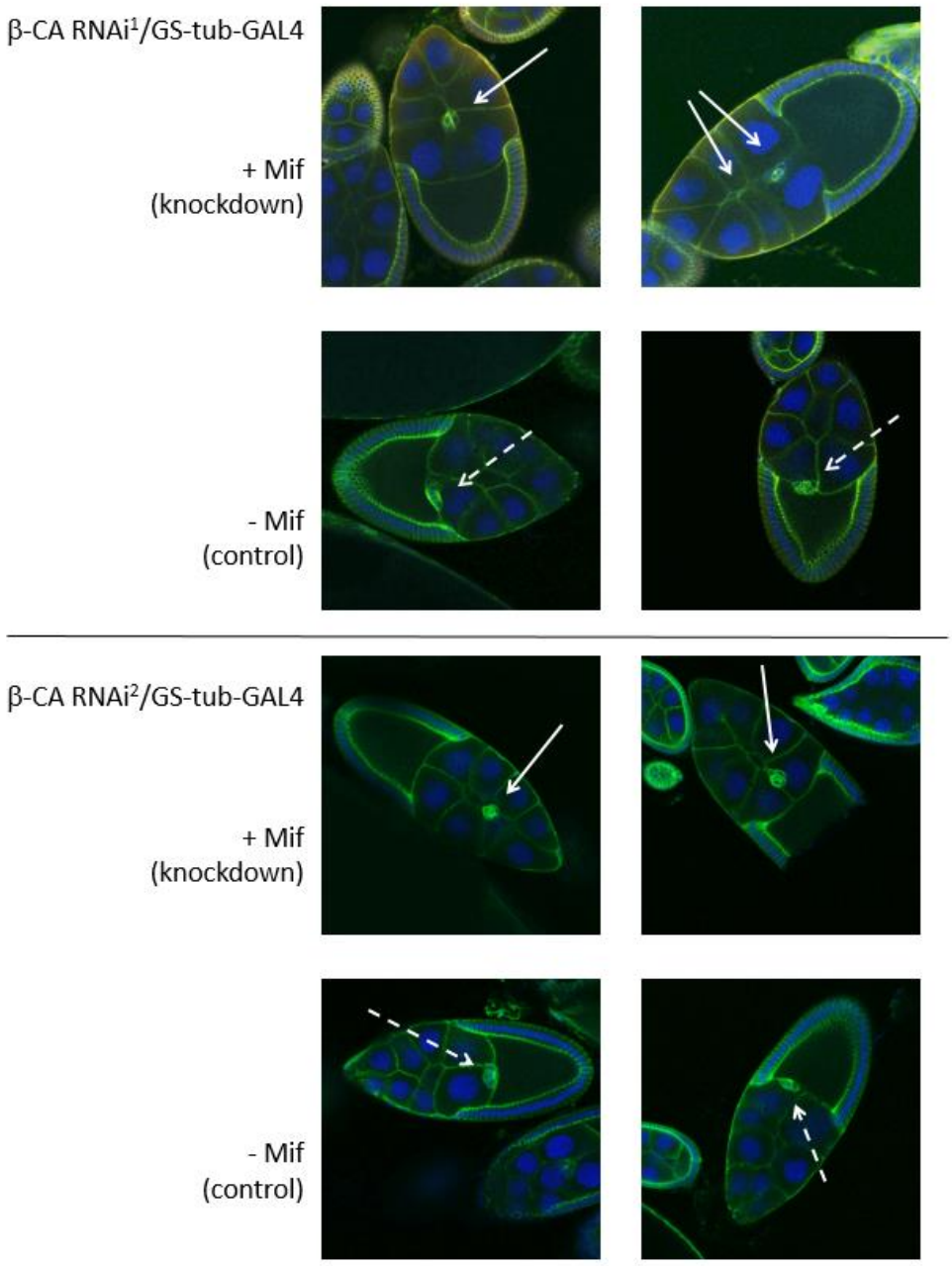

Figure 9. RNAi-mediated silencing of β-CA expression causes delayed border cell migration in *Drosophila* oogenesis. Migration of DCAD2-labeled border cells towards the developing oocyte is delayed upon *β-CA* knockdown (white arrows) compared to controls (dashed white arrows).

5.5.4 Measurement of mitochondrial oxygen consumption by High-resolution respirometry

With resolution respirometry (Kemppainen et al., 2014) it was measured if knockdown of the *β-CA* gene affects mitochondrial respiration. No significant differences using complex I- (pyruvate+proline), complex III- (sn-glycerol-3-phosphate) or complex IV-linked (ascorbate+TMPD) substrates in the presence of ADP were seen. In addition, mitochondrial density was not altered by *β-CA* RNAi. This further supports the fact that knockdown of *β-CA* is not affecting mitochondrial respiration since mitochondrial biogenesis is associated with disruption in the electron transport chain (Stefanatos et al., 2012). In conclusion, ubiquitous silencing of the *β-CA* gene in adult flies did not affect the mitochondrial oxygen consumption.

5.5.5 In vivo studies with Leishmania parasites

Inhibitory effects of different CA inhibitors (Charts 1-3) were tested on two *Leishmania* species, *L. chagasi and L. amazonensis* promastigotes.

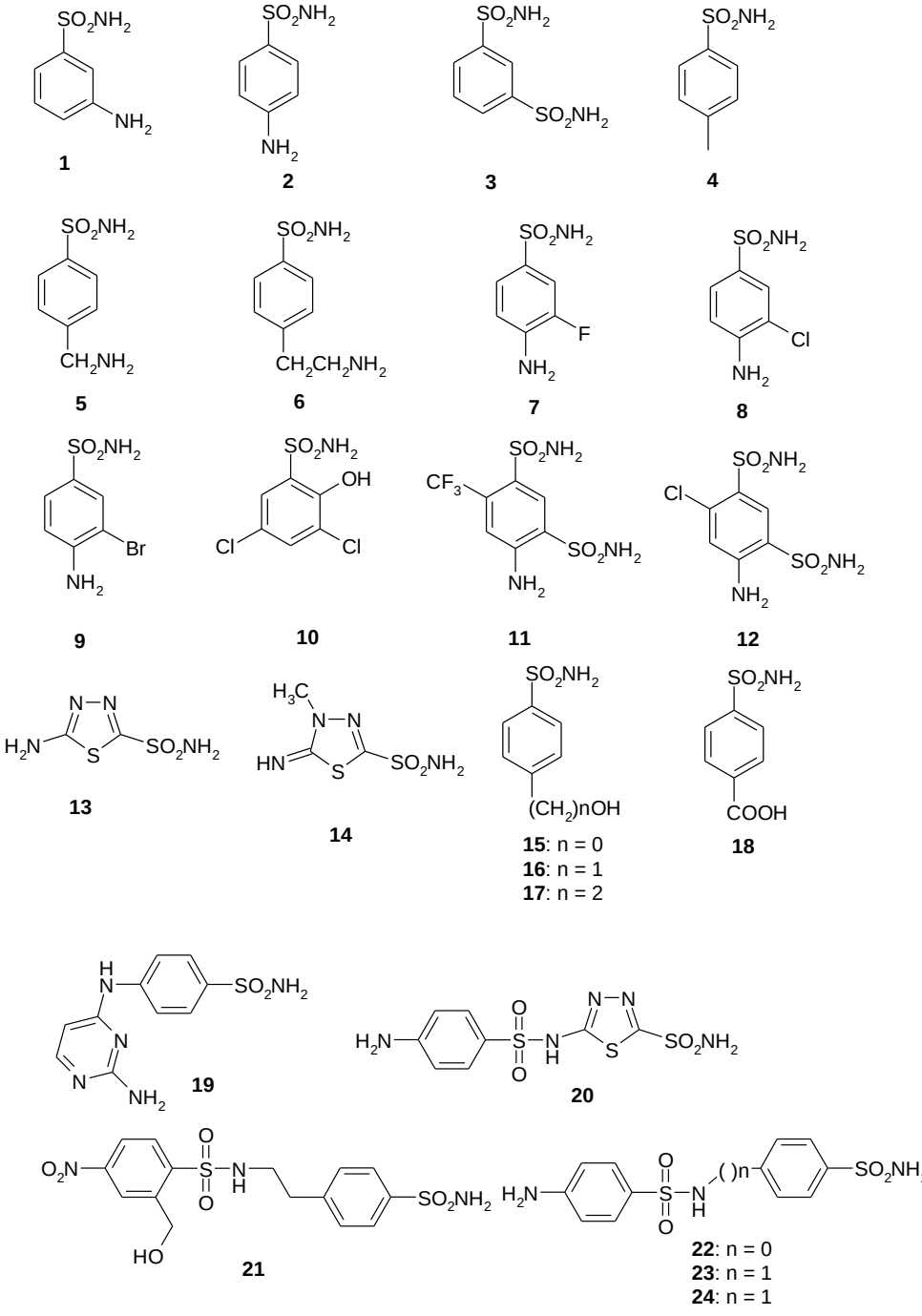

Chart 1. See a more detailed description in (III).

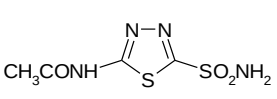

AAZ

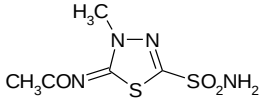

MZA

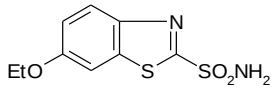

EZA

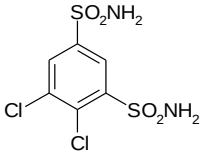

DCP

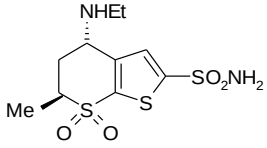

DZA

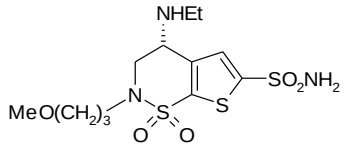

BRZ

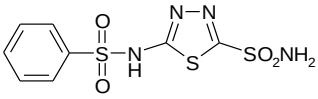

BZA

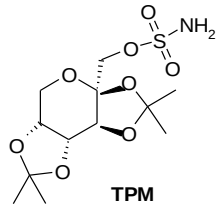

TPM

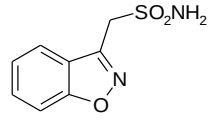

ZNS

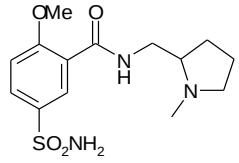

SLP

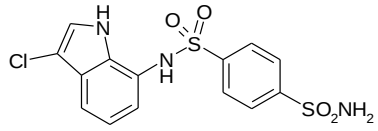

IND

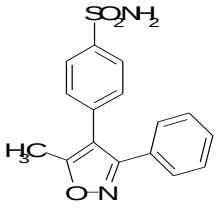

VLX

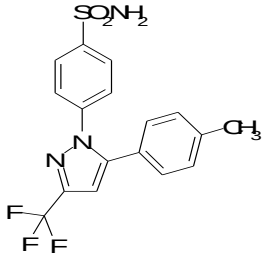

CLX

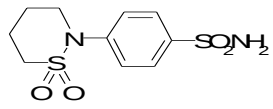

SLT

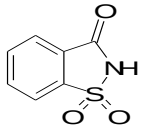

SAC

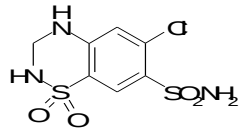

HCT

Chart 2. See a more detailed description in (III).

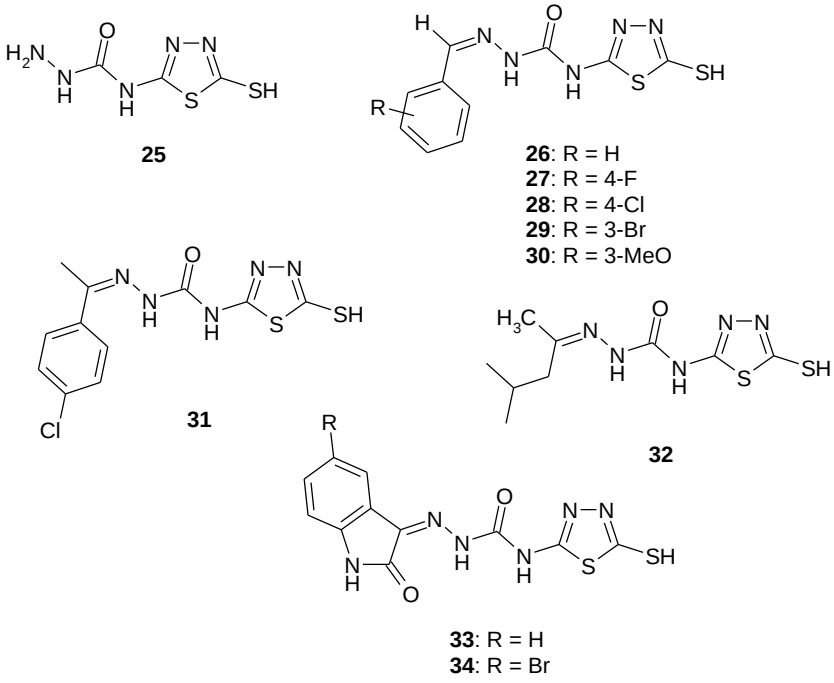

Chart 3. See a more detailed description in (III).

After 120 h treatment, some compounds exhibited a significant antileishmanial activity at concentrations of 256 μM (Tables 5 and 6). The best result was obtained with 1,3,4-thiadiazole-5-mercaptosemicarbazone derivative 29, which demonstrated an inhibition of growth of both *L. chagasi* and *L. amazonensis* in the range of 97 – 100 %. Only this compound was able to completely abrogate *Leishmania* growth, with a minimum inhibitory concentration (MIC) of 256 μM. When parasites were treated with this compound and concentration, and were subsequently reincubated in fresh medium, they were no longer able to grow. Also photomicrographs of *L. chagasi* treated with the compound 29 were obtained. After 24 h treatment with the compound, some morphological alterations of the parasites were observed. They included electron-dense granules in the cytoplasm and the presence of many cytoplasmic vesicles. An increase in flagellar pocket size was also noted in most of the treated parasites. In addition, some photomicrographs showed autophagic vacuoles indicative of cell degradation.

Table 5. Inhibition of human isoforms hCA I and hCA II, as well as the protozoan CAs from *T. cruzi* (TcCA) and *L. donovani chagasi* (LdcCA) with sulfonamides 1-24 and the clinically used agents AAZ – HCT. For more details, see table 2 and text in (III)

Inhibitor	KI (nM)			
	hCA I	hCA II	TcCA	LdcCA
1	28000	300	25460	5960
2	25000	240	57300	9251
3	79	8	63800	8910
4	78500	320	44200	> 100,000
5	25000	170	7231	> 100,000
6	21000	160	9238	> 100,000
7	8300	60	8130	15600
8	9800	110	6925	9058
9	6500	40	8520	8420
10	7300	54	9433	9135
11	5800	63	842	9083
12	8400	75	820	4819
13	8600	60	534	584
14	9300	19	652	433
15	5500	80	73880	927
16	9500	94	71850	389
17	21000	125	66750	227
18	164	46	84000	59.6
19	109	33	810	> 100,000
20	6	2	88.5	95.1
21	69	11	134	50.2
22	164	46	365	136
23	109	33	243	87.1
24	95	30	192	73.4
AAZ	250	12	61.6	91.7
MZA	50	14	74.9	87.1
EZA	25	8	88.2	51.5
DCP	1200	38	128	189
DZA	50000	9	92.9	806
BRZ	45000	3	87.3	764
BZA	15	9	93.6	236
TPM	250	10	85.5	> 100,000
ZNS	56	35	867	> 100,000

Table 5 (continued).

SLP	1200	40	87.9	> 100,000
IND	31	15	84.5	316
VLX	54000	43	82.7	338
CLX	50000	21	91.1	705
SLT	374	9	71.9	834
SAC	18540	5959	8210	> 100,000
HCT	328	290	134	50.2

Table 6. hCA I, hCA II and LdcCA inhibition data with thiols 25-34, and anti-leishmanial *in vivo* data with some of these derivatives. Promastigote forms of *L. chagasi* and *L. amazonensis* Raimundo strains have been use for the in vivo experiments. Concentrations of test compounds ranging from 2 to 256 μM were used. For more details, see table 2 and text in (III).

Compound	**KI (nM)**			**% Inhibition of growth**	
	hCA I	**hCA II**	**LdcCA**	**L. chagasi**	**L. amazonensis**
25	7100	9200	74.1	nt	nt
26	3000	354000	27.9	36.3	45.8
27	30770	3830	33.1	18	56
28	18740	13460	18.4	51.5	62.3
29	71600	235000	13.4	100	97
30	8540	2670	40.1	32.2	76.4
31	144000	3890	95.3	0	7
32	8530	8850	19.5	74.8	91.9
33	7890	8360	144	0	0
34	3710	7970	152	0	0

6. Discussion

6.1 Invertebrate β-CAs are dimeric mitochondrial enzymes

Our experiments made with DLS, analytical gel filtration and DmBCA-GFP fusion protein showed that *D. melanogaster* β-CA is a dimeric, mitochondrial protein, a finding which was also supported by bioinformatic predictions. A recently published study also suggested that invertebrate β-CAs are mitochondrial proteins (Zolfaghari Emameh, Barker, Tolvanen, Ortutay, & Parkkila, 2014). It can be speculated that either the animal *β-CA* gene in chordates might have been silenced or lost after a mitochondrial α-CA emerged and subsequently substituted the CA function in mitochondria; or that CA V acquired an exon to code for a mitochondrial targeting peptide after β-CA was lost.

In mammals, the roles of mitochondrial CAs have been linked to important metabolic functions like gluconeogenesis, ureagenesis, and lipogenesis (Hazen, Waheed, Sly, LaNoue, & Lynch, 1996; Sly & Hu, 1995). In a recent study, effects of targeted mutagenesis were tested in both CA VA and VB deficient mice (Shah et al., 2013). CA VA null mice were smaller than wild-types and bred poorly. However, when sodium–potassium citrate-supplemented water was given, the production of offspring was normal. Their blood ammonia concentrations were elevated, but fasting blood sugars were normal. On the other hand, CA VB null mice showed normal growth, normal blood ammonia levels as well as normal fasting blood sugars. CA VA/B double-knockout (DKO) mice showed additional abnormalities. Impairment of growth and hyperammonemia were more severe than for CA VA null mice. DKO animals were produced in less-than-predicted numbers even when supplemented with sodium-potassium citrate in their drinking water. Survival after weaning was also reduced, especially for males. Additionally, fasting blood glucose levels for DKO mice were significantly lower compared to controls. Clearly, these enzyme deficiencies on mice (and probably other vertebrates) are not lethal but cause significant metabolic problems and also have effect on breeding. Even though a period in evolution when animals did not have any mitochondrial CA is quite feasible, the order of the loss of β-CA and acquisition of mitochondrial CA V cannot be determined by current information.

Most of the β-CAs described so far are tetramers. To date, 14 β-CA crystal structures have been reported (Lehneck et al., 2014; Rowlett, 2014). Of these, two show octameric quaternary structure and 11 are tetramers. *Methanobacterium thermoautotrophicum* β-CA forms dimeric crystals (Strop et al., 2001), but there is also some evidence that this enzyme actually exists in solution as a tetramer (Smith & Ferry, 1999; Smith et al., 2000). The only truly dimeric enzyme characterized so far is *Mycobacterium tuberculosis* β-CA (Suarez Covarrubias et al., 2005). However, the thiocyanate complex of this enzyme crystallizes as a dimer-of-dimers homotetramer (Covarrubias, Bergfors, Jones, & Hogbom, 2006). Additionally, this enzyme seems to exist primarily as a tetramer at high pH. When pH is lowered from 8.4 to 7.5, it dissociates into dimers, suggesting that high pH is required for tetramerization. Thus, a dimeric appearance of β-CAs is relatively uncommon. Our experiments made with DLS and analytical gel filtration consistently suggested that *D. melanogaster* β-CA exists as a dimer in pH 7.0. Nevertheless, crystal structure is needed for detailed structural analysis of this enzyme.

6.2 β-CAs are found in invertebrates, but not in mammals

β-CAs have been previously reported from *Archaea* and *Bacteria* domains in addition to *Fungi*. Our studies suggested that at least one copy of *β-CA* gene can be found in all species among *Animalia*, excluding those in *Chordata*. A single *β-CA* gene was found in most invertebrates. Nematodes seem to have two *β-CA* genes in their genomes, which is specific for their lineage. Active site motifs and several other key residues seemed to be perfectly conserved. According to our studies, animal β-CAs form a separate subgroup in the β-CA enzyme family. Studied invertebrate β-CAs fell into category of "BCA_CladeB" like all plant β-CAs. Thus invertebrate β-CAs can be classified as "plant-type", "BCA_CladeB", β-CAs. The fact that β-CAs are found in animals makes them the CA class with the widest distribution in the tree of life. β-CAs are present in every domain (*Bacteria*, *Archaea* and *Eukarya*) and every kingdom (*Fungi*, *Animalia*, *Protista* and *Plantae*), unlike any other class of CAs.

Many parasites and disease carrying vectors are invertebrates. On the other hand, β-CA is missing from (at least most) chordates, including vertebrates and humans. This finding has significant potential for the development of parasite specific β-CA inhibitors with low incidence of side-effects in humans. These inhibitors could be used to prevent malaria propagation and to treat patients suffering from parasitic infections. Examples of β-CA-positive pathogens and pathogen vectors are the malaria mosquito *Anopheles*, the yellow fever mosquito

Aedes, the filariasis vector *Culex*, *Ancylostoma* hookworms, *Brugia* filarial nematodes, the blood fluke *S. mansoni*, the liver fluke *S. sinensis* and *Leishmania* parasites that cause leishmaniasis.

6.3 β-CA is the only mitochondrial CA in *D. melanogaster*

According to our bioinformatics studies, CAH1 and the mammalian cytoplasmic isozymes (CAs I, II, III, VII and XIII) share a common ancestor, whereas CAH2 has evolved from the same common ancestor as the mammalian extracellular isozymes (CAs IV, VI, IX, XII, XIV, and XV). Sequence identities suggest that CAH1 is the more strongly conserved of these two *Drosophila* CA isozymes. The predicted localizations are consistent with the phylogenetic results. *CAH1* is expressed in the cytoplasm, and CAH2 is an extracellular, membrane-attached isozyme. Based on high-throughput expression studies reported in Fly-Base, *CAH1* has the highest expression levels and widest expression pattern of all CA isozymes in *D. melanogaster*.

In addition to β-CA, and α-CAs CAH1 and CAH2, there are seven α-CAs and as many as five CARPs in *D. melanogaster* genome (Ortutay et al., 2010). Of these CARPs, three (CAH 13, 14 and 15) are *Drosophila* specific and other two (CARP-A and CARP-B) are found in all insects. In fact, CARP-B has His-His-Gln configuration in the active site and it may represent a newly proposed class of η-CAs (M. Tolvanen, unpublished observation). At least in *D. melanogaster*, β-CA is the only mitochondrial CA (Ortutay et al., 2010). It is likely that this is the case also in other invertebrates.

6.4 Kinetic properties of invertebrate CAs

6.4.1 Activity and inhibition of β-CAs

D. melanogaster β-CA (DmBCA) was found to be a highly active enzyme with k_{cat}/K_m of 1.1×10^8 $M^{-1}s^{-1}$. Studies made with different anionic CA inhibitors did not reveal any specific inhibitors of DmBCA. As with LdcCA, the inhibition profile was unique for this enzyme. DmBCA was appreciably inhibited by the classical CA inhibitor, acetazolamide (K_I 49 nM).

L. donovani chagasi β-CA (LdcCA) was also found to be a highly active enzyme with a k_{cat}/K_m of 5.9×10^7 M^{-1} s^{-1}, only slightly less active than DmBCA. Kinetic properties of LdcCA are in the same range with human isoform hCA I. A wide range of sulfonamides and thiols were tested against this enzyme (Charts 1-3). Most of the sulfonamides were not highly effective CAIs against LdcCA (Tables 5 and 6). However, the inhibition profile of LdcCA with the investigated sulfonamides was very different from hCA I and II. This can be considered as a positive feature in light of antiparasitic drug development. When the inhibitory potential of thiols was tested, it was observed immediately that the simple semicarbazido derivative 25 was an effective LdcCA inhibitor. Many of its semicarbazone derivatives were even more effective, with chloro and bromo derivatives 28 and 29 being the best inhibitors. The K_I value for the most effective thiol compound 29 was 13.4 nM, which indicates that it inhibits very efficiently β-CA. In contrast, the K_I values for hCA I and hCA II were 71.6 μM and 235.0 μM, respectively, which means that the possible effect on these human enzymes is minimal.

6.4.2 Activity and inhibition of α-CAs

The results from stopped-flow kinetic studies showed that both CAH1 and CAH2 from *D. melanogaster* enzymes are highly active (Table 3). Activity levels were in the same range with hCA II. Acetazolamide inhibited enzyme activities at submicromolar levels. Inhibition was somewhat weaker when compared to CA II and DmBCA. Also dithiocarbamates were tested against these enzymes. The inhibition profile was different from hCA II and also differed between CAH1 and CAH2. Some compounds efficiently inhibited both hCA II and CAH1/CAH2. On the other hand, some other compounds inhibited hCA II efficiently but not CAH1/CAH2, and also the other way around. The use of α-CA inhibitors is restricted by the fact that many inhibitors probably also have effects on some mammalian CAs, which predisposes these to adverse effects.

6.5 β-CA function seems to be crucial for the studied organisms

6.5.1 β-CA inhibition causes infertility of female fruit flies

β-CA function was shown to be essential for reproduction in female *D. melanogaster* flies. On the other hand, *β-CA* RNAi had no effect on survival of adult flies. Our study suggests that disturbance of DmBCA function leads to disturbances in border cell migration during *D. melanogaster* oogenesis. Previously it has been shown that defective border cell migration leads to sterility of female flies due to impaired formation of micropyle which is needed in fertilization (Montell et al., 1992; Montell, 2003). Additionally, even mature virgin *Drosophila* females should spontaneously ovulate at a low rate (~1 egg/day) (Heifetz, Lung, Frongillo, & Wolfner, 2000), but the RNAi-treated flies typically did not lay any eggs in our study. The mechanism by which oocytes are released from the *Drosophila* ovary is largely unknown. The absence of β-CA possibly affects the conditions in the ovulatory tract so that ovulation does not occur. As mentioned, the highest expression levels of β-CA in adult flies are found in spermatheca (female), fat body, and heart. Spermatheca is an organ whose purpose is to store sperm. It is possible that female sterility is related to both disturbances in border cell migration and function of spermatheca, in addition to the possible effect on ovulation itself.

It is unclear, how DmBCA would affect cell migration. Within human CAs, isozymes CA IX and XII have been linked to tumour invasiveness and migration (Parkkila et al., 2000; Svastova et al., 2004). It is suggested that CAs facilitate migration by affecting pH in extracellular matrix, which facilitates the action of matrix metalloproteinases. However, these enzymes are membrane-bound, whereas DmBCA is mitochondrial. Since HCO_3^- does not readily diffuse across mitochondrial membrane, DmBCA is unable to affect extracellular pH. The impaired movement of border cells might result from disturbances in biosynthetic pathways.

6.5.2 Disturbance of β-CA function causes growth inhibition of Leishmania parasites

L. donovani chagasi β-CA was found to be a highly active enzyme. Some thiol compounds were shown to be very efficient inhibitors of this enzyme both *in vitro* and *in vivo*. After 120 h treatment, some thiol compounds (26−30 and 32) exhibited

a significant antileishmanial activity at concentrations of 256 μM. Best results were obtained with the compound 29, which led to death of the parasites. These results show that β-CA is a crucial enzyme for *Leishmania* parasites and might be a potential target for antileishmanial drug development. However, it has to be remembered that *Leishmania* parasites also contain one α-CA which was not studied. Hence, some of the effects may emerge from the inhibition of α-CA. The physiological function of *Leishmania* β-CA is unclear and warrants further investigations.

6.6 β-CA inhibitors – new possibilities for antiparasitic drug and pesticide development?

Invertebrate genomes seem to encode at least one copy of a *β-CA* gene. Many of these invertebrates are parasites or parasite vectors. Moreover, many of these invertebrates cause problems related to agriculture or livestock husbandry, not forgetting diseases related to fish farming or veterinary medicine. Given that β-CA enzymes are present in invertebrates but not in vertebrate species, including mammals like humans, these enzymes could be potential targets for the development of novel pesticides or anti-parasitic drugs with minimal side effects to vertebrate α-CAs. However, this requires high isoform specificity, which in turn requires detailed structural information of the enzymes. At this point, some crystal structures of β-CAs including some algae, archaea, bacteria, yeast and a plant *P. sativum* are available in the PDB database (http://www.rcsb.org/). Currently, crystal structures of invertebrate or protozoan β-CAs are yet to be determined.

As shown in our studies, invertebrate β-CAs seem to be mitochondrial enzymes. Blocking of β-CAs in invertebrate cells can affect mitochondrial metabolic cycles and possibly damage the pathogens or pathogen vectors. Inhibition of CA activity could reduce the efficacy of some biochemical pathways. These include gluconeogenesis, nucleotide biosynthesis and fatty acid synthesis. As shown with *D. melanogaster*, interference of β-CA function can also affect physiological processes like reproduction. Thus far, the inhibition profiles of studied β-CAs have been completely different. Nowadays, completely β-CA specific inhibitors are not known, but based on this thesis and other studies, their development would have profitable possibilities in the control of protozoan and arthropod parasites and disease vectors.

7. Summary and conclusions

In conclusion, this study presents the characterization of *D. melanogaster* and *L. donovani chagasi* β-CAs and two α-CAs from *D. melanogaster*. This study provides novel information about a somewhat unknown group of invertebrate CAs – especially invertebrate β-CAs. The major conclusions are:

- *D. melanogaster* β-CA is highly active, dimeric, mitochondrial enzyme. Disruption of activity of this enzyme with RNA interference causes total but reversible infertility of female fruit flies.
- β-CAs seem to be present in virtually all invertebrates but is not found in mammals. The presence of β-CAs in chordates is still unclear.
- Two α-CAs were characterized from *D. melanogaster*. Both were shown to be highly active enzymes.
- β-CA was also characterized from the protozoan parasite *L. donovani chagasi* which causes a parasitic disease called leishmaniasis. In this parasite, disruption of CA function with a CA inhibitor caused growth inhibition.
- Inhibition of invertebrate and protozoan β-CAs could be considered a potential mechanism of action for novel anti-parasitic drugs.

8. Acknowledgements

This work was carried out at the School of Medicine and BioMediTech, University of Tampere during the years 2008-2015. I want to thank the dean of School of Medicine, Professor Matti Lehto (MD, PhD), and the dean of BioMediTech, Dr. Hannu Hanhijärvi (DDS, PhD), for the excellent facilities and pleasant working environment during these years.

I wish to express my gratitude to my supervisor, Professor Seppo Parkkila (MD, PhD). I want to thank you for the hours of discussion that have involved both scientific and not so scientific issues. Your optimism and friendship have played a huge role during this process. I also want to say thank you for the opportunity to teach medical students during these years. I have found it extremely interesting and rewarding.

I would like to thank the external reviewers of my thesis, Associate Professor Marc A. Ilies (PhD) and Professor Matti Karp (PhD), for their valuable comments and kind words. I would also like to thank Professor Kalervo Väänänen (MD, PhD) for giving me the honor of being my opponent.

I wish to thank the thesis committee members, docent Mika Hilvo (PhD) and Professor Markku Kulomaa (PhD) for their guidance during the project.

I also want to thank Docent Mika Hilvo (PhD) again. You were the one to introduce me to the field of carbonic anhydrases. Special thanks are also going for Dr. Martti Tolvanen (PhD). You have been involved in two out of four papers in this thesis. It has been pleasure to work with you. Your passionate attitude towards science has been inspiring for me during the process and I still can´t understand how you can remember all those details.

I wish to express my gratitude to Professor Claudiu Supuran (PhD) for the great collaboration. You are involved in three out of four publications in this thesis, and it is obvious that it would not be ready without you.

I also want to thank Dr. Susanna Valanne (PhD) for introducing me to the interesting world of fruit flies. Your support has been extremely valuable. A couple of years ago I couldn´t imagine that I would be breeding flies, but it actually became an essential part of my life for a couple of months. I also want to thank Professor Mika Rämet (MD, PhD) for the opportunity to use your lab facilities. In addition, I want to thank Professor Howard Jacobs (PhD), Dr. Suvi Vartiainen (PhD) and Tea Tuomela for the help with fly studies.

I want to thank all the other collaborators and co-authors for their valuable contribution: Andrea Scozzafava (PhD), Alane Vermelho (PhD), Alessio Innocenti (PhD), Ayodeji Olatubosun (MSc), Barbara Taskinen (PhD), Clemente Capasso (PhD), Daniela Vullo (PhD), Fabrizio Carta (PhD), Igor Rodriguez (PhD), Jenni Leppiniemi (PhD), Suzana Corte-Real (PhD), Terhi Salonen, Thomas Gorr (PhD) and Vesa Hytönen (PhD). Without you this wouldn´t be possible.

My scientific career already started before joining the CA-group. I would like to thank Professor Olli Silvennoinen (MD, PhD) for giving me the opportunity to be part of your group. My special gratitude goes to Dr. Tuuli Välineva (PhD) who was the first one to introduce me to the world of science. You taught how to do lab work precisely.

I want to thank all other persons who have worked with me during the past years: Alejandra Rodríguez Martínez (PhD), Alise Hyrskyluoto (PhD), Arja Ahola, Ashok Aspatwar (PhD), Daniela Ungureanu (PhD), Harlan Barker (MSc), Heimo Syvälä (PhD), Heini Kallio (PhD), Henna Luukkonen (MSc, tech.), Hilkka Mäkinen, Juha Grönholm (MD, PhD), Juha Saarikettu (PhD), Jukka Lehtonen, Maarit Patrikainen (MSc), Marko Pesu (MD, PhD), Merja Lehtinen, Niina Ikonen, Pasi Pennanen (PhD), Paula Kosonen, Peiwen Pan (PhD), Reza Zolfaghari Emameh (MSc), Sami Purmonen (MSc) and Sari Vanhatupa (PhD). Our laboratory technicians Marianne Kuuslahti and Aulikki Lehmus deserve special thanks for spending countless of hours with my proteins and fruit flies, not to forget the nice discussions. I also want to thank all the other people who have been helpful and friendly for me during these years. Thanks, Harlan, for the quick and effective language revision of this thesis.

I want to thank the Emil Aaltonen Foundation that provided me with two grants that pushed my research work forward.

I want to thank all of my friends, especially Mikko, Juha, Erkka, Rane, Olli, Niko, Ville R, Ville V, Jonne & Hanna, Aune & Jouni and Suvi & Timo, not to forget everyone else. Thank you for drawing my attention from research and work to something else every now and then. I also want to thank all of my colleagues from Cursus Seppo, Medical School of Tampere University, as well as all friends from Biotechnology program. Both former and current workmates also deserve thanks for their support. I think that some of you might have even understood what I´ve been doing.

I would like to express my thanks to my family. First, I would like to thank my parents Ritva and Sampo for never ending support in everything that I´ve attempted during my 30 years. I also want to thank Suvi for being the best little sister I could imagine. In addition, I want to thank my future parents-in-law Irja and Jukka. Also, I want to thank my grandparents that are unfortunately already

gone. Moreover, I want to thank all of my other relatives. Furthermore, I want to thank our dogs Taro and Kido for keeping my mental health in tolerable shape!

Finally I would like to express my deepest gratitude for my beloved Vilma. I want to thank for your love and support during these years. I wouldn´t be here without you.

This thesis was financially supported by Academy of Finland, Jane & Aatos Erkko Foundation and Sigrid Jusélius Foundation. It was also supported by the competitive Research Funding of the Tampere University Hospital and in part by grants from the 6th Framework Programme of the European Union (DeZnIT project).

Jyväskylä/Tampere, September 2015

Leo Syrjänen

9. References

Adams, M. D., Celniker, S. E., Holt, R. A., Evans, C. A., Gocayne, J. D., Amanatides, P. G., Scherer, S.E., Li, P.W., Hoskins, R.A., Galle, R.F., George, R.A., Lewis, S.E., Richards, S., Ashburner, M., Henderson, S.N., Sutton, G.G., Wortman, J.R., Yandell, M.D., Zhang, Q., Chen, L.X., Brandon, R.C., Rogers, Y.H., Blazej, R.G., Champe, M., Pfeiffer, B.D., Wan, K.H., Doyle, C., Baxter, E.G., Helt, G., Nelson, C.R., Gabor, G.L., Abril, J.F., Agbayani, A., An, H.J., Andrews-Pfannkoch, C., Baldwin, D., Ballew, R.M., Basu, A., Baxendale, J., Bayraktaroglu, L., Beasley, E.M., Beeson, K.Y., Benos, P.V., Berman, B.P., Bhandari, D., Bolshakov, S., Borkova, D., Botchan, M.R., Bouck, J., Brokstein, P., Brottier, P., Burtis, K.C., Busam, D.A., Butler, H., Cadieu, E., Center, A., Chandra, I., Cherry, J.M., Cawley, S., Dahlke, C., Davenport, L.B., Davies, P., de Pablos, B., Delcher, A., Deng, Z., Mays, A.D., Dew, I., Dietz, S.M., Dodson, K., Doup, L.E., Downes, M., Dugan-Rocha, S., Dunkov, B.C., Dunn, P., Durbin, K.J., Evangelista, C.C., Ferraz, C., Ferriera, S., Fleischmann, W., Fosler, C., Gabrielian, A.E., Garg, N.S., Gelbart, W.M., Glasser, K., Glodek, A., Gong, F., Gorrell, J.H., Gu, Z., Guan, P., Harris, M., Harris, N.L., Harvey, D., Heiman, T.J., Hernandez, J.R., Houck, J., Hostin, D., Houston, K.A., Howland, T.J., Wei, M.H., Ibegwam, C., Jalali, M., Kalush, F.,

Karpen, G.H., Ke, Z., Kennison, J.A., Ketchum, K.A., Kimmel, B.E., Kodira, C.D., Kraft, C., Kravitz, S., Kulp, D., Lai, Z., Lasko, P., Lei, Y., Levitsky, A.A., Li, J., Li, Z., Liang, Y., Lin, X., Liu, X., Mattei, B., McIntosh, T.C., McLeod, M.P., McPherson, D., Merkulov, G., Milshina, N.V., Mobarry, C., Morris, J., Moshrefi, A., Mount, S.M., Moy, M., Murphy, B., Murphy, L., Muzny, D.M., Nelson, D.L., Nelson, D.R., Nelson, K.A., Nixon, K., Nusskern, D.R., Pacleb, J.M., Palazzolo, M., Pittman, G.S., Pan, S., Pollard, J., Puri, V., Reese, M.G., Reinert, K., Remington, K., Saunders, R.D., Scheeler, F., Shen, H., Shue, B.C., Siden-Kiamos, I., Simpson, M., Skupski, M.P., Smith, T., Spier, E., Spradling, A.C., Stapleton, M., Strong, R., Sun, E., Svirskas, R., Tector, C., Turner, R., Venter, E., Wang, A.H., Wang, X., Wang, Z.Y., Wassarman, D.A., Weinstock, G.M., Weissenbach, J., Williams, S.M., WoodageT, Worley, K.C., Wu, D., Yang, S., Yao, Q.A., Ye, J., Yeh, R.F., Zaveri, J.S., Zhan, M., Zhang, G., Zhao, Q., Zheng, L., Zheng, X.H., Zhong, F.N., Zhong, W., Zhou, X., Zhu, S., Zhu, X., Smith, H.O., Gibbs, R.A., Myers, E.W., Rubin, G.M., Venter, J. C. (2000). The genome sequence of drosophila melanogaster. *Science (New York, N.Y.), 287*(5461), 2185-2195.

Alber, B. E., & Ferry, J. G. (1994). A carbonic anhydrase from the archaeon methanosarcina thermophila. *Proceedings of the National Academy of Sciences of the United States of America, 91*(15), 6909-6913.

Aspatwar, A., Tolvanen, M. E., & Parkkila, S. (2013). An update on carbonic anhydrase-related proteins VIII, X and XI. *Journal of Enzyme Inhibition and Medicinal Chemistry, 28*(6), 1129-1142.

Bastock, R., & St Johnston, D. (2008). Drosophila oogenesis. *Current Biology : CB, 18*(23), R1082-7.

Bloch Qazi, M.C., Heifetz Y., & Holfner M.F. (2003). The developments between gametogenesis and fertilization: ovulation and female sperm storage in Drosophila melanogaster. *Developmental Biology*. 15;256(2):195-211.

Boone, C. D., Pinard, M., McKenna, R., & Silverman, D. (2014). Catalytic mechanism of alpha-class carbonic anhydrases: CO2 hydration and proton transfer. *Sub-Cellular Biochemistry, 75*, 31-52.

Brand, A. H., & Perrimon, N. (1993). Targeted gene expression as a means of altering cell fates and generating dominant phenotypes. *Development (Cambridge, England), 118*(2), 401-415.

Burghout, P., Cron, L. E., Gradstedt, H., Quintero, B., Simonetti, E., Bijlsma, J. J., Bootsma H.J., & Hermans, P. W. (2010). Carbonic anhydrase is essential for streptococcus pneumoniae growth in environmental ambient air. *Journal of Bacteriology, 192*(15), 4054-4062.

Burnell, J. N., Gibbs, M. J., & Mason, J. G. (1990). Spinach chloroplastic carbonic anhydrase: Nucleotide sequence analysis of cDNA. *Plant Physiology, 92*(1), 37-40.

Bury-Mone, S., Mendz, G. L., Ball, G. E., Thibonnier, M., Stingl, K., Ecobichon, C., Avé P., Huerre M., Labigne A., Thiberge J.M., & De Reuse, H. (2008). Roles of alpha and beta carbonic anhydrases of helicobacter pylori in the urease-dependent response to acidity and in colonization of the murine gastric mucosa. *Infection and Immunity, 76*(2), 497-509.

Chegwidden WR, C. N. (2000). Introduction to the carbonic anhydrases. in: The carbonic anhydrases: New horizons, pp. 13–28. Eds: Chegwidden WR, Carter ND and Edwards YH, Birkhäuser Verlag, Basel.

Clark, D., Rowlett, R. S., Coleman, J. R., & Klessig, D. F. (2004). Complementation of the yeast deletion mutant DeltaNCE103 by members of the beta class of carbonic anhydrases is dependent on carbonic anhydrase activity rather than on antioxidant activity. *The Biochemical Journal, 379*(Pt 3), 609-615.

Corena, M., Seron, T. J., Lehman, H. K., Ochrietor, J. D., Kohn, A., Tu, C., & Linser, P. J. (2002). Carbonic anhydrase in the midgut of larval aedes aegypti: Cloning, localization and inhibition. *The Journal of Experimental Biology, 205*(Pt 5), 591-602.

Covarrubias, A. S., Bergfors, T., Jones, T. A., & Hogbom, M. (2006). Structural mechanics of the pH-dependent activity of beta-carbonic anhydrase from mycobacterium tuberculosis. *The Journal of Biological Chemistry, 281*(8), 4993-4999.

Cox, E. H., McLendon, G. L., Morel, F. M., Lane, T. W., Prince, R. C., Pickering, I. J., & George, G. N. (2000). The active site structure of thalassiosira weissflogii carbonic anhydrase 1. *Biochemistry, 39*(40), 12128-12130.

De Cian, M. C., Andersen, A. C., Bailly, X., & Lallier, F. H. (2003). Expression and localization of carbonic anhydrase and ATPases in the symbiotic tubeworm riftia pachyptila. *The Journal of Experimental Biology, 206*(Pt 2), 399-409.

Del Prete, S., Vullo, D., Fisher, G. M., Andrews, K. T., Poulsen, S. A., Capasso, C., & Supuran, C. T. (2014). Discovery of a new family of carbonic anhydrases in the malaria pathogen plasmodium falciparum--the eta-carbonic anhydrases. *Bioorganic & Medicinal Chemistry Letters, 24*(18), 4389-4396.

DeRosa, A. A., Chirgwin, S. R., Williams, J. C., & Klei, T. R. (2008). Isolation and characterization of a gene encoding carbonic anhydrase from ostertagia ostertagi and quantitative measurement of expression during in vivo exsheathment. *Veterinary Parasitology, 154*(1-2), 58-66.

Dietzl, G., Chen, D., Schnorrer, F., Su, K. C., Barinova, Y., Fellner, M., Gasser, B., Kinsey, K., Oppel, S., Scheiblauer, S., Couto, A., Marra, V., Keleman, K., & Dickson, B. J. (2007). A genome-wide transgenic RNAi library for conditional gene inactivation in drosophila. *Nature, 448*(7150), 151-156.

Elleuche, S., & Poggeler, S. (2009a). Beta-carbonic anhydrases play a role in fruiting body development and ascospore germination in the filamentous fungus sordaria macrospora. *PloS One, 4*(4), e5177.

Elleuche, S., & Poggeler, S. (2009b). Evolution of carbonic anhydrases in fungi. *Current Genetics, 55*(2), 211-222.

Fabre, N., Reiter, I. M., Becuwe-Linka, N., Genty, B., & Rumeau, D. (2007). Characterization and expression analysis of genes encoding alpha and beta carbonic anhydrases in arabidopsis. *Plant, Cell & Environment, 30*(5), 617-629.

Fasseas, M. K., Tsikou, D., Flemetakis, E., & Katinakis, P. (2009). Molecular and biochemical analysis of the beta class carbonic anhydrases in caenorhabditis elegans. *Molecular Biology Reports.* 37(6), 2941-50.

Fasseas, M. K., Tsikou, D., Flemetakis, E., & Katinakis, P. (2011). Molecular and biochemical analysis of the alpha class carbonic anhydrases in caenorhabditis elegans. *Molecular Biology Reports, 38*(3), 1777-1785.

Fernandez-Ayala, D. J., Sanz, A., Vartiainen, S., Kemppainen, K. K., Babusiak, M., Mustalahti, E., Costa R., Tuomela T., Zeviani M., Chung J., O'Dell K.M., Rustin P., & Jacobs, H. T. (2009). Expression of the ciona intestinalis alternative oxidase (AOX) in drosophila complements defects in mitochondrial oxidative phosphorylation. *Cell Metabolism, 9*(5), 449-460.

Fleming, R. E., Crouch, E. C., Ruzicka, C. A., & Sly, W. S. (1993). Pulmonary carbonic anhydrase IV: Developmental regulation and cell-specific expression in the capillary endothelium. *The American Journal of Physiology, 265*(6 Pt 1), L627-35.

Fujikawa-Adachi, K., Nishimori, I., Taguchi, T., & Onishi, S. (1999). Human mitochondrial carbonic anhydrase VB. cDNA cloning, mRNA expression,

subcellular localization, and mapping to chromosome x. *The Journal of Biological Chemistry, 274*(30), 21228-21233.

Fukuzawa, H., Suzuki, E., Komukai, Y., & Miyachi, S. (1992). A gene homologous to chloroplast carbonic anhydrase (icfA) is essential to photosynthetic carbon dioxide fixation by synechococcus PCC7942. *Proceedings of the National Academy of Sciences of the United States of America, 89*(10), 4437-4441.

Gotz, R., Gnann, A., & Zimmermann, F. K. (1999). Deletion of the carbonic anhydrase-like gene NCE103 of the yeast saccharomyces cerevisiae causes an oxygen-sensitive growth defect. *Yeast (Chichester, England), 15*(10A), 855-864.

Guilloton, M. B., Korte, J. J., Lamblin, A. F., Fuchs, J. A., & Anderson, P. M. (1992). Carbonic anhydrase in escherichia coli. A product of the cyn operon. *The Journal of Biological Chemistry, 267*(6), 3731-3734.

Guyton AC, H. J. (2006). Regulation of acid-base balance. in textbook of medical physiology, pp. 383-401. Elsevier Saunders, Philadelphia.

Hazen, S. A., Waheed, A., Sly, W. S., LaNoue, K. F., & Lynch, C. J. (1996). Differentiation-dependent expression of CA V and the role of carbonic anhydrase isozymes in pyruvate carboxylation in adipocytes. *The FASEB Journal : Official Publication of the Federation of American Societies for Experimental Biology, 10*(4), 481-490.

Heifetz, Y., Lung, O., Frongillo, E. A.,Jr, & Wolfner, M. F. (2000). The drosophila seminal fluid protein Acp26Aa stimulates release of oocytes by the ovary. *Current Biology : CB, 10*(2), 99-102.

Hewett-Emmett, D. (2000). Evolution and distribution of the carbonic anhydrase gene families. *Exs, (90)*(90), 29-76.

Hilvo, M., Baranauskiene, L., Salzano, A. M., Scaloni, A., Matulis, D., Innocenti, A., Scozzafava A., Monti S.M., Di Fiore A., De Simone G., Lindfors M., Jänis J., Valjakka J., Pastoreková S., Pastorek J., Kulomaa M.S., Nordlund H.R., Supuran C.T. &, Parkkila, S. (2008). Biochemical characterization of CA IX, one of the most active carbonic anhydrase isozymes. *The Journal of Biological Chemistry, 283*(41), 27799-27809.

Innocenti, A., Leewattanapasuk, W., Muhlschlegel, F. A., Mastrolorenzo, A., & Supuran, C. T. (2009). Carbonic anhydrase inhibitors. inhibition of the beta-class enzyme from the pathogenic yeast candida glabrata with anions. *Bioorganic & Medicinal Chemistry Letters, 19*(16), 4802-4805.

Ivanov, S., Liao, S. Y., Ivanova, A., Danilkovitch-Miagkova, A., Tarasova, N., Weirich, G., Merrill M.J., Proescholdt M.A., Oldfield E.H., Lee J., Zavada J., Waheed A., Sly W., Lerman M.I., & Stanbridge, E. J. (2001). Expression of hypoxia-inducible cell-surface transmembrane carbonic anhydrases in human cancer. *The American Journal of Pathology, 158*(3), 905-919.

Iverson, T. M., Alber, B. E., Kisker, C., Ferry, J. G., & Rees, D. C. (2000). A closer look at the active site of gamma-class carbonic anhydrases: High-resolution crystallographic studies of the carbonic anhydrase from methanosarcina thermophila. *Biochemistry, 39*(31), 9222-9231.

Kemppainen, K. K., Rinne, J., Sriram, A., Lakanmaa, M., Zeb, A., Tuomela, T., Popplestone A., Singh S., Sanz A., Rustin P., & Jacobs, H. T. (2014). Expression of alternative oxidase in drosophila ameliorates diverse phenotypes due to cytochrome oxidase deficiency. *Human Molecular Genetics, 23*(8), 2078-2093.

Kim, G., Lee, T. H., Wetzel, P., Geers, C., Robinson, M. A., Myers, T. G., Owens J.W., Wehr N.B., Eckhaus M.W., Gros G., Wynshaw-Boris A., & Levine, R. L. (2004). Carbonic anhydrase III is not required in the mouse for normal growth, development, and life span. *Molecular and Cellular Biology, 24*(22), 9942-9947.

Kimber, M. S., & Pai, E. F. (2000). The active site architecture of pisum sativum beta-carbonic anhydrase is a mirror image of that of alpha-carbonic anhydrases. *The EMBO Journal, 19*(7), 1407-1418.

Krishnamurthy, V. M., Kaufman, G. K., Urbach, A. R., Gitlin, I., Gudiksen, K. L., Weibel, D. B., & Whitesides, G. M. (2008). Carbonic anhydrase as a model for biophysical and physical-organic studies of proteins and protein-ligand binding. *Chemical Reviews, 108*(3), 946-1051.

Krungkrai, S. R., Suraveratum, N., Rochanakij, S., & Krungkrai, J. (2001). Characterisation of carbonic anhydrase in plasmodium falciparum. *International Journal for Parasitology, 31*(7), 661-668.

Kumar, V., & Kannan, K. K. (1994). Enzyme-substrate interactions. structure of human carbonic anhydrase I complexed with bicarbonate. *Journal of Molecular Biology, 241*(2), 226-232.

Lane, T. W., Saito, M. A., George, G. N., Pickering, I. J., Prince, R. C., & Morel, F. M. (2005). Biochemistry: A cadmium enzyme from a marine diatom. *Nature, 435*(7038), 42.

Lehneck, R., Neumann, P., Vullo, D., Elleuche, S., Supuran, C. T., Ficner, R., & Poggeler, S. (2014). Crystal structures of two tetrameric beta-carbonic anhydrases from the filamentous ascomycete sordaria macrospora. *The FEBS Journal, 281*(7), 1759-1772.

Lehtonen, J., Shen, B., Vihinen, M., Casini, A., Scozzafava, A., Supuran, C. T., Parkkila A. K., Saarnio J., Kivelä A. J., Waheed A, Sly W. S, & Parkkila, S. (2004). Characterization of CA XIII, a novel member of the carbonic anhydrase isozyme family. *The Journal of Biological Chemistry, 279*(4), 2719-2727.

Linser, P. J., Smith, K. E., Seron, T. J., & Neira Oviedo, M. (2009). Carbonic anhydrases and anion transport in mosquito midgut pH regulation. *The Journal of Experimental Biology, 212*(Pt 11), 1662-1671.

Macauley, S. R., Zimmerman, S. A., Apolinario, E. E., Evilia, C., Hou, Y. M., Ferry, J. G., & Sowers, K. R. (2009). The archetype gamma-class carbonic anhydrase (cam) contains iron when synthesized in vivo. *Biochemistry, 48*(5), 817-819.

Majeau, N., Arnoldo, M. A., & Coleman, J. R. (1994). Modification of carbonic anhydrase activity by antisense and over-expression constructs in transgenic tobacco. *Plant Molecular Biology, 25*(3), 377-385.

Majeau, N., & Coleman, J. R. (1996). Effect of CO2 concentration on carbonic anhydrase and ribulose-1,5-bisphosphate Carboxylase/Oxygenase expression in pea. *Plant Physiology, 112*(2), 569-574.

Mass, T., Drake, J. L., Peters, E. C., Jiang, W., & Falkowski, P. G. (2014). Immunolocalization of skeletal matrix proteins in tissue and mineral of the coral stylophora pistillata. *Proceedings of the National Academy of Sciences of the United States of America, 111*(35), 12728-12733.

McCall, L. I., Zhang, W. W., & Matlashewski, G. (2013). Determinants for the development of visceral leishmaniasis disease. *PLoS Pathogens, 9*(1), e1003053.

McGinn, P. J., & Morel, F. M. (2008). Expression and regulation of carbonic anhydrases in the marine diatom thalassiosira pseudonana and in natural phytoplankton assemblages from great bay, New Jersey. *Physiologia Plantarum, 133*(1), 78-91.

McKenna, R., & Supuran, C. T. (2014). Carbonic anhydrase inhibitors drug design. *Sub-Cellular Biochemistry, 75*, 291-323.

Merlin, C., Masters, M., McAteer, S., & Coulson, A. (2003). Why is carbonic anhydrase essential to escherichia coli? *Journal of Bacteriology, 185*(21), 6415-6424.

Mitsuhashi, S., Ohnishi, J., Hayashi, M., & Ikeda, M. (2004). A gene homologous to beta-type carbonic anhydrase is essential for the growth of corynebacterium glutamicum under atmospheric conditions. *Applied Microbiology and Biotechnology, 63*(5), 592-601.

Montell, D. J. (2003). Border-cell migration: The race is on. *Nature Reviews.Molecular Cell Biology, 4*(1), 13-24.

Montell, D. J., Rorth, P., & Spradling, A. C. (1992). Slow border cells, a locus required for a developmentally regulated cell migration during oogenesis, encodes drosophila C/EBP. *Cell, 71*(1), 51-62.

Neish, A. C. (1939). Studies on chloroplasts: Their chemical composition and the distribution of certain metabolites between the chloroplasts and the remainder of the leaf. *The Biochemical Journal, 33*(3), 300-308.

Ortutay, C., Olatubosun, A., Parkkila, S., Vihinen, M., & Tolvanen, M. (2010). An evolutionary analysis of insect carbonic anhydrases. in: Advances in medicine and biology. pp. 145-168. Ed: Berhardt LV.

Pan, P., Vermelho, A. B., Capaci Rodrigues, G., Scozzafava, A., Tolvanen, M. E., Parkkila, S., Capasso, C. & Supuran, C. T. (2013). Cloning, characterization, and sulfonamide and thiol inhibition studies of an alpha-carbonic anhydrase from trypanosoma cruzi, the causative agent of chagas disease. *Journal of Medicinal Chemistry,* 28;56(4):1761-71.

Pandey, U. B., & Nichols, C. D. (2011). Human disease models in drosophila melanogaster and the role of the fly in therapeutic drug discovery. *Pharmacological Reviews, 63*(2), 411-436.

Parisi, G., Perales, M., Fornasari, M. S., Colaneri, A., Gonzalez-Schain, N., Gomez-Casati, D., Zimmermann S., Brennicke A., Araya A., Ferry J. G., Echave J., & Zabaleta, E. (2004). Gamma carbonic anhydrases in plant mitochondria. *Plant Molecular Biology, 55*(2), 193-207.

Parkkila, S., Rajaniemi, H., Parkkila, A. K., Kivela, J., Waheed, A., Pastorekova, S., Pastorek J., & Sly, W. S. (2000). Carbonic anhydrase inhibitor suppresses invasion of renal cancer cells in vitro. *Proceedings of the National Academy of Sciences of the United States of America, 97*(5), 2220-2224.

Patrikainen, M., Pan, P., Kulesskaya, N., Voikar, V., & Parkkila, S. (2014). The role of carbonic anhydrase VI in bitter taste perception: Evidence from the Car6(-)/(-) mouse model. *Journal of Biomedical Science, 21*, 82-014-0082-2.

Pfaffl, M. W. (2001). A new mathematical model for relative quantification in real-time RT-PCR. *Nucleic Acids Research, 29*(9), e45.

Reiter, L. T., Potocki, L., Chien, S., Gribskov, M., & Bier, E. (2001). A systematic analysis of human disease-associated gene sequences in drosophila melanogaster. *Genome Research, 11*(6), 1114-1125.

Rorth, P. (2009). Collective cell migration. *Annual Review of Cell and Developmental Biology, 25*, 407-429.

Rowlett, R. S. (2014). Structure and catalytic mechanism of beta-carbonic anhydrases. *Sub-Cellular Biochemistry, 75*, 53-76.

Rubin, G. M., & Lewis, E. B. (2000). A brief history of drosophila's contributions to genome research. *Science (New York, N.Y.), 287*(5461), 2216-2218.

Ruusuvuori, E., Li, H., Huttu, K., Palva, J. M., Smirnov, S., Rivera, C., Kaila K., &Voipio, J. (2004). Carbonic anhydrase isoform VII acts as a molecular switch in the development of synchronous gamma-frequency firing of hippocampal CA1 pyramidal cells. *The Journal of Neuroscience : The Official Journal of the Society for Neuroscience, 24*(11), 2699-2707.

Schlicker, C., Hall, R. A., Vullo, D., Middelhaufe, S., Gertz, M., Supuran, C. T., Mühlschlegel F.A., & Steegborn, C. (2009). Structure and inhibition of the CO2-sensing carbonic anhydrase Can2 from the pathogenic fungus cryptococcus neoformans. *Journal of Molecular Biology, 385*(4), 1207-1220.

Shah, G. N., Rubbelke, T. S., Hendin, J., Nguyen, H., Waheed, A., Shoemaker, J. D., & Sly, W. S. (2013). Targeted mutagenesis of mitochondrial carbonic anhydrases VA and VB implicates both enzymes in ammonia detoxification and glucose metabolism. *Proceedings of the National Academy of Sciences of the United States of America, 110*(18), 7423-7428.

Shah, G. N., Ulmasov, B., Waheed, A., Becker, T., Makani, S., Svichar, N., Chesler M., &Sly, W. S. (2005). Carbonic anhydrase IV and XIV knockout mice: Roles of the respective carbonic anhydrases in buffering the extracellular space in

brain. *Proceedings of the National Academy of Sciences of the United States of America, 102*(46), 16771-16776.

Sly, W. S., Hewett-Emmett, D., Whyte, M. P., Yu, Y. S., & Tashian, R. E. (1983). Carbonic anhydrase II deficiency identified as the primary defect in the autosomal recessive syndrome of osteopetrosis with renal tubular acidosis and cerebral calcification. *Proceedings of the National Academy of Sciences of the United States of America, 80*(9), 2752-2756.

Sly, W. S., & Hu, P. Y. (1995). Human carbonic anhydrases and carbonic anhydrase deficiencies. *Annual Review of Biochemistry, 64*, 375-401.

Smith, K. S., Cosper, N. J., Stalhandske, C., Scott, R. A., & Ferry, J. G. (2000). Structural and kinetic characterization of an archaeal beta-class carbonic anhydrase. *Journal of Bacteriology, 182*(23), 6605-6613.

Smith, K. S., & Ferry, J. G. (1999). A plant-type (beta-class) carbonic anhydrase in the thermophilic methanoarchaeon methanobacterium thermoautotrophicum. *Journal of Bacteriology, 181*(20), 6247-6253.

Smith, K. S., Ingram-Smith, C., & Ferry, J. G. (2002). Roles of the conserved aspartate and arginine in the catalytic mechanism of an archaeal beta-class carbonic anhydrase. *Journal of Bacteriology, 184*(15), 4240-4245.

Stams, T., & Christianson, D. (2000). X-ray crystallographic studies of mammalian carbonic anhydrase isozymes. in: The carbonic anhydrases: New horizons, pp. 159–174. Eds. Chegwidden WR, Carter ND and Edwards YH, Birkhäuser Verlag, Basel.

Stefanatos, R., Sriram, A., Kiviranta, E., Mohan, A., Ayala, V., Jacobs, H. T., Pamplona R., & Sanz, A. (2012). Dj-1beta regulates oxidative stress, insulin-like signaling and development in drosophila melanogaster. *Cell Cycle (Georgetown, Tex.), 11*(20), 3876-3886.

Stephenson, R., & Metcalfe, N. H. (2013). Drosophila melanogaster: A fly through its history and current use. *The Journal of the Royal College of Physicians of Edinburgh, 43*(1), 70-75.

Strop, P., Smith, K. S., Iverson, T. M., Ferry, J. G., & Rees, D. C. (2001). Crystal structure of the "cab"-type beta class carbonic anhydrase from the archaeon methanobacterium thermoautotrophicum. *The Journal of Biological Chemistry, 276*(13), 10299-10305.

Suarez Covarrubias, A., Larsson, A. M., Hogbom, M., Lindberg, J., Bergfors, T., Bjorkelid, C., Mowbray S. L., Unge T., & Jones, T. A. (2005). Structure and function of carbonic anhydrases from mycobacterium tuberculosis. *The Journal of Biological Chemistry, 280*(19), 18782-18789.

Supuran, C. (2004). Carbonic anhydrases: Catalytic and inhibition mechanisms, distribution and physiological roles. in: Carbonic anhydr ase: Its inhibitors and activators, pp. 1–23. Eds. Supuran CT, Scozzafava A and Conway J, CRC Press, Boca Raton.

Supuran, C. T. (2008). Carbonic anhydrases: Novel therapeutic applications for inhibitors and activators. *Nature Reviews.Drug Discovery, 7*(2), 168-181.

Supuran, C. T. (2011). Bacterial carbonic anhydrases as drug targets: Toward novel antibiotics? *Frontiers in Pharmacology, 2*, 34.

Svastova, E., Hulikova, A., Rafajova, M., Zat'ovicova, M., Gibadulinova, A., Casini, A., Cecchi A., Scozzafava A., Supuran C. T., Pastorek J., & Pastorekova, S. (2004). Hypoxia activates the capacity of tumor-associated carbonic anhydrase IX to acidify extracellular pH. *FEBS Letters, 577*(3), 439-445.

Tripp, B. C., Bell, C. B.,3rd, Cruz, F., Krebs, C., & Ferry, J. G. (2004). A role for iron in an ancient carbonic anhydrase. *The Journal of Biological Chemistry, 279*(8), 6683-6687.

Whittington, D. A., Grubb, J. H., Waheed, A., Shah, G. N., Sly, W. S., & Christianson, D. W. (2004). Expression, assay, and structure of the extracellular domain of murine carbonic anhydrase XIV: Implications for selective inhibition of membrane-associated isozymes. *The Journal of Biological Chemistry, 279*(8), 7223-7228.

Wu, X., Tanwar, P. S., & Raftery, L. A. (2008). Drosophila follicle cells: Morphogenesis in an eggshell. *Seminars in Cell & Developmental Biology, 19*(3), 271-282.

Xu, Y., Feng, L., Jeffrey, P. D., Shi, Y., & Morel, F. M. (2008). Structure and metal exchange in the cadmium carbonic anhydrase of marine diatoms. *Nature, 452*(7183), 56-61.

Zabaleta, E., Martin, M. V., & Braun, H. P. (2012). A basal carbon concentrating mechanism in plants? *Plant Science : An International Journal of Experimental Plant Biology, 187*, 97-104.

Zimmerman, S. A., & Ferry, J. G. (2008). The beta and gamma classes of carbonic anhydrase. *Current Pharmaceutical Design, 14*(7), 716-721.

Zolfaghari Emameh, R., Barker, H., Tolvanen, M. E., Ortutay, C., & Parkkila, S. (2014). Bioinformatic analysis of beta carbonic anhydrase sequences from protozoans and metazoans. *Parasites & Vectors, 7*, 38-3305-7-38.

10. Original communications

BMC Biochemistry

RESEARCH ARTICLE Open Access

Characterization of the first beta-class carbonic anhydrase from an arthropod (*Drosophila melanogaster*) and phylogenetic analysis of beta-class carbonic anhydrases in invertebrates

Leo Syrjänen[1,2,3*], Martti Tolvanen[1], Mika Hilvo[1], Ayodeji Olatubosun[1], Alessio Innocenti[4], Andrea Scozzafava[4], Jenni Leppiniemi[1], Barbara Niederhauser[1], Vesa P Hytönen[1], Thomas A Gorr[5], Seppo Parkkila[1,2,3], Claudiu T Supuran[4]

Abstract

Background: The β-carbonic anhydrase (CA, EC 4.2.1.1) enzymes have been reported in a variety of organisms, but their existence in animals has been unclear. The purpose of the present study was to perform extensive sequence analysis to show that the β-CAs are present in invertebrates and to clone and characterize a member of this enzyme family from a representative model organism of the animal kingdom, e.g., *Drosophila melanogaster*.

Results: The novel β-CA gene, here named *DmBCA*, was identified from FlyBase, and its orthologs were searched and reconstructed from sequence databases, confirming the presence of β-CA sequences in 55 metazoan species. The corresponding recombinant enzyme was produced in Sf9 insect cells, purified, kinetically characterized, and its inhibition was investigated with a series of simple, inorganic anions. Holoenzyme molecular mass was defined by dynamic light scattering analysis and gel filtration, and the results suggested that the holoenzyme is a dimer. Double immunostaining confirmed predictions based on sequence analysis and localized DmBCA protein to mitochondria. The enzyme showed high CO_2 hydratase activity, with a k_{cat} of 9.5×10^5 s^{-1} and a k_{cat}/K_M of 1.1×10^8 $M^{-1}s^{-1}$. DmBCA was appreciably inhibited by the clinically-used sulfonamide acetazolamide, with an inhibition constant of 49 nM. It was moderately inhibited by halides, pseudohalides, hydrogen sulfide, bisulfite and sulfate (K_I values of 0.67 - 1.36 mM) and more potently by sulfamide (K_I of 0.15 mM). Bicarbonate, nitrate, nitrite and phenylarsonic/boronic acids were much weaker inhibitors (K_Is of 26.9 - 43.7 mM).

Conclusions: The Drosophila β-CA represents a highly active mitochondrial enzyme that is a potential model enzyme for anti-parasitic drug development.

Background

Carbonic anhydrases (CAs, EC 4.2.1.1) catalyze the reversible hydration of carbon dioxide according to the following reaction: $CO_2 + H_2O \leftrightarrow HCO_3^- + H^+$ [1]. CAs are zinc-containing metalloenzymes, except for the ζ form, which uses cadmium [2,3] as alternative metal cofactor. Additionally γ-CAs contain iron *in vivo*, at least in anaerobic *Archaea* [4,5]. The reaction catalyzed by CAs is crucial in the regulation of acid-base balance in organisms. In addition, CAs participate in many other physiological processes such as bone resorption in vertebrates, gluconeogenesis, production of body fluids, and transport of CO_2 and HCO_3^- to name but a few [1].

To date, five different classes of CAs have been identified: α, β, γ, δ and ζ [6]. A previously known ε-CA class [7] has been reclassified as a new type of β-CA based on its crystallographic structure [8], which shows a fold nearly identical to those of the archaeal cab-type [9] and plant-type [10] β-CAs. In ζ-CA, the geometry of the active site is nearly identical to that of β-CAs, and there is also some similarity in the fold, which has led to the

* Correspondence: leo.syrjanen@uta.fi
[1]Institute of Medical Technology, University of Tampere and Tampere University Hospital, Tampere, Finland

suggestion that even ζ-CAs might represent a distantly diverged subtype of β-CAs [3].

The ζ-CAs are found only in diatoms, and the δ-CAs in diatoms and other marine phytoplankton, whereas the three major classes (α, β and γ) are widely distributed. γ-CA orthologs are present in *Archaea, Bacteria* and plants [6,11] but have been secondarily lost in animals and fungi [12] (M. Tolvanen, unpublished observation). The α class is missing from *Archaea* (M. Tolvanen, unpublished observation) but is nearly ubiquitously present in *Bacteria* and *Eukarya*, with the exception of *Fungi*, in which only filamentous ascomycetes have α-CAs [12]. In plants and animals, α-CAs exist as numerous isoforms. For example, 16 and 15 α-CAs have been described in non-primate mammals and primates including humans, respectively [1,13]. β-CAs appear to be the class with the widest distribution as they have been described in multiple lineages throughout the tree of life, including most species belonging to the *Archaea* and *Bacteria* domains and probably all species of plants and fungi among *Eukarya* ([14] and M. Tolvanen, unpublished data). β-CAs have also been characterized in a number of human pathogens such as fungi/yeasts (e.g., *Candida albicans*, *Candida glabrata, Cryptococcus neoformans* and *Saccharomyces cerevisiae*) [15-20] and bacteria (*Helicobacter pylori*, *Mycobacterium tuberculosis*, *Haemophilus influenzae*, *Brucella suis* etc.) [21-25], and their inhibition profiles by various agents such as sulfonamides, anions, carboxylates and boronic acids have been explored [15-24,26-30]. Given that β-CA genes appear to be missing in invertebrates, novel antimicrobial compounds based on the inhibition of β-CAs from pathogenic organisms may soon become available.

Although β-CAs catalyze the same reaction as α-CAs and other CA forms, important structural differences between these classes exist. First, instead of functioning as obligate monomers like most α-forms or trimers like γ-forms, β-CAs are found in many oligomerization states. Crystal structures of dimeric, tetrameric and octameric β-CAs have been reported [9,10,31]. In the active site of β-CAs, the zinc atom is coordinated by one histidine and two cysteine residues instead of three histidine residues present in α-, γ- and δ-CAs [32]. Despite this difference, β-class CAs basically share the same molecular mechanism for reversible hydration of carbon dioxide as α-class CAs [9]. β-CAs possess a highly conserved dyad comprising an aspartate and an arginine residue that seem to be crucial for the catalytic mechanism since mutation of these residues severely reduces the catalytic activity of the enzyme [33]. The aspartate makes a hydrogen bond with the Zn(II) coordinated water molecule, activating it for nucleophilic attack of the CO_2 molecule [29].

β-CAs have been reported in many photosynthetic organisms, including plants and algae [6]. In plants, β-class CAs are strongly expressed in both roots and green tissues and are located in chloroplasts, cytoplasm and mitochondria with isozyme-specific patterns [13,34]. The cytoplasmic and chloroplastic CAs are suggested to be crucial in CO_2 accumulation and carbon fixation. The green algae *Chlamydomonas reinhardtii* also contains β-class CAs that are localized to mitochondria [35]. In fungi like *Cryptococcus neoformans* and *Candida albicans*, β-CAs have an important role in CO_2 sensing and, consequently, in the pathogenesis of these species [36]. In addition, many fungal β-CAs have been shown to be mitochondrial [12]. These and many other similar findings confirm that β-CAs are physiologically important enzymes with variable localization and function like α-CAs in vertebrates.

The presence of β-CAs in the animal kingdom has been controversial or ignored due to the paucity and poor quality of the available sequences [6,14]. Here we show, however, that β-CAs are widespread among invertebrates. The aim of this study was to express, purify and characterize a β-CA enzyme from fruit fly (*D. melanogaster*), a commonly used model organism in biological sciences. The recombinant enzyme was produced in Sf9 insect cells using the baculovirus/insect cell expression system. Along with the characterization of the first arthropod β-CA, this study also describes its inhibition profile with inorganic anions. These results might open new strategies for developing novel anti-parasitic drugs against common diseases like schistosomiasis and malaria.

Results

Sequence analysis

We found β-CAs in all complete non-chordate animal genomes and in almost all invertebrates with at least 20,000 EST sequences in the NCBI database, plus in some with fewer sequences. We confirmed the existence of β-CA sequences in *Placozoa, Cnidaria, Platyhelminthes, Nematoda, Arthropoda*, and *Annelida*, and even in many classes of *Deuterostomia*, namely in *Hemichordata, Echinodermata*, and *Xenoturbellida*. The only major taxon of *Protostomia* with poor evidence for β-CA is *Mollusca*, in which we found only one EST to match 55 residues in other β-CAs. Of special interest were numerous pathogenic helminth species with complete β-CA sequences or substantial fragments, namely, filaria-causing *Brugia malayi*, mouse whipworm *Trichuris muris*, dog hookworm *Ancylostoma caninum*, and the flukes *Schistosoma mansoni* and *Schistosoma sinensis*.

In the case of chordates, the existence of a functional β-CA is currently unclear. The genomes and NCBI EST

sequence collections (as of 1st Oct, 2009) of *Ciona intestinalis* and *Ciona savignyi* (tunicates) lack β-CA, whereas we found two recognizable but incomplete β-CA sequences in the genome of the cephalochordate *Branchiostoma floridae* (of one locus from both haplotypes in the genome). The encoded proteins seem to lack more than 60 residues at the N-terminus, including the active site. In addition, there are two even less complete partial EST transcripts, GenBank BW824885 and BW803919. The latter contains an unrelated sequence in place of the active-site-containing exon. We can only conclude that it remains an open question whether β-CA in *B. floridae* is a pseudogene or an incompletely sequenced active gene.

Our survey discovered and assembled 38 seemingly complete and correct β-CA sequences from the genome and sequence databases of 33 metazoan species, including improved gene models for sequences already in sequence databases. Fragmentary β-CA sequences were found in additional 22 species. Multiple sequence alignment of all animal β-CAs shows perfect conservation of the known active site motifs CxDxR and HxxC and several other key residues. Figure 1 shows an alignment of the first 120 residues of selected β-CA sequences, including the N-terminal mitochondrial targeting peptide and active site regions (See Table 1 for identification of species). Of the active-site residues indicated below the alignment, two cysteines and one histidine are zinc-binding residues. Additional files 1 and 2 show the full alignment of the same sequences and of all of the identified sequences, respectively. The phylogenetic tree of the selected animal β-CA sequences is shown in Figure 2 (See Table 1 for identification of species). The tree indicates that the duplication of β-CA genes in nematodes is specific for the nematode lineage. Out of the two copies, the one labeled BCA2 is more strongly conserved, as shown by shorter branches in the tree of Figure 2 and in trees we made with all available sequences. The placement of the β-CA from acorn worm (*S. kowalevskii*, a hemichordate) seems contrary to conventional invertebrate taxonomy, but since some of the bootstrap values are under 50%, the tree is not perfectly resolved outside the insect and nematode blocks.

No β-*CA* sequences exist in vertebrate genomes. A false positive is found in the *X. tropicalis* genome, scaffold_1719, which we attribute to bacterial contamination, since the β-CA sequence and every other gene in this scaffold are highly similar (>80% identical) with known genes of *Pseudomonas*-related bacteria.

All of the complete sequences are classified as β-CA domains of type "BCA_CladeB" in the NCBI Conserved Domain Database. All plant β-CAs are also classified as BCA_CladeB domains, so animal β-CAs can well be said to be "plant-type β-CAs". There are also hundreds of bacterial β-CA sequences of type "BCA_CladeB", and some of them cluster closest to animal sequences, and some closest to plant sequences in phylogenetic trees (data not shown).

Expression of β-CA in Sf9 insect cells

Sf9 insect cells were transfected with the β-CA gene (*DmBCA*) obtained from *D. melanogaster* cDNA. The amount of protein obtained from 500 ml of culture supernatant was approximately 1 mg. According to SDS-PAGE, the relative molecular mass of DmBCA was approximately 28 and 27 kDa before and after thrombin treatment, respectively (Figure 3).

Subcellular localization of DmBCA

When the collection of 38 complete animal β-CA sequences was analyzed for subcellular targeting with

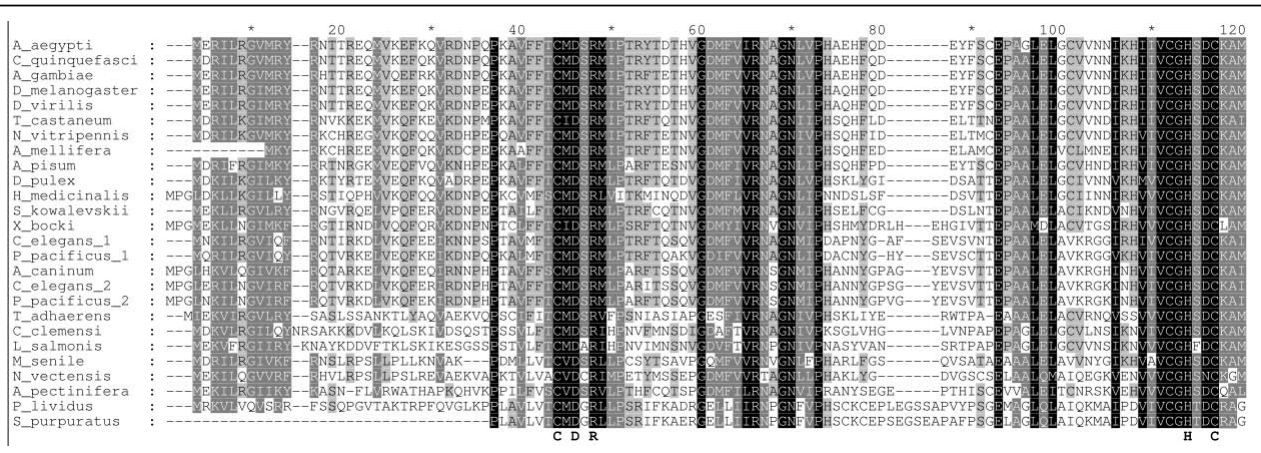

Figure 1 Alignment of 26 β-CA sequences from invertebrate species. Only the first 120 residues are shown. Active-site residues C, D, R, H and C are highlighted below the alignment. These residues are found in all β-CAs. See Table 1 for identification of species.

Table 1 Identification of sequences and species in the sequence alignment and phylogenetic tree

Abbreviation	Full name	Common name and classification	gi or accession numbers
A_aegypti	*Aedes aegypti*	Yellow fever mosquito, insects	157110803 + 77891004
C_quinquefasciatus	*Culex quinquefasciatus*	Southern house mosquito, insects	170043321
A_gambiae	*Anopheles gambiae*	Malaria mosquito, insects	57968460
D_melanogaster	*Drosophila melanogaster*	Fruit fly, insects	24645213
D_virilis	*Drosophila virilis*	Fruit fly, insects	194152748
T_castaneum	*Tribolium castaneum*	Red flour beetle, insects	91084165
N_vitripennis	*Nasonia vitripennis*	Wasp, insects	156547528
A_mellifera	*Apis mellifera*	Honeybee, insects	110764310
A_pisum	*Acyrthosiphon pisum*	Pea aphid, insects	193713675
D_pulex	*Daphnia pulex*	Water flea, crustaceans	FE417346 + FE409868
H_medicinalis	*Hirudo medicinalis*	Medical leech, Annelid worms	EY481200 + EY505051 + EY490477
S_kowalevskii	*Saccoglossus kowalevskii*	Acorn worm, hemichordate	187043763
X_bocki	*Xenoturbella bocki*	Xenoturbella, Xenoturbellidae	117195962
C_elegans_1	*Caenorhabditis elegans* BCA1	Nematode	NP_741809.1
P_pacificus_1	*Pristionchus pacificus* BCA1	Nematode	FG098717 + GeneWise
A_caninum	*Ancylostoma caninum*	Dog hookworm, nematodes	FC551456 + FC550353
C_elegans_2	*Caenorhabditis elegans* BCA2	Nematode	NP_001041015
P_pacificus_2	*Pristionchus pacificus* BCA2	Nematode	FG106379 + GeneWise
T_adhaerens	*Trichoplax adhaerens*	Trichoplax, Placozoa	190581916
C_clemensi	*Caligus clemensi*	Sea louse, crustaceans	225719368
L_salmonis	*Lepeophtheirus salmonis*	Sea louse, crustaceans	225713548
M_senile	*Metridium senile*	Sea anemone, Cnidaria	FC835283
N_vectensis	*Nematostella vectensis*	Sea anemone, Cnidaria	XP_001632619
A_pectinifera	*Asterina pectinifera*	Starfish, Echinodermata	DB424979 + DB440523
P_lividus	*Paracentrotus lividus*	Sea urchin, Echinodermata	139313180 + 139245724
S_purpuratus	*Strongylocentrotus purpuratus*	Purple sea urchin, Echinodermata	XP_001189115

TargetP, 22 sequences were predicted to be mitochondrial, with low reliability, and most of the remaining sequences were predicted to be cytoplasmic, again with low reliability. The results from WolF PSORT, Secretome 2.0 and MitoProt II v. 1.101 also supported the hypothesis that it is a mitochondrial enzyme, with a possibility for non-classical secretion (without a signal peptide) suggested by Secretome 2.0. A mitochondrial targeting signal sequence is also predicted in the N-terminus (prediction lengths varying from 14 in MitoProt to 49 in TargetP). Based on these findings, a DmBCA-GFP construct was designed to study the subcellular localization of the protein in Sf9 cells.

According to our experiments on the DmBCA-GFP fusion protein, DmBCA is indeed a mitochondrial protein, supporting the predictions made by bioinformatic tools. Figure 4A shows the DmBCA-GFP recombinant protein in Sf9 insect cells in which the positive signal was located in intracellular granular structures. Figure 4B shows the same cells labeled with a mitochondrial marker, MitoTracker Red CMXros™. Figure 4C presents an overlay of the previous panels, demonstrating the colocalization of DmBCA-GFP and MitoTracker Red CMXros™.

Catalytic activity and inhibition of DmBCA

DmBCA purified from Sf9 cells was kinetically analyzed in the presence or absence of acetazolamide or inorganic anions. The kinetic parameters of DmBCA (k_{cat} and k_{cat}/K_m) were then compared with those of the thoroughly investigated CAs such as the cytosolic and ubiquitous human isozymes α-CA I (HCA I) and II (HCA II), as well as the recently described fungal β-CAs, *C. neoformans* Can2, *C. albicans* Nce103, *S. cerevisiae* CA (ScCA) and *C. glabrata* CA (CgCA). All of these fungal enzymes are orthologous to *Nce103*, a protein found in all fungi/yeasts studied to date (Table 2).

One can appreciate from the data shown in Table 2 that DmBCA, similar to the other recently investigated α- and β-CAs, possesses considerable CO_2 hydratase activity. A k_{cat} of 9.5×10^5 s^{-1} and a k_{cat}/K_m of 1.1×10^8 $M^{-1}s^{-1}$ make DmBCA one the most efficient β-CA described to date. Data from Table 2 also show that DmBCA was appreciably inhibited by the clinically-used sulfonamide acetazolamide (5-acetamido-1,3,4-thiadiazole-2-sulfonamide), with an inhibition constant of 49 nM. Table 3 shows the DmBCA inhibition screening data with anionic physiological species (such as chloride, bicarbonate, sulfate, etc.) as well as other non-

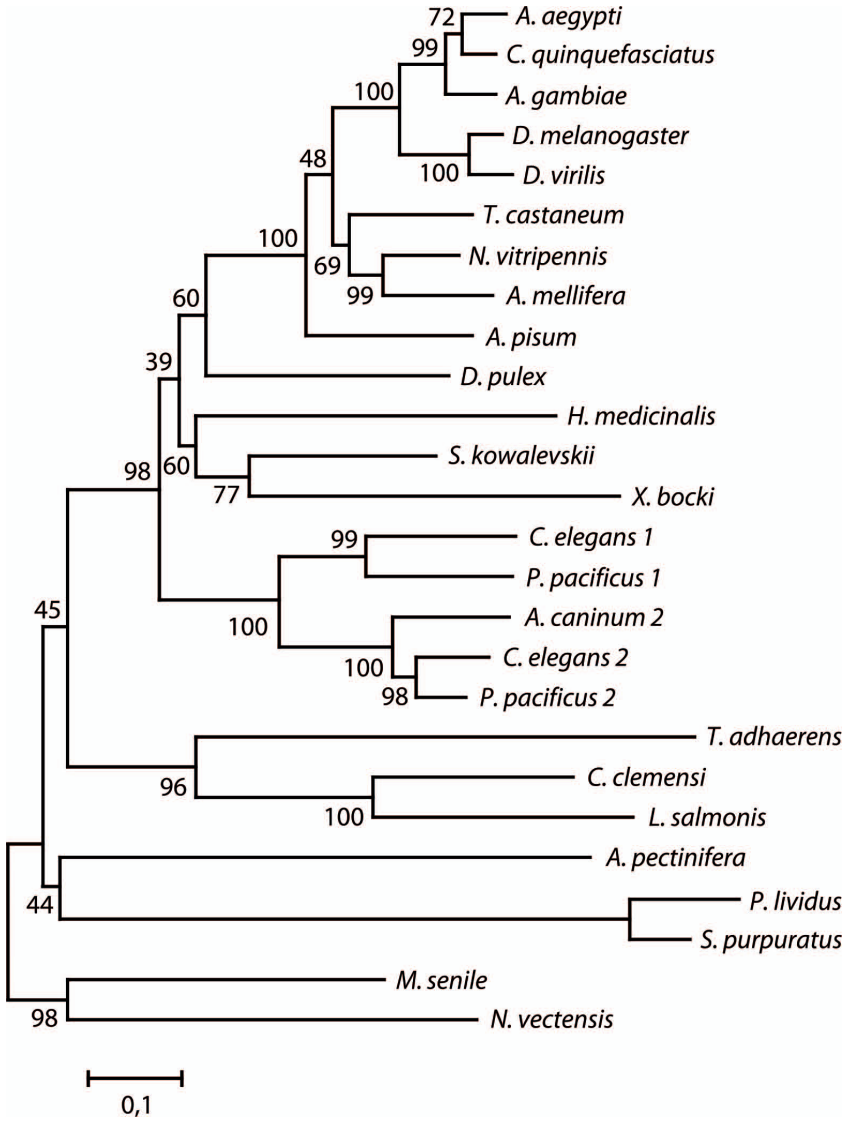

Figure 2 Minimum-evolution tree of 26 invertebrate β-CA sequences. Bootstrap consensus tree of 1,000 replicates. The percentage of replicate trees in which the associated taxa clustered together in the bootstrap test are shown next to the branches. See Table 1 for identification of species.

physiological anions. Note that similar to other investigated α- and β-CAs, DmBCA has an inhibition profile with anions characteristic only for this enzyme. Several species such as bicarbonate, nitrate, nitrite, perchlorate, phenylboronic acid and phenylarsonic acid behaved as weak inhibitors (K_Is in the range of 22.4 - 200 mM), whereas other anions inhibited the enzyme more potently (e.g., cyanide, cyanate, and sulfamide, with inhibition constants in the range of 150 - 730 μM).

Dynamic light scattering and gel filtration analysis

The hydrodynamic diameters of the proteins were measured by dynamic light scattering (DLS). At a temperature range from 4°C to 37°C the hydrodynamic diameter of DmBCA was 6.3 ± 0.8 nm and the diameter was found to slightly increase during the heating. According to the hydrodynamic diameter the average molecular weight of DmBCA was estimated to be 48.9 kDa, the lowest estimate being 35.4 kDa, and the highest 64.9 kDa (n = 30). When temperature was raised above 43°C the hydrodynamic diameter of DmBCA started to clearly increase and DmBCA had a transition state at temperature range 46-49°C, where large protein aggregates appeared. This might be associated with protein denaturation.

At the temperature range from 4°C to 37°C the hydrodynamic diameter of HCA II was 3.9 ± 0.6 nm leading to estimated average molecular weight of 16.1 kDa, the

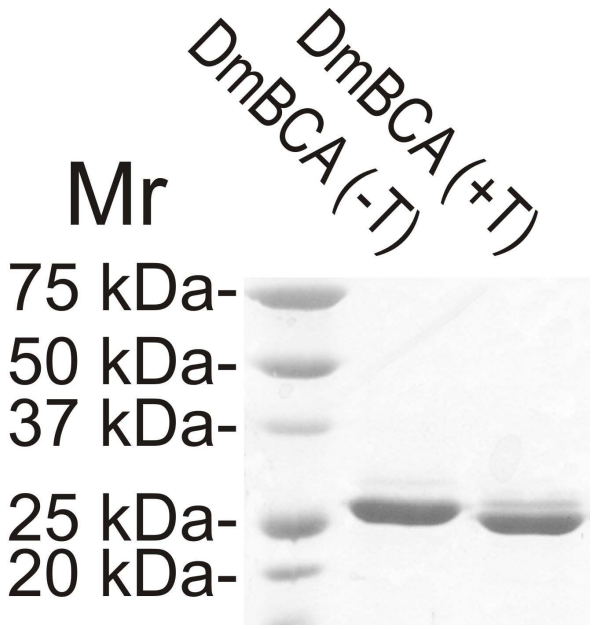

Figure 3 SDS-PAGE of the produced DmBCA. T = thrombin treatment.

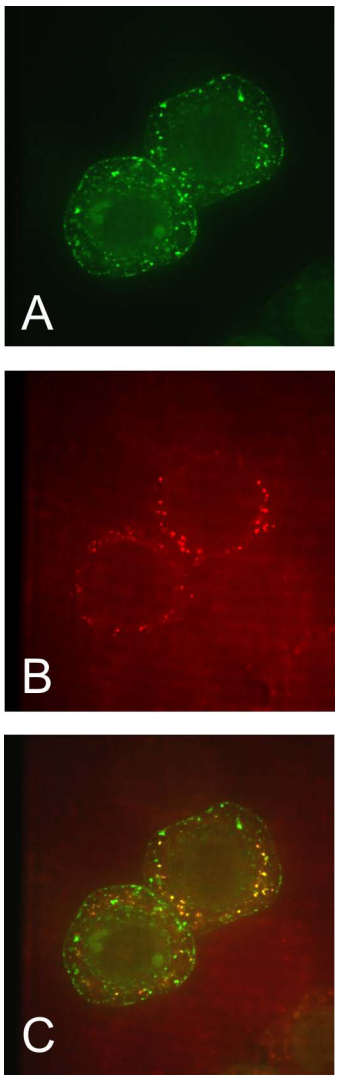

Figure 4 Double immunofluorescence staining of DmBCA-GFP and mitochondria in Sf9 cells. Green fluorescent signal shows the location of the DmBCA-GFP fusion protein (A), and the red color labels the mitochondria (B). The yellow color in panel C indicates the colocalization of these two labels.

lowest estimate being 10.8 kDa, and the highest 22.8 kDa (n = 12). When HCA II was heated from 4°C to 43° C there was a slight increase in hydrodynamic diameter. However, no transition states were observed.

The estimated molecular weights determined by DLS are in agreement with the values obtained by analytical gel filtration which gave a molecular weight estimate for DmBCA of 38.1 ± 3.0 kDa and for HCA II of 23.4 ± 4.0 kDa. The molecular weight of HCA II monomer is 29 kDa. Therefore, gel filtration analysis appears to underestimate the molecular size of CAs. Overall, DLS and gel filtration analyses suggest dimeric state for DmBCA whereas HCA II appears predominantly monomeric in solution.

Discussion

In the present study, we identified and characterized a novel β-CA enzyme (DmBCA) from an arthropod, *D. melanogaster*. Although β-CAs have been previously reported in *Archaea* and *Bacteria* domains, in addition to plants and fungi in *Eukarya*, our results suggest the widespread occurrence of at least a single-copy β-CA gene among animal species distinct from chordates. The loss of β-*CA* gene in the chordate lineage may have occurred either in the last common ancestor of all chordates or in the last common ancestor of tunicates and craniates. Whether cephalochordates have a functional β-*CA* gene remains an unresolved question.

Using bioinformatic tools, we discovered a single β-*CA* gene in most invertebrates with reasonable sequence coverage. The exception is nematodes, which seem to have two β-*CA* genes in their genomes. A very recent article [37] reported the cloning and characterization of *C. elegans* β-CAs and the authors found that one of the two isoforms, BCA-1, has no activity and does not work in complementation assay. This might, however, be due to incorrect sequence: the sequence they show for *C. elegans* BCA-1 contains the coding sequence of the preceding *MTP18* gene fused to the β-*CA* reading frame. This sequence is a result of an incorrect gene prediction which has no support at the mRNA level and which remained in WormBase and UniProt until May 2008, subsequently corrected from our initiative. The previously fused

Table 2 Kinetic parameters for the CO2 hydration reaction catalyzed by various CAs

Isozyme	Activity level	k_{cat} (s^{-1})	k_{cat}/K_m ($M^{-1}s^{-1}$)	K_I (nM)[c]
HCA I[a]	moderate	2.0×10^5	5.0×10^7	250
HCA II[a]	very high	1.4×10^6	1.5×10^8	12
Can2[a]	moderate	3.9×10^5	4.3×10^7	10.5
Nce103[a]	high	8.0×10^5	9.7×10^7	132
ScCA[a]	high	9.4×10^5	9.8×10^7	82
CgCA[a]	moderate	3.8×10^5	4.8×10^7	11
DmBCA[b]	high	9.5×10^5	1.1×10^8	49

Kinetic parameters for the human cytosolic isozymes human HCA I and II (α-class CAs) at 20°C and pH 7.5 in 10 mM HEPES buffer and 20 mM Na_2SO_4, in addition to the β-CAs Can2, Nce103 (from *C. neoformans* and *C. albicans*, respectively), ScCA (from *S. cerevisiae*), CgCA (from *C. glabrata*) and DmBCA (from *Drosophila melanogaster*) measured at 20°C, pH 8.3 in 20 mM Tris buffer and 20 mM $NaClO_4$ are shown. Inhibition data with the clinically used sulfonamide acetazolamide (5-acetamido-1,3,4-thiadiazole-2-sulfonamide) are also provided.

[a]Reference [30]

[b]This work

[c]acetazolamide

Table 3 Inhibition constants of anionic inhibitors against various CAs

Inhibitor	K_I [mM][#]				
	HCA II	Nce103	ScCA	CgCA	DmBCA
F^-	>300	0.69	2.85	0.36	0.80
Cl^-	200	0.85	0.85	0.58	0.97
Br^-	63	0.94	0.0108	27	1.04
I^-	26	1.40	0.0103	42.4	1.18
CNO^-	0.03	1.18	31.7	0.60	0.73
SCN^-	1.6	0.65	55.6	0.73	1.28
CN^-	0.02	0.011	16.8	1.12	0.67
N_3^-	1.5	0.52	27.9	1.03	1.12
HCO_3^-	85	0.62	0.78	0.086	26.9
NO_3^-	35	0.69	13.9	0.097	43.7
NO_2^-	63	0.53	0.46	0.088	28.6
HS^-	0.04	0.37	0.33	0.10	1.01
HSO_3^-	89	0.54	0.33	0.10	1.29
SO_4^{2-}	>200	14.15	0.58	0.58	1.36
ClO_4^-	>200	>200	>200	>200	>200
$H_2NSO_2NH_2$	1.13	0.30	0.0087	0.42	0.15
H_2NSO_3H[§]	0.39	0.70	0.84	0.11	2.45
Ph-$B(OH)_2$	23.1	30.8	38.2	0.10	22.4
Ph-AsO_3H_2[§]	49.2	30.8	0.40	0.098	32.6

Inhibition constants against isozymes HCA II (α-CA class), and the β-CAs Nce103 (from *C. albicans*), ScCA (from *S. cerevisiae*), CgCA (from *C. glabrata*) and DmBCA (*D. melanogaster*) for the CO_2 hydration reaction at 20°C are shown.

[§]As sodium salt.

[#] Errors in the range of 5-10% of the shown data, from three different assays, by a CO2 hydration stopped-flow assay.

UniProt entry Q8T3C8 now represents only MTP18, and a new entry BCA1_CAEEL contains the more plausible BCA-1 sequence. Since *C. elegans* BCA-1 has all of the active-site residues and is also well conserved in other nematodes, we think it is probable that both isozymes in nematodes would be functional β-CAs.

Our larger phylogenetic analysis (M. Tolvanen, unpublished data) and NCBI domain classification of animal β-CAs clearly show them to be "plant-type" β-CAs. The "plant-type" group also includes hundreds of bacterial β-CAs, and this group contains plant/bacterial and animal/bacterial subgroups. The presence of such polyphyletic subgroups may indicate horizontal gene transfer, and further investigations are underway to study this phenomenon.

Fasseas *et al.* [37] state that the 3D structure of their *C. elegans* β-CA models would resemble archaeal "cab-type" β-CAs, but we cannot agree with their conclusion. In our eyes, the models are nearly identical to the pea BCA (panel a in their Figure 2), and in our hands Swiss-Model http://swissmodel.expasy.org/ in fact chooses the pea β-CA structure as a template for both insect and nematode β-CAs.

In the recent paper by Fasseas *et al.* [37], the enzyme activity of *C. elegans* Y116A8C.28 was reported to be typical for β-CAs, with a k_{cat} and k_{cat}/K_m of 2.77×10^4 s^{-1} and $6,383 \times 10^5 M^{-1}s^{-1}$, respectively. These values are significantly lower than the k_{cat} of 9.5×10^5 s^{-1}, and k_{cat}/K_m of 1.1×10^8 $M^{-1}s^{-1}$ that we report here for DmBCA. The enzymatic activity of DmBCA is one of the highest reported so far for a β-CA, suggesting an important physiological role for this enzyme.

Our studies with different anionic CA inhibitors did not reveal specific inhibitors of DmBCA, which is in fact normal for such simple inorganic ions [38]. The inhibition profile of DmBCA was unique for this enzyme, however, and differed significantly from other β-CAs studied previously.

Indeed, fluoride, chloride, cyanate, cyanide and sulfamide showed submillimolar inhibitory activity against DmBCA, with inhibition constants in the range of 150 μM - 970 μM. Another groups of anions, including bromide, iodide, thiocyanate, azide, hydrogen sulfide, bisulfite and sulfate showed inhibition constants close to 1 mM (K_Is in the range of 1.01 - 1.36 mM), thus making them weak DmBCA inhibitors. Other anions such as bicarbonate, nitrate and nitrite, as well as the non-anionic species phenylboronic acid and phenylarsonic acid, were much less effective inhibitors, with inhibition constants of 22.4 - 43.7 mM. It is interesting to note that bicarbonate, a CA substrate, is a weak DmBCA inhibitor, but it appreciably inhibits the fungal enzymes Nce103 (C. Albicans), ScCA and CgCA, with K_Is in the submillimolar range (of 86 μM - 0.78 mM). Even though the low apparent K_I value for bicarbonate could be a reflection of allosteric inactivation of the enzyme ([39,40]), the value is still in the same range with the other anion inhibitors, suggesting that their mechanism

of inhibition might be quite similar. The present inhibition data may suggest a different physiological role for DmBCA in the insect compared to the corresponding β-CAs in fungal or yeast species studied previously. One should also note that DmBCA has a completely different inhibition profile not only compared to other β-CAs but also compared to the highly investigated α-CA of human origin, HCA II (Table 3).

Animal β-CAs constitute a separate subgroup in the β-CA family according to our bioinformatic analysis. Because the main target, β-CA, is present in many parasites and disease carrying vectors but absent in humans, this discovery clearly carries the significant potential for the design of parasite-specific β-CA inhibitors. Such drugs would presumably combine high specificity with a low incidence of side-effects in humans. These drugs could, for example, provide novel opportunities to restrict malaria propagation and to treat patients suffering from helminth infections.

Predictions of subcellular localization placed most, but not all, animal β-CAs in the mitochondria. Our hypothesis is that all of them will be mitochondrial based on three main reasons. First, we have direct experimental evidence of mitochondrial localization of DmBCA. Second, all of the TargetP predictions were either mitochondrial or cytoplasmic, both with low-reliability. Third, the neural network used in TargetP is trained with human and Arabidopsis mitochondrial proteins; thus, it is perhaps not perfectly adjusted to detect the signals in invertebrate mitochondrial transit peptides. Because of this mitochondrial localization of animal β-CAs, we speculate that the β-CA gene in chordates might have been silenced and ultimately lost after the emergence of mitochondrial α-CAs (CA V) to substitute for this function. The presence of an active CA in mitochondria has been linked to maintaining fundamental metabolic functions such as gluconeogenesis, ureagenesis and lipogenesis [1,41]. Although our experiments were not focused on the role of the DmBCA enzyme, its mitochondrial localization and high enzymatic activity suggest that knockdown studies in *D. melanogaster* are warranted to further investigate the physiological function of β-CAs in animals.

The expression of DmBCA has been studied at mRNA level in two publicly available DNA microarray datasets. In FlyAtlas (http://flyatlas.org/atlas.cgi?name=CG11967-RA, [42]) expression levels in 17 adult and 8 larval *D. melanogaster* tissues are given. The highest upregulated values in adult are found in spermatheca (female), fat body, and heart. In larval tissues (third instar) downregulated or average expression levels are seen for all tissues. A time course study published in FlyBase (http://flybase.org/reports/FBgn0037646.html, under Microarray data, Personal communications to FlyBase, Gaurav et al. 2008), shows upregulated expression of DmBCA in early larval stages and late in metamorphosis, but downregulated levels in embryonal, late larval, early metamorphosis, and adult stages. The specific temporal and tissue patterns of expression suggest relevant functional and/or physiological roles for DmBCA.

Conclusions

In conclusion, fruit fly (*Drosophila melanogaster*) β-CA (DmBCA) is an active mitochondrial enzyme for the physiological reaction catalyzed by CAs, the hydration of CO_2 to bicarbonate and protons. It is inhibited by various inorganic anions, boronic/arsonic acids or sulfonamides. Mammals do not possess β-class CAs, but these enzymes are widespread throughout the phylogenetic tree, making them exciting new targets for parasitic drug development. Indeed, β-CAs are found in many pathogenic organisms and pathogen vectors of the animal kingdom, including the malaria mosquito *Anopheles*, the yellow fever mosquito *Aedes*, the filariasis vector *Culex, Ancylostoma* hookworms, *Brugia* filarial nematodes, the blood fluke *Schistosoma mansoni* and the liver fluke *Schistosoma sinensis*. Because animal-derived β-CAs probably have a different predicted structure compared to the β-CAs investigated so far in detail from Archaea, plants, algae and fungi, as well as the α-CAs, specific inhibitors against these enzymes could be designed with minimal effect on human CAs and normal bacterial flora.

Methods

Bioinformatic analysis

Taking advantage of the known pea β-CA (UniProt P17067) as an initial query, and subsequently the found invertebrate β-CAs (*D. melanogaster*, AAF54311; *C. elegans* CAJ43916), the animal CA sequences were retrieved from NCBI protein databases using Blast [43] http://blast.ncbi.nlm.nih.gov/Blast.cgi and from complete genomes at the UCSC Genome Bioinformatics Site http://genome.ucsc.edu using BLAT search algorithms [44]. Hits were taken through iterated cycles of multiple sequence alignment (ClustalW; [45]), evaluation and revision. For revision, sequences with poorly matching or missing regions were subjected to gene model generation with GeneWise ([46]; http://www.ebi.ac.uk/Tools/Wise2/), taking the genomic sequences from the UCSC site. EST and mRNA sequence data from NCBI were used to confirm gene models, sometimes to bridge gaps or fill ends in the genomic sequences, and to discover and assemble β-CAs from less than genome-wide sequenced organisms.

Phylogenetic trees were constructed from the multiple sequence alignments using MEGA 4 [47]. Preliminary Neighbour-Joining trees [48] were constructed with all

sequences, and a representative set of 26 sequences was then selected for a final tree, eliminating excessive insect and nematode sequences and severely incomplete sequences. The final tree was inferred using the Minimum evolution method [49] from a multiple sequence alignment containing columns corresponding to positions 31 to 255 (of 255) of DmBCA. The bootstrap consensus tree inferred from 1,000 replicates [50] was taken to represent the evolutionary history of the analyzed sequences. The tree was drawn to scale, with branch lengths proportional to the evolutionary distances used to infer the phylogenetic tree and rooted using the Cnidarian sequences as outgroup. The evolutionary distances were computed using the Poisson correction method and are presented in the units of the number of amino acid substitutions per site. The minimum evolution tree was searched using the Close-Neighbor-Interchange algorithm [51] at a search level of 3. The Neighbor-Joining algorithm [48] was used to generate the initial tree. All positions containing alignment gaps and missing data were eliminated only in pairwise sequence comparisons (Pairwise deletion option).

Predictions of subcellular localization were made using TargetP v1.1 ([52]; http://www.cbs.dtu.dk/services/TargetP/), Secretome 2.0 http://www.cbs.dtu.dk/services/SecretomeP/, WolF PSORT, http://wolfpsort.org/ and MitoProt II v. 1.101 http://ihg2.helmholtz-muenchen.de/ihg/mitoprot.html. Conserved domain types were identified at the NCBI Conserved Domains Database http://www.ncbi.nlm.nih.gov/Structure/cdd/cdd.shtml.

Construction of recombinant baculoviruses

Two constructs were engineered to study functional aspects of *D. melanogaster* β-CA (DmBCA). The first one contained a *GFP* (Green Fluorescent Protein) sequence fused C-terminally to the *DmBCA* cDNA for detection of the recombinant protein with confocal microscopy. The second construct contained a C-terminal histidine tag for protein purification. Both constructs contained full length β-CA gene, including the proposed N-terminal signal sequence. *Bgl*II and *Xho*I restriction sites and a thrombin cleavage site (for tag removal) were introduced into both constructs.

Total RNA extracted from *D. melanogaster* S2 cells (TRIzol® reagent and protocol, Invitrogen) was precipitated using sodium acetate at a final concentration of 100 mM and 100% ethanol. The solution was centrifuged at 13,000×*g* for 15 min at +4°C. The RNA sample was washed once with 70% ethanol and recentrifuged in the same manner. The sample was evaporated at room temperature and then suspended in sterile water. Precipitated RNA was transcribed into cDNA using a First strand cDNA Synthesis Kit #K1612 (Fermentas) according to the manufacturer's instructions.

The *DmBCA* gene was identified and amplified from cDNA by PCR using Phusion™ Hot Start High Fidelity DNA Polymerase (Finnzymes, Espoo, Finland). Sequence-specific primers were ordered from Sigma-Aldrich (St. Louis, MO). The forward primer was 5'-ATGGAGCGTATTTTGAGGGGAATC-3' (F1), and the reverse primer was 3'-CTACGAATAGAATCTTCT-GACCTC-5' (R1). PCR was performed in a PTC 2000 thermal cycler (MJ Research, Waltham, MA), and the program consisted of a single 98°C denaturation step for 30 s, followed by 33 cycles of denaturation at 98°C for 10 s, annealing at 53°C for 15 s and extension at 72°C for 25 s. A final extension was performed at 72°C for 5 min. The PCR product band was separated from the gel and dissolved using Illustra™ GFX PCR DNA and GEL Band Purification Kit (GE Healthcare Life Sciences, Buckinghamshire, UK).

To engineer the *DmBCA-GFP* construct, the sequences of *DmBCA* and *GFP* were first amplified separately using sequence specific primers. The templates used for *DmBCA* and *GFP* were *DmBCA* gene product obtained from cDNA and pEGFP-N1™ Vector (Clontech), respectively. The constructs were then combined using PCR reactions whose R2 and F3 primer sequences partly overlapped (bolded in the primer sequences, see below). This allowed the ends of the PCR products to recognize each other. The forward primer used for *DmBCA* amplification was 5'- GGCCAGATC-TATGGAGCGTATTTTGAGGGGA-3' (F2), and the reverse primer was 5'-**CACGGAACCACGGGGCAC-CAG**CGAATAGAATCTTCTGACCTC-3' (R2). The bolded sequence was designed to recognize the thrombin site and part of the *GFP* PCR product, while the other half recognized the *DmBCA* PCR product.

The forward primer used for GFP amplification was 5'-**TCGCTGGTGCCCCGTGGTTCCGTG**AGCAAG GGCGAGGAGCTG-3' (F3), and the reverse primer was 5'-CCGCTCGAGTTACTTGTACAGCTCGTCCAT-3' (R3). The bolded sequence in the F3 primer was designed to recognize the thrombin site and part of the *DmBCA* PCR product, while the other half recognized the *GFP* PCR product. The PCR program was as follows: 98°C for 2 min; then 33 cycles of 98°C for 10 s, 55°C for 15 s, and 72°C for 30 s; and finally 72°C for 7 min.

Both PCR products were run on agarose gel, purified and used as templates in the next PCR reaction. The PCR program was as follows: 98°C for 2 min; then 33 cycles of 98°C for 10 s, 55°C for 15 s and 72°C for 40 s; and finally 72°C for 8 min. The forward primer used in this PCR was (F2), and the reverse primer was (R3). The extra sequence overlaps at the 3' end of *DmBCA* and at the 5' end of the *GFP* allowed these PCR products to anneal to each other.

The PCR product was run on an agarose gel, and the obtained band was purified. pFastBac™ 1 plasmid (Invitrogen) and the PCR product were digested at +37°C overnight with *BamHI* and *XhoI* restriction enzymes (New England Biolabs). The digested plasmid and *DmBCA-GFP* construct were purified and then ligated overnight at +4°C using T4 DNA ligase (New England Biolabs). The ligated product was transformed into TOP10 bacteria (Invitrogen). Overnight cultures (8 ml) were made from these colonies, and plasmids were purified using a QIAprep Spin Miniprep Kit™ (Qiagen, Hilden, Germany). Sequencing was performed to verify the validity of the *DmBCA-GFP* construct. The construction of baculoviral genomes encoding the recombinant proteins has been described previously [53].

For recombinant protein production, the *DmBCA* gene construct with a C-terminal polyhistidine tag of six histidines was constructed and cloned into the pFastBac1™ vector. The forward primer used in the initial amplification of the *DmBCA* gene was (F2), and the reverse primer was 5'- GCCCTCGAGTTA**ATGGTGGTGATGGTGGTG**GGAACCACGGGGCACCAGCGAATAGAATCTTCTGACCTC -3' (R4). The latter primer contains nucleotide repeats to create the polyhistidine tag (bolded in the primer sequence). The PCR program was as follows: 98°C for 60 s; then 35 cycles of 98°C for 10 s, 66°C for 15 s, and 72°C for 60 s; and finally 72°C for 5 min. Otherwise, the construct was made essentially in the same way as the *DmBCA-GFP* construct described above.

Study of the subcellular localization of DmBCA

A total of 100 μl of Sf9 insect cells (2 million cells/ml) were infected with 10 μl of baculovirus stock. The cells were kept at +27°C in incubator for three days in Lab-Tek™ Chamber Slide™ System™ plates (Nunc). The medium was then removed, and the cells were incubated in 600 μl of medium containing 100 nM Mitotracker Red CMXros™ (Invitrogen) for 20 minutes at +27°C. The cells were washed three times with 600 μl of medium and kept at +27°C in an incubator for two hours. The cells were then washed with PBS, fixed with 4% paraformaldehyde for five minutes and washed again with PBS. The cells were mounted in Vecta-Shield® Mounting Medium (Vector Laboratories), covered with cover slips and analyzed using a confocal scanning laser microscope (Perkin Elmer-Cetus/Wallac UltraView LCI system™) with two different wavelengths: 488 nm for GFP detection and 579 nm for MitoTracker™. Image acquisition was performed with an Andor iXon™ DV885 EMCCD camera and the Andor iQ™ software (Andor).

Production and Purification of Recombinant Insect β-CA

The Sf9 insect cells were grown in HyQ SFX-Insect serum-free cell culture medium (HyClone, Logan, UT) in an orbital shaker at 27°C (125 rpm) for three days after infection. Although much of the DmBCA was associated with the cell pellet, protein purification was performed after centrifugation (5000 × g, 20°C, 8 min) from the supernatant and yielded highly pure DmBCA protein for characterization. Purification was performed using the Probond™ Purification System (Invitrogen) under native binding conditions, with wash and elution buffers made according to the manufacturer's instructions. The purification procedure per 500 ml of insect cell medium was as follows: 1 liter of native binding buffer and 25 ml of the nickel-chelating resin were added to the medium, and the His-tagged protein was then allowed to bind to the resin on a magnetic stirrer at 25°C for 3 h. The resin was washed with 100 + 30 ml of washing buffer (Invitrogen). The protein was then eluted with elution buffer (50 mM NaH_2PO_4, 500 mM NaCl, 250 mM imidazole, pH 8.0).

The purified DmBCA recombinant protein was transferred to a buffer of 50 mM Tris-HCl, pH 7.5, using an Amicon Ultracel™ - 10 k centrifugal filter device (Millipore) according to the manufacturer's instructions. To remove the His tag, the recombinant protein was treated with 60 μl of resin-coupled thrombin (Thrombin Clean-Cleave KIT™, Sigma) per 1 mg of protein with gentle shaking at 25°C for 1 h, according to the manufacturer's instructions. Protein concentration was determined using the DC Protein Assay™ (Bio-Rad) with three different dilutions. Purified recombinant DmBCA proteins were analyzed using 10% sodium dodecyl sulfate polyacrylamide gel electrophoresis (SDS-PAGE) under reducing conditions. The gels were stained using the Colloidal Blue Staining Kit™ (Invitrogen).

CA activity measurements

An Applied Photophysics stopped-flow instrument was used to assay the CA-catalyzed CO_2 hydration activity. Phenol red (at a concentration of 0.2 mM) was used as an indicator, working at the absorbance maximum of 557 nm, with 10 - 20 mM HEPES (pH 7.5) or Tris(pH 8.3) as buffers and 20 mM Na_2SO_4 or 20 mM $NaClO_4$ (for maintaining constant ionic strength), following the initial rates of the CA-catalyzed CO_2 hydration reaction for a period of 10 - 100 s. The CO_2 concentrations ranged from 1.7 to 17 mM for the determination of kinetic parameters and inhibition constants. For each inhibitor at least six traces of the initial 5-10% of the reaction were used to determine the initial velocity. The uncatalyzed rates were determined in the same manner and subtracted from the total observed rates. Stock solutions of inhibitor (100 mM)

were prepared in distilled-deionized water, and dilutions up to 0.01 μM were made thereafter with distilled-deionized water. Inhibitor and enzyme solutions were pre-incubated together for 15 min at room temperature prior to the assay to allow for the formation of the E-I complex. The inhibition constants were obtained by non-linear least-squares methods using PRISM 3, whereas the kinetic parameters for the uninhibited enzymes were obtained from Lineweaver-Burk plots, each representing the mean of at least three different determinations.

Kinetic measurements have been performed also with m-cresol purple (as indicator) - bicine (as buffer) (data not shown), and the results were the same (±5-10% of the reported values, which is the error range of this method) both for the kinetic parameters of CO_2 hydration and for the inhibition constants of anionic inhibitors investigated here. Thus, the standard method reported in this paper is reliable for the investigation of β-CAs (in addition to the α-CAs) as reported by this group for several enzymes, such as the three β-class enzymes from *Mycobacterium tuberculosis*, *Helicobacter pylori* and *Brucella suis*, and the fungal class enzymes (for example [25]).

Dynamic light scattering analysis

The hydrodynamic diameters of the proteins were determined by dynamic light scattering (DLS) using Zetasizer ZS (Malvern Instruments Ltd., Worcestershire, United Kingdom). A 100 μl sample of DmBCA (200 μg/ml) in elution buffer (50 mM NaH_2PO_4, 500 mM NaCl, 250 mM imidazole, pH 8.0) was analyzed. Human CA II (HCA II) (180 μg/ml) in 0.1 M Tris, 0.4 M NaN_3, 1 mM benzamidine, 20% glycerol, pH 7.0 was analyzed to support the results of DmBCA analysis. The small molecules such as imidazole and glycerol of the elution buffers seemed to dominate in the DLS analysis, since most of the light scattering was from particles having diameter smaller than one nm. Therefore, proteins were exchanged to 50 mM Na_2HPO_4 pH 7.0 containing 100 mM NaCl using protein desalting spin columns (Pierce). DLS analysis was then performed for 100 μl sample by using temperature scanning mode where the temperature was raised from 4°C to 50°C at 3°C intervals. Sample was let to equilibrate to each measurement temperature two minutes before data acquisition. For DmBCA three parallel measurements were carried out at each temperature and for HCA II only one measurement was performed at each temperature. The molecular weight of the protein was estimated from hydrodynamic diameter using globular protein standard curve provided by the manufacturer.

Analytical gel filtration

The molecular size of the protein in solution was measured by size-exclusion chromatography using Superdex200 10/300GL column (GE Healthcare) connected to ÄKTA ™purifier-100 equipped with UV-900 monitor (GE Healthcare). The analysis was done using 50 mM Na_2HPO_4, 650 mM NaCl (pH 7.0) as mobile phase. 20-30 μg protein was injected per run. All the analyses were done with flow rate 0.3 ml/min, and absorbencies at 280 nm and 205 nm were used to locate the protein peaks in the chromatograms. Molecular weight calibration curve was prepared by analyzing gel filtration standard protein mixture containing thyroglobulin (670kDa), γ-globulin (158kDa), ovalbumin (44kDa), myoglobin (17kDa) and vitamin B_{12} (1,35kDa) (Bio-Rad).

Additional material

Additional file 1: The full alignment of the 26 invertebrate β-CA sequences (partly shown in Figure 1).

Additional file 2: The full sequence alignment of all of the identified invertebrate β-CA sequences.

Acknowledgements

We thank Professor Hans Spelbrink and Dr. Peter Martinsson for help with fluorescence confocal microscopy and Aulikki Lehmus and Jukka Lehtonen for skilful technical assistance. We thank Joanna Zmurko for assistance in gel filtration analysis. This research was financed in part by grants from the 6th Framework Programme of the European Union (DeZnIT project) and the Competitive Research Funding of the Tampere University Hospital (9L071).

Author details

[1]Institute of Medical Technology, University of Tampere and Tampere University Hospital, Tampere, Finland. [2]School of Medicine, University of Tampere and Tampere University Hospital, Tampere, Finland. [3]Centre for Laboratory Medicine, Tampere University Hospital, Tampere, Finland. [4]Laboratorio di Chimica Bioinorganica, Università degli Studi di Firenze, Sesto Fiorentino (Firenze), Italy. [5]Vetsuisse Faculty and Zurich Center for Integrative Human Physiology (ZIHP), Institute of Veterinary Physiology, University of Zurich, Zurich, Switzerland.

Authors' contributions

LS carried out protein construct design, protein production and purification, colocalization studies and drafted the manuscript. MH contributed to protein construct design and co-localization studies. MT made all the bioinformatic analysis and helped to draft the manuscript. AO contributed in bioinformatic analyses. CTS, AI and AS carried out the kinetic measurements. JL and VPH carried out the DLS analysis. BN and VPH performed the gel filtration studies. TAG conceived the study, provided materials and helped to draft the manuscript. CTS and SP conceived the study, and participated in its design and coordination and helped to draft the manuscript. All authors read and approved the final manuscript.

Received: 22 February 2010 Accepted: 26 July 2010
Published: 26 July 2010

References

1. Sly WS, Hu PY: **Human carbonic anhydrases and carbonic anhydrase deficiencies.** *Annu Rev Biochem* 1995, **64**:375-401.
2. Lane TW, Saito MA, George GN, Pickering IJ, Prince RC, Morel FM: **Biochemistry: a cadmium enzyme from a marine diatom.** *Nature* 2005, **435(7038)**:42.
3. Xu Y, Feng L, Jeffrey PD, Shi Y, Morel FM: **Structure and metal exchange in the cadmium carbonic anhydrase of marine diatoms.** *Nature* 2008, **452(7183)**:56-61.

4. Tripp BC, Bell CB, Cruz F, Krebs C, Ferry JG: **A role for iron in an ancient carbonic anhydrase.** *J Biol Chem* 2004, **279(8)**:6683-6687.
5. Macauley SR, Zimmerman SA, Apolinario EE, Evilia C, Hou YM, Ferry JG, Sowers KR: **The archetype gamma-class carbonic anhydrase (Cam) contains iron when synthesized in vivo.** *Biochemistry* 2009, **48(5)**:817-819.
6. Zimmerman SA, Ferry JG: **The beta and gamma classes of carbonic anhydrase.** *Curr Pharm Des* 2008, **14(7)**:716-721.
7. So AK, Espie GS, Williams EB, Shively JM, Heinhorst S, Cannon GC: **A novel evolutionary lineage of carbonic anhydrase (epsilon class) is a component of the carboxysome shell.** *J Bacteriol* 2004, **186(3)**:623-630.
8. Sawaya MR, Cannon GC, Heinhorst S, Tanaka S, Williams EB, Yeates TO, Kerfeld CA: **The structure of beta-carbonic anhydrase from the carboxysomal shell reveals a distinct subclass with one active site for the price of two.** *J Biol Chem* 2006, **281(11)**:7546-7555.
9. Strop P, Smith KS, Iverson TM, Ferry JG, Rees DC: **Crystal structure of the "cab"-type beta class carbonic anhydrase from the archaeon *Methanobacterium thermoautotrophicum*.** *J Biol Chem* 2001, **276(13)**:10299-10305.
10. Kimber MS, Pai EF: **The active site architecture of *Pisum sativum* beta-carbonic anhydrase is a mirror image of that of alpha-carbonic anhydrases.** *EMBO J* 2000, **19(7)**:1407-1418.
11. Parisi G, Perales M, Fornasari MS, Colaneri A, Gonzalez-Schain N, Gomez-Casati D, Zimmermann S, Brennicke A, Araya A, Ferry JG, Echave J, Zabaleta E: **Gamma carbonic anhydrases in plant mitochondria.** *Plant Mol Biol* 2004, **55(2)**:193-207.
12. Elleuche S, Poggeler S: **Evolution of carbonic anhydrases in fungi.** *Curr Genet* 2009, **55(2)**:211-222.
13. Fabre N, Reiter IM, Becuwe-Linka N, Genty B, Rumeau D: **Characterization and expression analysis of genes encoding alpha and beta carbonic anhydrases in *Arabidopsis*.** *Plant Cell Environ* 2007, **30(5)**:617-629.
14. Hewett-Emmett D: **Evolution and distribution of the carbonic anhydrase gene families.** *EXS* 2000, **90(90)**:29-76.
15. Klengel T, Liang WJ, Chaloupka J, Ruoff C, Schroppel K, Naglik JR, Eckert SE, Mogensen EG, Haynes K, Tuite MF, Levin LR, Buck J, Muhlschlegel FA: **Fungal adenylyl cyclase integrates CO2 sensing with cAMP signaling and virulence.** *Curr Biol* 2005, **15(22)**:2021-2026.
16. Bahn YS, Cox GM, Perfect JR, Heitman J: **Carbonic anhydrase and CO2 sensing during *Cryptococcus neoformans* growth, differentiation, and virulence.** *Curr Biol* 2005, **15(22)**:2013-2020.
17. Innocenti A, Muhlschlegel FA, Hall RA, Steegborn C, Scozzafava A, Supuran CT: **Carbonic anhydrase inhibitors: inhibition of the beta-class enzymes from the fungal pathogens *Candida albicans* and *Cryptococcus neoformans* with simple anions.** *Bioorg Med Chem Lett* 2008, **18(18)**:5066-5070.
18. Isik S, Kockar F, Arslan O, Guler OO, Innocenti A, Supuran CT: **Carbonic anhydrase inhibitors. Inhibition of the beta-class enzyme from the yeast *Saccharomyces cerevisiae* with anions.** *Bioorg Med Chem Lett* 2008, **18(24)**:6327-6331.
19. Zimmerman SA, Ferry JG, Supuran CT: **Inhibition of the archaeal beta-class (Cab) and gamma-class (Cam) carbonic anhydrases.** *Curr Top Med Chem* 2007, **7(9)**:901-908.
20. Isik S, Kockar F, Aydin M, Arslan O, Guler OO, Innocenti A, Scozzafava A, Supuran CT: **Carbonic anhydrase inhibitors: inhibition of the beta-class enzyme from the yeast *Saccharomyces cerevisiae* with sulfonamides and sulfamates.** *Bioorg Med Chem* 2009, **17(3)**:1158-1163.
21. Nishimori I, Minakuchi T, Kohsaki T, Onishi S, Takeuchi H, Vullo D, Scozzafava A, Supuran CT: **Carbonic anhydrase inhibitors: the beta-carbonic anhydrase from *Helicobacter pylori* is a new target for sulfonamide and sulfamate inhibitors.** *Bioorg Med Chem Lett* 2007, **17(13)**:3585-3594.
22. Minakuchi T, Nishimori I, Vullo D, Scozzafava A, Supuran CT: **Molecular cloning, characterization, and inhibition studies of the Rv1284 beta-carbonic anhydrase from *Mycobacterium tuberculosis* with sulfonamides and a sulfamate.** *J Med Chem* 2009, **52(8)**:2226-2232.
23. Nishimori I, Minakuchi T, Vullo D, Scozzafava A, Innocenti A, Supuran CT: **Carbonic anhydrase inhibitors. Cloning, characterization, and inhibition studies of a new beta-carbonic anhydrase from *Mycobacterium tuberculosis*.** *J Med Chem* 2009, **52(9)**:3116-3120.
24. Cronk JD, Rowlett RS, Zhang KY, Tu C, Endrizzi JA, Lee J, Gareiss PC, Preiss JR: **Identification of a novel noncatalytic bicarbonate binding site in eubacterial beta-carbonic anhydrase.** *Biochemistry* 2006, **45(14)**:4351-4361.
25. Joseph P, Turtaut F, Ouahrani-Bettache S, Montero JL, Nishimori I, Minakuchi T, Vullo D, Scozzafava A, Kohler S, Winum JY, Supuran CT: **Cloning, characterization, and inhibition studies of a beta-carbonic anhydrase from *Brucella suis*.** *J Med Chem* 2010, **53(5)**:2277-2285.
26. Innocenti A, Hall RA, Schlicker C, Muhlschlegel FA, Supuran CT: **Carbonic anhydrase inhibitors. Inhibition of the beta-class enzymes from the fungal pathogens *Candida albicans* and *Cryptococcus neoformans* with aliphatic and aromatic carboxylates.** *Bioorg Med Chem* 2009, **17(7)**:2654-2657.
27. Innocenti A, Hall RA, Schlicker C, Scozzafava A, Steegborn C, Muhlschlegel FA, Supuran CT: **Carbonic anhydrase inhibitors. Inhibition and homology modeling studies of the fungal beta-carbonic anhydrase from *Candida albicans* with sulfonamides.** *Bioorg Med Chem* 2009, **17(13)**:4503-4509.
28. Innocenti A, Winum JY, Hall RA, Muhlschlegel FA, Scozzafava A, Supuran CT: **Carbonic anhydrase inhibitors. Inhibition of the fungal beta-carbonic anhydrases from *Candida albicans* and *Cryptococcus neoformans* with boronic acids.** *Bioorg Med Chem Lett* 2009, **19(10)**:2642-2645.
29. Schlicker C, Hall RA, Vullo D, Middelhaufe S, Gertz M, Supuran CT, Muhlschlegel FA, Steegborn C: **Structure and inhibition of the CO2-sensing carbonic anhydrase Can2 from the pathogenic fungus *Cryptococcus neoformans*.** *J Mol Biol* 2009, **385(4)**:1207-1220.
30. Innocenti A, Leewattanapasuk W, Muhlschlegel FA, Mastrolorenzo A, Supuran CT: **Carbonic anhydrase inhibitors. Inhibition of the beta-class enzyme from the pathogenic yeast *Candida glabrata* with anions.** *Bioorg Med Chem Lett* 2009, **19(16)**:4802-4805.
31. Smith KS, Cosper NJ, Stalhandske C, Scott RA, Ferry JG: **Structural and kinetic characterization of an archaeal beta-class carbonic anhydrase.** *J Bacteriol* 2000, **182(23)**:6605-6613.
32. Cox EH, McLendon GL, Morel FM, Lane TW, Prince RC, Pickering IJ, George GN: **The active site structure of *Thalassiosira weissflogii* carbonic anhydrase 1.** *Biochemistry* 2000, **39(40)**:12128-12130.
33. Smith KS, Ingram-Smith C, Ferry JG: **Roles of the conserved aspartate and arginine in the catalytic mechanism of an archaeal beta-class carbonic anhydrase.** *J Bacteriol* 2002, **184(15)**:4240-4245.
34. Tetu SG, Tanz SK, Vella N, Burnell JN, Ludwig M: **The *Flaveria bidentis* beta-carbonic anhydrase gene family encodes cytosolic and chloroplastic isoforms demonstrating distinct organ-specific expression patterns.** *Plant Physiol* 2007, **144(3)**:1316-1327.
35. Mitra M, Lato SM, Ynalvez RA, Xiao Y, Moroney JV: **Identification of a new chloroplast carbonic anhydrase in *Chlamydomonas reinhardtii*.** *Plant Physiol* 2004, **135(1)**:173-182.
36. Bahn YS, Muhlschlegel FA: **CO2 sensing in fungi and beyond.** *Curr Opin Microbiol* 2006, **9(6)**:572-578.
37. Fasseas MK, Tsikou D, Flemetakis E, Katinakis P: **Molecular and biochemical analysis of the beta class carbonic anhydrases in *Caenorhabditis elegans*.** *Mol Biol Rep* 2010, **37(6)**:2941-50.
38. Supuran CT: **Carbonic anhydrases: novel therapeutic applications for inhibitors and activators.** *Nat Rev Drug Discov* 2008, **7(2)**:168-181.
39. Rowlett RS, Tu C, Lee J, Herman AG, Chapnick DA, Shah SH, Gareiss PC: **Allosteric site variants of *Haemophilus influenzae* beta-carbonic anhydrase.** *Biochemistry* 2009, **48(26)**:6146-6156.
40. Rowlett RS, Hoffmann KM, Failing H, Mysliwiec MM, Samardzic D: **Evidence for a bicarbonate "escort" site in *Haemophilus influenzae* beta-carbonic anhydrase.** *Biochemistry* 2010, **49(17)**:3640-3647.
41. Hazen SA, Waheed A, Sly WS, LaNoue KF, Lynch CJ: **Differentiation-dependent expression of CA V and the role of carbonic anhydrase isozymes in pyruvate carboxylation in adipocytes.** *FASEB J* 1996, **10(4)**:481-490.
42. Chintapalli VR, Wang J, Dow JA: **Using FlyAtlas to identify better *Drosophila melanogaster* models of human disease.** *Nat Genet* 2007, **39(6)**:715-720.
43. Altschul SF, Gish W, Miller W, Myers EW, Lipman DJ: **Basic local alignment search tool.** *J Mol Biol* 1990, **215(3)**:403-410.
44. Kent WJ: **BLAT–the BLAST-like alignment tool.** *Genome Res* 2002, **12(4)**:656-664.
45. Larkin MA, Blackshields G, Brown NP, Chenna R, McGettigan PA, McWilliam H, Valentin F, Wallace IM, Wilm A, Lopez R, Thompson JD,

Gibson TJ, Higgins DG: **Clustal W and Clustal X version 2.0.** *Bioinformatics* 2007, **23(21)**:2947-2948.
46. Birney E, Clamp M, Durbin R: **GeneWise and Genomewise.** *Genome Res* 2004, **14(5)**:988-995.
47. Tamura K, Dudley J, Nei M, Kumar S: **MEGA4: Molecular Evolutionary Genetics Analysis (MEGA) software version 4.0.** *Mol Biol Evol* 2007, **24(8)**:1596-1599.
48. Saitou N, Nei M: **The neighbor-joining method: a new method for reconstructing phylogenetic trees.** *Mol Biol Evol* 1987, **4(4)**:406-425.
49. Rzhetsky A, Nei M: **METREE: a program package for inferring and testing minimum-evolution trees.** *Comput Appl Biosci* 1994, **10(4)**:409-412.
50. Zharkikh A, Li WH: **Estimation of confidence in phylogeny: the complete-and-partial bootstrap technique.** *Mol Phylogenet Evol* 1995, **4(1)**:44-63.
51. Nei M: **Phylogenetic analysis in molecular evolutionary genetics.** *Annu Rev Genet* 1996, **30**:371-403.
52. Emanuelsson O, Nielsen H, Brunak S, von Heijne G: **Predicting subcellular localization of proteins based on their N-terminal amino acid sequence.** *J Mol Biol* 2000, **300(4)**:1005-1016.
53. Hilvo M, Baranauskiene L, Salzano AM, Scaloni A, Matulis D, Innocenti A, Scozzafava A, Monti SM, Di Fiore A, De Simone G, Lindfors M, Janis J, Valjakka J, Pastorekova S, Pastorek J, Kulomaa MS, Nordlund HR, Supuran CT, Parkkila S: **Biochemical characterization of CA IX, one of the most active carbonic anhydrase isozymes.** *J Biol Chem* 2008, **283(41)**:27799-27809.

doi:10.1186/1471-2091-11-28
Cite this article as: Syrjänen *et al.*: Characterization of the first beta-class carbonic anhydrase from an arthropod (*Drosophila melanogaster*) and phylogenetic analysis of beta-class carbonic anhydrases in invertebrates. *BMC Biochemistry* 2010 **11**:28.

Bioorganic & Medicinal Chemistry 21 (2013) 1516–1521

Contents lists available at SciVerse ScienceDirect

Bioorganic & Medicinal Chemistry

journal homepage: www.elsevier.com/locate/bmc

Characterization, bioinformatic analysis and dithiocarbamate inhibition studies of two new α-carbonic anhydrases, CAH1 and CAH2, from the fruit fly *Drosophila melanogaster*

Leo Syrjänen [a,b,†,*], Martti E. E. Tolvanen [a,†,*], Mika Hilvo [c], Daniela Vullo [d], Fabrizio Carta [d], Claudiu T. Supuran [d,e], Seppo Parkkila [a,b,f]

[a] Institute of Biomedical Technology, University of Tampere and Tampere University Hospital, Tampere, Finland
[b] School of Medicine, University of Tampere and Tampere University Hospital, Tampere, Finland
[c] Bio and Process Technology, VTT Technical Research Centre of Finland, Espoo, Finland
[d] Università degli Studi di Firenze, Laboratorio di Chimica Bioinorganica, 50019 Sesto Fiorentino (Firenze), Italy
[e] Università degli Studi di Firenze, Dipartimento di Scienze Farmaceutiche, Via Ugo Schiff 6, 50019 Sesto Fiorentino (Firenze), Italy
[f] Fimlab Laboratories Ltd, Tampere, Finland

ARTICLE INFO

Article history:
Received 9 July 2012
Revised 23 August 2012
Accepted 24 August 2012
Available online 31 August 2012

Keywords:
Carbonic anhydrase
Inhibition
Phylogenetics
Drosophila melanogaster

ABSTRACT

Carbonic anhydrases (CAs) are essential and ubiquitous enzymes. Thus far, there are no articles on characterization of *Drosophila melanogaster* α-CAs. Data from invertebrate CA studies may provide opportunities for anti-parasitic drug development because α-CAs are found in many parasite or parasite vector invertebrates. We have expressed and purified *D. melanogaster* CAH1 and CAH2 as proteins of molecular weights 30 kDa and 28 kDa. CAH1 is cytoplasmic whereas CAH2 is a membrane-attached protein. Both are highly active enzymes for the CO_2 hydration reaction, being efficiently inhibited by acetazolamide. CAH2 in the eye of *D. melanogaster* may provide a new animal model for CA-related eye diseases. A series of dithiocarbamates were also screened as inhibitors of these enzymes, with some representatives showing inhibition in the low nanomolar range.

1. Introduction

Carbonic anhydrases (CAs, EC 4.2.1.1) catalyze the reversible hydration of carbon dioxide according to the following reaction: $CO_2 + H_2O \leftrightarrow HCO_3^- + H^+$.[1] CAs are zinc-containing metalloenzymes, except for the δ and ζ forms, which may use cobalt[2] and cadmium,[3,4] respectively, as alternative metal cofactors. Additionally γ-CA contains iron in vivo, at least in anaerobic *Archaea*.[5,6] The reaction catalyzed by CAs is crucial in the regulation of acid–base balance in organisms. In addition, CAs participate in many other physiological processes, such as bone resorption in vertebrates, gluconeogenesis, production of body fluids, and transport of CO_2 and HCO_3^-.[1]

α-CAs have been considered the CA class with the widest distribution among different species. However, recent studies have described β-class CAs in invertebrates *Caenorhabditis elegans* and *Drosophila melanogaster* (fruit fly), which may alter the conception of prevalence of the CAs in different species.[7,8] Our recent investigations[8] showed that the *D. melanogaster* β-CA (DmBCA) has a high CO_2 hydratase activity, with a k_{cat} of 9.5×10^5 s^{-1} and a k_{cat}/K_M of 1.1×10^8 M^{-1} s^{-1}. DmBCA was appreciably inhibited by the clinically-used sulfonamide acetazolamide, with an inhibition constant of 49 nM. Thus far, there are no articles on characterization of *D. melanogaster* α-CAs, even though some α-CAs from other Dipteran species, especially the malaria mosquito *Anopheles gambiae* and yellow fever mosquito *Aedes aegypti* are well characterized.[9,10] These CAs have generally shown high enzymatic activity. Publications concerning *D. melanogaster* α-CAs have focused on the pH regulation in *D. melanogaster* midgut and electrolyte transport in the Malpighian tubules,[11,12] but no specific CA isozymes were identified in these studies.

The aim of this study was to express, purify and characterize two abundantly expressed α-CA enzymes CAH1 and CAH2 from an important model organism, the fruit fly *D. melanogaster*. In addition to biochemical characterization, we have performed bioinformatic analyses for their subcellular localization and phylogenetic relationships, and studied publicly available gene expression data. We selected these two isozymes for experimental work based on their high expression levels and existence of orthologs in many other insects. An inhibition study with a large series of dithiocarbamates has also been performed.

* Corresponding authors. Address: School of Medicine, Medisiinarinkatu 3, 33014, University of Tampere, Finland.
E-mail addresses: leo.syrjanen@uta.fi (L. Syrjänen), martti.tolvanen@uta.fi (M.E.E. Tolvanen).
† These authors contributed equally to this work.

0968-0896/$ - see front matter © 2012 Elsevier Ltd. All rights reserved.
http://dx.doi.org/10.1016/j.bmc.2012.08.046

2. Materials and methods

2.1. Data sources

Drosophila protein and DNA sequences were obtained from EnsemblMetazoa Release 14 (http://www.metazoa.ensembl.org).[13] CAH1 protein was FBpp0080116, transcript FBtr0080539, and CAH2 protein was FBpp0075733, transcript FBtr0076001. One-to-one orthologs were studied using the ortholog tables in comparative data of EnsemblMetazoa. Instead of the obviously truncated Ensembl entry AGAP010052 for the *Anopheles gambiae* ortholog, we used ABF66618.1 from the NCBI protein database (http://www.ncbi.nlm.nih.gov/protein/).[14] Selected human CAs and mouse CA XV were retrieved from UniProtKB (http://www.uniprot.org).[15] Table 1 shows the list of CAH1 and CAH2 orthologs which we used in analyses of subcellular localization.

Gene expression data was retrieved from FlyBase[16] on Dec 5, 2011, from the gene report pages of CAH1 (http://www.flybase.org/reports/FBgn0027844.html) and CAH2 (http://www.flybase.org/reports/FBgn0027843.html), under High-Throughput Expression Data.[17] We used the modENCODE Temporal Expression Data, FlyAtlas Anatomical Expression Data, and modENCODE developmental timecourse RNA-Seq data for expression levels at different developmental stages and in different larval and adult tissues.

2.2. Bioinformatic analyses

Sequence identity percentages were calculated as the number of identical residues in two aligned protein sequences divided by the number of residues in the shorter of the two proteins (×100%). Multiple sequence alignment of protein sequences was performed with ClustalW (http://www.ebi.ac.uk/Tools/msa/clustalw2/).[18,19]

Evolutionary analyses were conducted in MEGA5.[20] The evolutionary history of 13 CA sequences was inferred using the Minimum Evolution method.[21] The bootstrap consensus tree inferred from 1000 replicates is taken to represent the evolutionary history of the taxa analyzed.[22] The percentage of replicate trees in which the associated taxa clustered together in the bootstrap test (1000 replicates) are shown next to the branches. The tree is rooted at the enzymatically inactive CAH10 (CA-related protein X) and drawn to scale, with branch lengths in the same units as those of the evolutionary distances used to infer the phylogenetic tree. The evolutionary distances were computed using the Poisson correction method[23] and are in the units of number of amino acid substitutions per site. The ME tree was searched using the Close-Neighbor-Interchange (CNI) algorithm[24] at a search level of 0. The Neighbor-joining algorithm[25] was used to generate the initial tree. All positions containing gaps and missing data were eliminated. There were a total of 230 positions in the final dataset. SignalP 4.0 and TargetP 1.1 at CBS, Denmark (http://www.cbs.dtu.dk/services/)[26,27] were used to predict signal peptides in the protein sequences. Glycosyl phoshpatidyl inositol anchor attachment sites (GPI sites) were predicted in the Pred-GPI server (http://www.gpcr.biocomp.unibo.it/predgpi/)[28] with the general model and taking the 99.0% specificity cutoff to represent a positive prediction.

2.3. Construction of GST-fusion proteins

CAH1- and CAH2-GST-fusion protein constructs were designed for enzyme production in BL21(DE3)pLysS Competent Cells (Promega), and purification. Both constructs included BamHI and XhoI restriction sites. Total RNA extracted from *D. melanogaster* S2 cells was precipitated using NaOAc with final concentration of 100 mM and 100% ethanol. Solution was centrifuged at 13,000×*g* for 15 min at +4 °C. After centrifugation RNA was washed with 70% ethanol and centrifuged again. The RNA pellet was dried at +25 °C and suspended in sterile water. A cDNA transcription was performed using First strand cDNA Synthesis Kit #K1612 (Fermentas) according to manufacturer's instructions.

The cDNA obtained from total RNA was copied with PCR using Phusion™ Hot Start High Fidelity DNA Polymerase (Finnzymes, Espoo, Finland). For PCR, sequence specific primers for CAH1 were ordered from Sigma-Aldrich. The forward primer was 5′-ATGAGCCACCACTGGGGATACACC-3′ (F1) and the reverse primer was 3′-TTAGTGGCCCCCGATCTCGCGCAG-5′ (R1). PCR was performed with PTC 2000 thermal cycler (MJ Research, Waltham, MA). The program consisted of a single 98 °C denaturation step for 30 s, followed by 33 cycles of denaturation at 98 °C for 10 s, annealing at 60 °C for 15 s and extension at 72 °C for 25 s, followed by a final extension at 72 °C for 5 min. The band was separated from the gel and dissolved using Illustra™ GFX™ PCR DNA and GEL Band Purification Kit (GE Healthcare Life Sciences, Buckinghamshire, UK).

The obtained PCR product was used as a template in the next PCR reaction in which the forward primer was 5′-CGCGGATCCAGCCACCACTGGGGATACACC-3′ (F2) and the reverse primer was 3′-CCGCTCGAGTTAGTGGCCCCCGATCTCGCG-5′ (R2). The PCR program used was identical to the first protocol, except that annealing temperature was 70 °C. pGEX-4T1 vector (Amersham Biosciences) and *CAH1* gene were digested overnight at +37 °C. pGEX plasmid was run into gel and purified. pGEX-4T1 and *CAH1* were ligated at +4 °C overnight using T4 DNA ligase (New England Biolabs). The Ligated pGEX-4T1 plasmid was transformed into BL-21(DE3)pLys Competent Cells (Promega) according to the manufacturer's instructions. Sequencing was performed to

Table 1
FlyBase identifiers for CAH1 and CAH2 orthologs in 12 Drosophila species

Orthologs of	CAH1		CAH2	
	FlyBase gene	Gene name	FlyBase gene	Gene name
Drosophila melanogaster	FBgn0027844	CAH1	FBgn0027843	CAH2
Drosophila ananassae	FBgn0091284	GF14257	FBgn0101798	GF24805
Drosophila erecta	FBgn0116020	GG23881	FBgn0107812	GG15564
Drosophila grimshawi	FBgn0118595	GH11114	FBgn0123625	GH16154
Drosophila mojavensis	FBgn0140976	GI18237	FBgn0135183	GI12426
Drosophila persimilis	FBgn0158823	GL21230	FBgn0162746	GL25159
Drosophila pseudoobscura	FBgn0080602	GA20608	FBgn0079943	GA19947
Drosophila sechellia	FBgn0170142	GM15222	FBgn0180192	GM25332
Drosophila simulans	FBgn0083469	CAH1	FBgn0186049	GD14364
Drosophila virilis	FBgn0205309	GJ18144	FBgn0199568	GJ12322
Drosophila willistoni	FBgn0226191	GK24229	FBgn0215291	GK13282
Drosophila yakuba	FBgn0236082	GE18682	FBgn0239132	GE21890

confirm that insert was accurate and free of defects. Amino acids 1–269 were included in the construct.

The cloning of *CAH2* gene was done exactly in the same way as with CAH1, except for the following parts. In the first PCR reaction the forward primer was 5′-ATGAGGAGGTGTCGCAACACCCCG-3′ (F3) and the reverse primer was 3′-TTAAAAACCCCGGAAAATG-GAGGT-5′ (R3). The PCR program used was: a single 98 °C denaturation step for 30 s, followed by 33 cycles of denaturation at 98 °C for 10 s, annealing at 65 °C for 15 s and extension at 72 °C for 40 s, followed by a final extension at 72 °C for 5 min.

In the next PCR reaction the forward primer was 5′-CGCGGATCCTACGAGGGCAGACATGGACCC-3′ (F4) and the reverse primer was 3′-CCGCTCGAGTTAGTAGTTCTTGTACAAGGT-5′ (R4). Amino acids 30–286 were included. The proposed signal sequence and membrane anchor region were excluded from the construct.

2.4. Expression and purification of CAH1 and CAH2

For production of CAH1 and CAH2 proteins, *Escherichia coli* were cultured in LB medium (5 ml) in the presence of ampicillin overnight. After 18 h, the culture media were diluted 100-fold and grown at +37 °C until optical density at 600 nm was between 0.6 and 0.8. The expression rates of CAH1 and CAH2 were induced by 1 mM isopropyl β-D-thiogalactoside (IPTG) and the culturing was continued for additional 3 h. The bacterial cells were harvested by centrifugation. The purification protocol for 500 ml culture of bacterial cells was the following: The bacterial cell pellet was lysed in 1× PBS containing 80 mg of lysozyme. The solution was incubated for 15 min on ice after which 20 μl (200 U) of DNAse was added. The solution was again incubated for 15 min on ice. The supernatant was gathered by centrifugation at 12 900×*g* for 15 min at +4 °C. 530 μl of glutathione sepharose slurry (GST Bulk Kit, GE Healthcare) was added to the supernatant and the solution was incubated with gentle shaking for 30 min at room temperature. For separation of the glutathione sepharose beads, the solution was transferred to a column containing filter paper in the bottom. The column was washed four times with 1 ml of PBS. 20 μl (20 U) of thrombin (GE Healthcare) was added to 700 μl of PBS and beads were gathered from column with this solution and incubated with gentle shaking for 1 h at room temperature. The solution was transferred to a column and the buffer containing the purified protein was collected followed by additional washes with 1400 μl of PBS. The fractions were analysed by SDS–PAGE under reducing conditions using 10% acrylamide gels.

2.5. CA activity measurements and inhibition studies

An Applied Photophysics stopped-flow instrument was used to assay the CA-catalyzed CO_2 hydration activity.[29] Phenol red (at a concentration of 0.2 mM) was used as an indicator, working at the absorbance maximum of 557 nm, with 10–20 mM HEPES (pH 7.5) or Tris (pH 8.3) as buffers and 20 mM Na_2SO_4 or 20 mM $NaClO_4$ (for maintaining constant ionic strength), following the initial rates of the CA-catalyzed CO_2 hydration reaction for a period of 10–100 s. The CO_2 concentrations ranged from 1.7 to 17 mM for the determination of kinetic parameters and inhibition constants. For each inhibitor at least six traces of the initial 5–10% of the reaction were used to determine the initial velocity. The uncatalyzed rates were determined in the same manner and subtracted from the total observed rates. Stock solutions of inhibitor (100 mM) were prepared in distilled-deionized water, and dilutions up to 0.01 μM were made thereafter with distilled-deionized water. Inhibitor and enzyme solutions were preincubated together for 15 min at room temperature prior to the assay to allow for the formation of the E–I complex. The inhibition constants were obtained by non-linear least-squares methods using PRISM 3, whereas the kinetic parameters for the uninhibited enzymes were obtained from Lineweaver–Burk plots, each representing the mean of at least three different determinations.

The dithiocarbamates investigated here were reported earlier by our group.[30]

3. Results and discussion

3.1. Bioinformatics

3.1.1. Phylogenetic analyses

Orthologs computed as one-to-one orthologs in Ensembl were found for CAH1 in all 23 available insect species in EnsemblMetazoa. In the Drosophila genomes, the protein sequence identities of these orthologs to *D. melanogaster* CAH1 range from 92% to 99%. In non-Drosophila insects, the protein sequence identities range from 51% to 66%. For comparison, the human many-to-one orthologs, the cytoplasmic CA isozymes CA I, CA II, CA III, CA XIII, and CA VII show protein sequence identities between 40% and 47% to *D. melanogaster* CAH1.

In case of CAH2 one-to-one orthologs, we find them annotated in 21 insect species in EnsemblMetazoa, including all 12 Drosophila genomes and missing just in the silkworm, *Bombyx mori*, and in the red flour beetle, *Tribolium castaneum*. In other Drosophila species, the protein sequence identities compared to the *D. melanogaster* ortholog range from 52% to 97%. In other insects than Drosophilas, they are in the range from 34% to 38%. Within mammalian many-to-one orthologs, namely the extracellular CA isozymes CA IV, CA VI, CA IX, CA XII, CA XIV, and CA XV, the similarity is considerably less than within the cytoplasmic CAH1 family. The sequence identities of these orthologs from human and mouse to CAH2 are only from 21% to 24%.

Figure 1 shows the phylogenetic tree that relates *D. melanogaster* CAH1 and CAH2 to mammalian CA isozymes. CAH1 and the mammalian cytoplasmic isozymes share a common ancestor, whereas CAH2 has descended from the same common ancestor as the mammalian extracellular isozymes. Our analyses (data not shown) also confirm that within *Anopheles gambiae* CAs AgCA9 (NCBI ABF66618.1) is ortholog to CAH1, and AgCA4 (Ensembl AGAP007550-PA) is ortholog to CAH2, as was shown by Linser et al.[31] The relationship of CAH1 and CAH2 to other alpha CAs in arthropods was studied more widely in our previous paper.[32]

Sequence identities suggest that CAH1 is more strongly conserved of the two Drosophila CA isozymes which we have analyzed

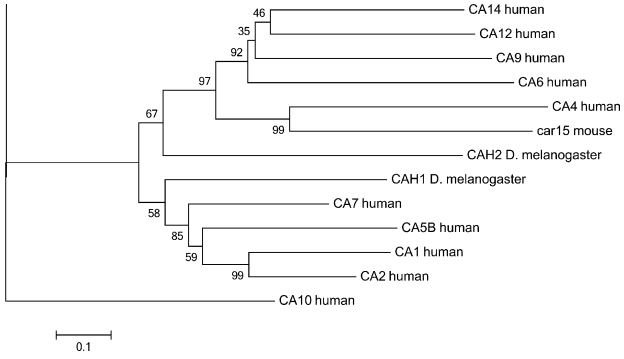

Figure 1. Phylogenetic tree of selected CAs. A minimum-evolution tree was constructed as described in Section 2.2 in more detail, with CA-related protein 10 as an outgroup. Numbers at internal nodes of the tree show the bootstrap support percentage for each node (from 1000 bootstrap replicate trees). The branch lengths are proportional to the evolutionary distances used to infer the phylogenetic tree. The scale bar at the bottom indicates the distance of 0.1 amino acid substitutions per site.

here. We have also analyzed the conservation of CAs in Drosophilas by their Ka/Ks ratios, or ratios between non-synonymous and synonymous substitution rates (Ortutay, C., Nair. P. S, Tolvanen, M. E. E., et al., unpublished). The results show that CAH1 is under very strong purifying selection. The median K_a/K_s ratio from all pairwise comparisons between 12 CAH1 genes from published Drosophila genomes is 0.023. For CAH2, the median K_a/K_s ratio is 0.198, which indicates that the gene is under purifying selection, but the selection pressure is not as strong as in the case of CAH1.

3.1.2. Subcellular localization

The CAH1 orthologs in all 12 Drosophila genomes are predicted to be cytoplasmic in localization, and give no positive predictions for signal peptides or GPI anchor attachment sites. Among the CAH2 orthologs, all except the ortholog from *D. willistoni* are predicted to have both signal peptide and GPI anchor. The *D. willistoni* ortholog is slightly shorter than all other CAH2 sequences, both in its N- and C-terminus. However, a Blast search in the *D. willistoni* genome (at Ensembl), with *D. persimilis* CAH2 as the query sequence, reveals that an alternative gene model can be built to give a 334-residue sequence which has both a signal peptide and a strongly predicted GPI site (data not shown). Therefore, all of the CAH2 orthologs in Drosophila are very probably located on the extracellular side of the plasma membrane, anchored to a phosphatidyl inositol lipid via a glycan linker in the C-terminus of the processed protein.

The predicted localizations conform with the phylogenetic results, that is, that CAH1 is expressed in the cytoplasm, and CAH2 is an extracellular, membrane-attached isozyme.

3.1.3. Gene expression

Based on high-throughput expression studies reported in FlyBase, *CAH1* has the highest expression levels and widest expression pattern of all CA isozymes in *D. melanogaster*. *CAH1* expression is highest in salivary gland, midgut and hindgut in both larva and adult and in larval trachea. Slightly lower (but still very high) levels are observed in adult head, eye, brain, and thoracic-abdominal ganglion, and in larval central nervous system. Out of all measured tissues, *CAH1* expression is low or absent only in ovary, testis, and male accessory gland. During development, *CAH1* transcription is high or very high from late embryo to white prepupae (12 h) and again high from late pupa to all of adult life, being low only in early embryo (up to 16 h) and in mid-metamorphosis.

Shanbhag and Tripathi[12] observed that CA activity is required to maintain acidification in Drosophila midgut. The high expression of CAH1 in the midgut suggests that it might be the isozyme which is responsible for this activity. Even more importantly CA activity is required in the alkalinization in the posterior midgut where it is rate-limiting for proton exit. In the malaria mosquito, the orthologous isozyme AgCA9 is needed in alkalinization of the midgut[31] The pH value is of course dependent on the transport activities in each species, but it is interesting to see how CAs may contribute to achieving pH values in the opposite extremes.

CAH2 has very high or high expression in larval hindgut and trachea, and in adult salivary gland, midgut and Malpighian tubules. Contrary to *CAH1*, *CAH2* has a low or no expression in nerve tissues or in reproductive tissues. In developmental time course there is a notable peak at hatching, with very high expression from 18 to 20 h embryo to larva L2. Interestingly, *CAH2* is upregulated in the adult fly eye, too, which parallels with the expression of *CA4* in the human eye.[33] *CA4* is the gene which codes for the only GPI-linked CA in human, and mutations in *CA4* are associated with one form of retinitis pigmentosa, RP17.[34] We suggest that CAH2 in Drosophila could be a potential new animal model for CA-associated eye disease, even though this can be considered a speculative idea at the moment.

3.2. Recombinant proteins

3.2.1. Production

Expression of CAH1 and CAH2 was performed with bacterial cells. BL21(DE3)pLysS Competent Cells (Promega) were transformed with *CAH1* and *CAH2* genes obtained from *D. melanogaster* cDNA. Purification was done with GST purification kit described above. According to SDS–PAGE the molecular weights of CAH1 and CAH2 were approximately 30 kDa and 28 kDa after the removal of the GST purification tags, respectively (Fig. 2).

3.2.2. Activity and inhibition studies

Catalytic activities of recombinant CAH1 and CAH2 enzymes were monitored using the sensitive stopped-flow method. The results indicated that both enzymes are highly active (Table 2), showing activity levels in the same range with human CA II, which is considered one of the most active enzymes. Inhibition properties of CAH1 and CAH2 were tested using acetazolamide, the classical sulfonamide CA inhibitor. The results showed that acetazolamide inhibited enzyme activities at submicromolar levels—slightly weaker when compared to CA II and DmBCA.

A series of dithiocarbamates were screened as inhibitors of these enzymes, with some representatives showing inhibition in the low nanomolar range. *n*-Hex and 2-thiazolyl thiocarbamates, for example, inhibited the enzymes very efficiently (Table 3). Inhibition profile is unique for both enzymes and differs notably from human CA II. Importantly, some compounds seem to inhibit significantly both human CA II and CAH1/CAH2, which offers opportunities for investigating the CA associated eye disease, for example. On the other hand, some compounds inhibit significantly human CA II but not CAH1/CAH2, and vice versa. This shows that there is poten-

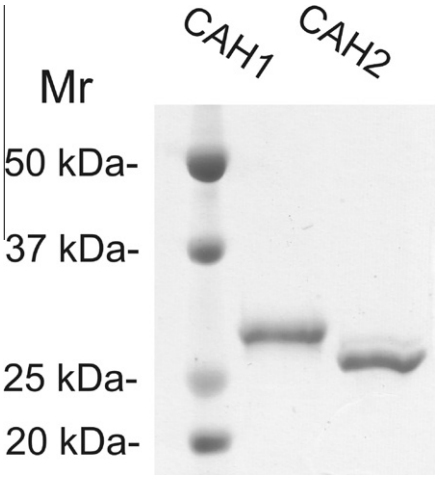

Figure 2. SDS–PAGE results from protein purification. The molecular weights of CAH1 and CAH2 were approximately 30 kDa and 28 kDa after the removal of the GST purification tags, respectively.

Table 2
Kinetic parameters for the CO_2 hydration reaction catalyzed by various CAs. Kinetic parameters for human (h) CA II (α-class CA), DmBCA (β-CA from *Drosophila melanogaster*) and CAH1 and 2 were monitored at 20 °C and pH 7.5 in 10 mM HEPES buffer and 20 mM Na_2SO_4. Inhibition data with the clinically used sulfonamide, acetazolamide (5-acetamido-1,3,4-thiadiazole-2-sulfonamide), is also shown. Data on hCA II and DmBCA have been reported in our previous work[8]

Isozyme	Activity level	k_{cat} (s^{-1})	k_{cat}/K_m (M^{-1} s^{-1})	K_I (nM)
hCA II	Very high	1.4×10^6	1.5×10^8	12
DmBCA	High	9.5×10^5	1.1×10^8	49
CAH1	High	6.4×10^6	1.2×10^8	106
CAH2	High	6.0×10^6	1.0×10^8	78

Table 3
Inhibition data of the human and insect α-CA isoform, with dithiocarbamates 1–27 by a stopped-flow, CO_2 hydrase assay[29]

R^1R^2N-CSSM

1-27

Compd	R^1	R^2	K_I (nM)[a]			M
			hCA II	CAH1	CAH2	
1	H	Ph	4.8	21.4 ± 0.2	33.9 ± 1.3	Et_3NH
2	H	$O[(CH_2CH_2)]_2N$	3.6	13.1 ± 0.9	20.7 ± 2.0	K
3	H	$MeN[(CH_2CH_2)]_2N$	33.0	0.9 ± 0.01	13.8 ± 1.2	K
4	H	2-Butyl	29.4	325 ± 21	0.9 ± 0.1	K
5	H	$O[(CH_2CH_2)]_2N(CH_2)_2$	36.3	12.1 ± 0.4	10.4 ± 0.1	K
6[b]	H	$N[(CH_2CH_2)N]_3$	13.5	134 ± 12	1.5 ± 0.2	K
7	H	$PhCH_2$	0.7	0.8 ± 0.02	213 ± 18	Na
8	H	4-PyridylCH_2	16.6	35.1 ± 1.9	58.8 ± 3.6	Et_3NH
9	H	$[(CH_2)_5N]CH_2CH_2$	20.3	57.1 ± 4.0	26.7 ± 1.8	K
10	H	2-Thiazolyl	4.6	0.5 ± 0.03	3.9 ± 0.2	Et_3NH
11	H	$KOOCCH_2$	325	123 ± 9.6	76.5 ± 5.1	K
12	H	Imidazol-1-yl-$(CH_2)_3$	24.7	0.9 ± 0.08	24.1 ± 1.3	A
13	Me	Me	6910	3461 ± 28	769 ± 21	Na
14	Et	Et	3100	2355 ± 130	654 ± 25	Na
15		$(CH_2)_5$	27.5	135 ± 5.6	4.7 ± 0.3	Na
16	*n*-Pr	*n*-Pr	55.5	23.4 ± 1.4	3.9 ± 0.2	Na
17	*n*-Bu	*n*-Bu	50.9	17.1 ± 0.8	0.5 ± 0.03	Na
18	*iso*-Bu	*iso*-Bu	0.95	20.2 ± 1.3	0.9 ± 0.02	Na
19	*n*-Hex	*n*-Hex	51.3	1.4 ± 0.11	3.8 ± 0.2	Na
20	Et	*n*-Bu	27.8	10.5 ± 0.7	21.9 ± 1.4	Na
21	$HOCH_2CH_2$	$HOCH_2CH_2$	4.0	3.2 ± 0.16	134 ± 9.5	Na
22	Me	Ph	21.5	67.1 ± 4.8	5.9 ± 0.32	Na
23	Me	$PhCH_2$	25.4	50.2 ± 3.9	12.4 ± 0.86	Na
24	$O[(CH_2CH_2)]_2$		0.95	13.8 ± 1.1	0.8 ± 0.07	Na
25	$NaS_2CN[(CH_2CH_2)]_2$		0.92	0.9 ± 0.04	21.6 ± 1.7	Na
26	$(NC)(Ph)C(CH_2CH_2)_2$		40.8	12.8 ± 1.0	3.7 ± 0.23	Na
27[c]	(*S*)-$[CH_2CH_2CH_2CH(COONa)]$		17.3	1.4 ± 0.13	13.6 ± 1.25	Na

[a] ±Standard errors of the mean (from three different measurements), by a CO_2 hydrase assay method.[29] A = imidazol-1-yl-$(CH_2)_3NH_3^+$.
[b] Tris–dithiocarbamate.
[c] (*S*)-Proline dithiocarbamate.

tial to discover selective CA inhibitors against arthropod CAs, to be used in control of disease vectors.

4. Conclusions

D. melanogaster CAH1 and CAH2 are highly active CA enzymes for hydration of CO_2 for bicarbonate and protons, which is the main physiological reaction catalysed by CAs. They can be efficiently inhibited by acetazolamide, although the inhibition constant was lower than in human CA II or drosophila β-CA. Besides evolutionary aspects, data from invertebrate CA studies may provide opportunities for anti-parasitic drug development. α-CAs are found in many invertebrate organisms which are parasites or parasite vectors. CAH2 in the eye of *D. melanogaster* may provide a new animal model for CA-related eye disease, and as many dithiocarbamates investigated here are low nanomolar or subnanomolar inhibitors of these enzymes, interesting pharmacological tools are available to check these hypotheses.

Acknowledgments

This work was supported by the competitive research funding of the Tampere University Hospital (Grant 9N054) and grants from the Academy of Finland and Sigrid Jusélius Foundation. Work from the Florence lab was supported by an FP7 EU grant (Metoxia).

References

1. (a) Sly, W. S.; Hu, P. Y. *Annu. Rev. Biochem.* **1995**, *64*, 375; (b) Supuran, C. T. *Nat. Rev. Drug Discov.* **2008**, *7*, 168.
2. Lane, T. W.; Morel, F. M. *Plant Physiol.* **2000**, *123*, 345.
3. Lane, T. W.; Saito, M. A.; George, G. N.; Pickering, I. J.; Prince, R. C.; Morel, F. M. *Nature* **2005**, *435*, 42.
4. Xu, Y.; Feng, L.; Jeffrey, P. D.; Shi, Y.; Morel, F. M. *Nature* **2008**, *452*, 56.
5. Tripp, B. C.; Bell, C. B., 3rd; Cruz, F.; Krebs, C.; Ferry, J. G. *J. Biol. Chem.* **2004**, *279*, 6683.
6. Macauley, S. R.; Zimmerman, S. A.; Apolinario, E. E.; Evilia, C.; Hou, Y. M.; Ferry, J. G.; Sowers, K. R. *Biochemistry* **2009**, *48*, 817.
7. Fasseas, M. K.; Tsikou, D.; Flemetakis, E.; Katinakis, P. *Mol. Biol. Rep.* **2009**, 37, 2941.
8. Syrjanen, L.; Tolvanen, M.; Hilvo, M.; Olatubosun, A.; Innocenti, A.; Scozzafava, A.; Leppiniemi, J.; Niederhauser, B.; Hytonen, V. P.; Gorr, T. A.; Parkkila, S.; Supuran, C. T. *BMC Biochem.* **2010**, *11*, 28.
9. Smith, K. E.; Vanekeris, L. A.; Linser, P. J. *J. Exp. Biol.* **2007**, *210*, 3919.
10. Fisher, S. Z.; Tariku, I.; Case, N. M.; Tu, C.; Seron, T.; Silverman, D. N.; Linser, P. J.; McKenna, R. *Biochim. Biophys. Acta* **2006**, *1764*, 1413.
11. Bertram, G.; Zierold, K.; Wessing, A. *J. Insect Physiol.* **1997**, *43*, 17.
12. Shanbhag, S.; Tripathi, S. *J. Exp. Biol.* **2009**, *212*, 1731.
13. Flicek, P.; Amode, M. R.; Barrell, D.; Beal, K.; Brent, S.; Carvalho-Silva, D.; Clapham, P.; Coates, G.; Fairley, S.; Fitzgerald, S.; Gil, L.; Gordon, L.; Hendrix, M.; Hourlier, T.; Johnson, N.; Kahari, A. K.; Keefe, D.; Keenan, S.; Kinsella, R.; Komorowska, M.; Koscielny, G.; Kulesha, E.; Larsson, P.; Longden, I.; McLaren, W.; Muffato, M.; Overduin, B.; Pignatelli, M.; Pritchard, B.; Riat, H. S.; Ritchie, G. R.; Ruffier, M.; Schuster, M.; Sobral, D.; Tang, Y. A.; Taylor, K.; Trevanion, S.; Vandrovcova, J.; White, S.; Wilson, M.; Wilder, S. P.; Aken, B. L.; Birney, E.; Cunningham, F.; Dunham, I.; Durbin, R.; Fernandez-Suarez, X. M.; Harrow, J.; Herrero, J.; Hubbard, T. J.; Parker, A.; Proctor, G.; Spudich, G.; Vogel, J.; Yates, A.; Zadissa, A.; Searle, S. M. *Nucleic Acids Res.* **2012**, *40*, D84.
14. Sayers, E. W.; Barrett, T.; Benson, D. A.; Bolton, E.; Bryant, S. H.; Canese, K.; Chetvernin, V.; Church, D. M.; Dicuccio, M.; Federhen, S.; Feolo, M.; Fingerman, I. M.; Geer, L. Y.; Helmberg, W.; Kapustin, Y.; Krasnov, S.; Landsman, D.; Lipman, D. J.; Lu, Z.; Madden, T. L.; Madej, T.; Maglott, D. R.; Marchler-Bauer, A.; Miller, V.; Karsch-Mizrachi, I.; Ostell, J.; Panchenko, A.; Phan, L.; Pruitt, K. D.; Schuler, G. D.; Sequeira, E.; Sherry, S. T.; Shumway, M.; Sirotkin, K.; Slotta, D.; Souvorov, A.; Starchenko, G.; Tatusova, T. A.; Wagner, L.; Wang, Y.; Wilbur, W. J.; Yaschenko, E.; Ye, J. *Nucleic Acids Res.* **2012**, *40*, D13.
15. UniProt Consortium. *Nucleic Acids Res.* **2012**, *40*, D71.
16. Tweedie, S.; Ashburner, M.; Falls, K.; Leyland, P.; McQuilton, P.; Marygold, S.; Millburn, G.; Osumi-Sutherland, D.; Schroeder, A.; Seal, R.; Zhang, H.; FlyBase Consortium *Nucleic Acids Res.* **2009**, *37*, D555.
17. Gelbart, W.; Emmert, D. (2010.10.13). FlyBase High Throughput Expression Pattern Data Beta Version.

18. Larkin, M. A.; Blackshields, G.; Brown, N. P.; Chenna, R.; McGettigan, P. A.; McWilliam, H.; Valentin, F.; Wallace, I. M.; Wilm, A.; Lopez, R.; Thompson, J. D.; Gibson, T. J.; Higgins, D. G. *Bioinformatics* **2007**, *23*, 2947.
19. Goujon, M.; McWilliam, H.; Li, W.; Valentin, F.; Squizzato, S.; Paern, J.; Lopez, R. *Nucleic Acids Res.* **2010**, *38*, W695.
20. Tamura, K.; Peterson, D.; Peterson, N.; Stecher, G.; Nei, M.; Kumar, S. *Mol. Biol. Evol.* **2011**, *28*, 2731.
21. Rzhetsky, A.; Nei, M. *Mol. Biol. Evol.* **1992**, *9*, 945–967.
22. Felsenstein, J. *Evolution* **1985**, *39*, 783–791.
23. Zuckerkandl, E.; Pauling, L. Evolving Genes and Proteins In Bryson, V., Vogel, H. J., Eds.; Academic Press: New York, 1965; pp 97–166.
24. Nei, M.; Kumar, S. Molecular Evolution and Phylogenetics Oxford University Press: New York, 2000.
25. Saitou, N.; Nei, M. *Mol. Biol. Evol.* **1987**, *4*, 406.
26. Petersen, T. N.; Brunak, S.; von Heijne, G.; Nielsen, H. *Nat. Methods* **2011**, *8*, 785.
27. Emanuelsson, O.; Brunak, S.; von Heijne, G.; Nielsen, H. *Nat. Protoc.* **2007**, *2*, 953.
28. Pierleoni, A.; Martelli, P. L.; Casadio, R. *BMC Bioinformatics* **2008**, *9*, 392.
29. Khalifah, R. G. *J. Biol. Chem.* **1971**, *246*, 2561.
30. (a) Carta, F.; Aggarwal, M.; Maresca, A.; Scozzafava, A.; McKenna, R.; Supuran, C. T. *Chem. Commun.* **2012**, *48*, 1868; (b) Carta, F.; Aggarwal, M.; Maresca, A.; Scozzafava, A.; McKenna, R.; Masini, E.; Supuran, C. T. *J. Med. Chem.* **2012**, *55*, 1721; (c) Monti, S. M.; Maresca, A.; Viparelli, F.; Carta, F.; De Simone, G.; Mühlschlegel, F. A.; Scozzafava, A.; Supuran, C. T. *Bioorg. Med. Chem. Lett.* **2012**, *22*, 859; (d) Maresca A, Carta F, Vullo D, Supuran C.T. J. Enzyme Inhib. Med. Chem. 2012; 27: in press.; (e) Kolayli, S.; Karahalil, F.; Sahin, H.; Dincer, B.; Supuran, C. T *J. Enzyme Inhib. Med. Chem.* **2011**, *26*, 895.
31. Linser, P. J.; Smith, K. E.; Seron, T. J.; Neira Oviedo, M. *J. Exp. Biol.* **2009**, *212*, 1662.
32. Ortutay, C.; Olatubosun, A.; Parkkila, S.; Vihinen, M.; Tolvanen, M. In *Advances in Medicine and Biology*; Bernhardt, L. E., Ed.; Nova Science Publishers, Inc.: Hauppauge, NY, 2010; Vol. 7, pp 145–168.
33. Hageman, G. S.; Zhu, X. L.; Waheed, A.; Sly, W. S. *Proc. Natl. Acad. Sci. U.S.A.* **1991**, *88*, 2716.
34. Datta, R.; Waheed, A.; Bonapace, G.; Shah, G. N.; Sly, W. S. *Proc. Natl. Acad. Sci. U.S.A.* **2009**, *106*, 3437.

Journal of Medicinal Chemistry

Article

pubs.acs.org/jmc

Cloning, Characterization, and Inhibition Studies of a β-Carbonic Anhydrase from *Leishmania donovani chagasi*, the Protozoan Parasite Responsible for Leishmaniasis

Leo Syrjänen,*[,†,‡] Alane Beatriz Vermelho,[§] Igor de Almeida Rodrigues,[§] Suzana Corte-Real,[∥] Terhi Salonen,[†,‡] Peiwen Pan,[†,‡] Daniela Vullo,[⊥] Seppo Parkkila,[†,‡,#] Clemente Capasso,[▽] and Claudiu T. Supuran*[,⊥,○]

[†]Institute of Biomedical Technology and BioMediTech, University of Tampere, 33520 Tampere, Finland

[‡]School of Medicine, University of Tampere and Tampere University Hospital, 33014 Tampere, Finland

[§]Biotechnology Center—BIOINOVAR: Bioenergy, Biocatalysis and Bioproducts, Federal University of Rio de Janeiro, 21941-901 Rio de Janeiro, Brazil

[∥]Laboratory of Structural Biology, Oswaldo Cruz Institute (OCI) Platform, Manguinhos, 21040-360, Rio de Janeiro, RJ Brazil

[⊥]Laboratorio di Chimica Bioinorganica, Dipartimento di Chimica, Università degli Studi di Firenze, Via della Lastruccia 3, 50019 Sesto Fiorentino, Firenze, Italy

[#]Fimlab Laboratories Ltd, 33101 Tampere, Finland

[▽]Istituto di Biochimica delle Proteine—CNR, Via Pietro Castellino 111, 80131 Napoli, Italy

[○]Neurofarba Dipartimento, Sezione di Scienza Farmaceutiche e Nutraceutiche, Università degli Studi di Firenze, Via Ugo Sciff 6, 50019 Sesto Fiorentino, Firenze, Italy

Supporting Information

ABSTRACT: Leishmaniasis is an infection provoked by protozoans belonging to the genus *Leishmania*. Among the many species and subsepecies of such protozoa, *Leishmania donovani chagasi* causes visceral leishmaniasis. A β-carbonic anhydrase (CA, EC 4.2.1.1) was cloned and characterized from this organism, denominated here LdcCA. LdcCA possesses effective catalytic activity for the CO_2 hydration reaction, with k_{cat} of 9.35×10^5 s^{-1} and k_{cat}/K_M of 5.9×10^7 M^{-1} s^{-1}. A large number of aromatic/heterocyclic sulfonamides and 5-mercapto-1,3,4-thiadiazoles were investigated as LdcCA inhibitors. The sulfonamides were medium potency to weak inhibitors (K_I values of 50.2 nM–9.25 μM), whereas some heterocyclic thiols inhibited the enzyme with K_Is in the range of 13.4–152 nM. Some of the investigated thiols efficiently inhibited the in vivo growth of *Leishmania chagasi* and *Leishmania amazonensis* promastigotes, by impairing the flagellar pocket and movement of the parasites and causing their death. The β-CA from *Leishmania* spp. is proposed here as a new antileishmanial drug target.

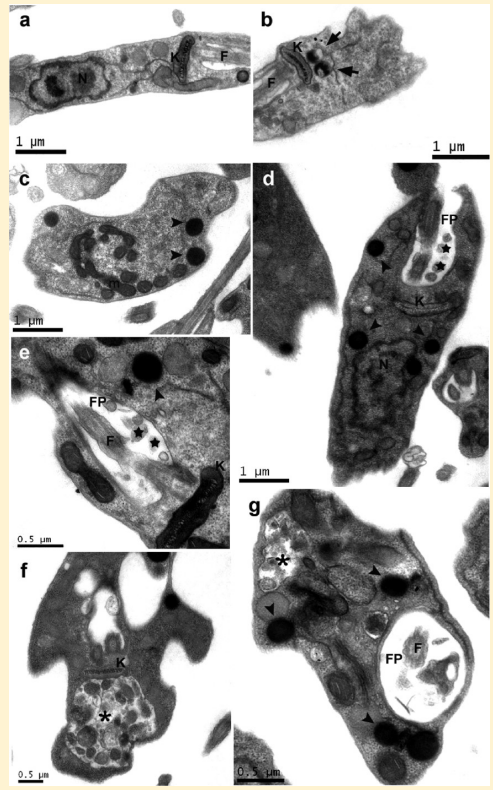

Received: June 22, 2013
Published: August 26, 2013

dx.doi.org/10.1021/jm400939k | J. Med. Chem. 2013, 56, 7372–7381

INTRODUCTION

Leishmaniasis is a vector-borne tropical disease caused by unicellular protozoan organisms from the genus *Leishmania*. The parasites are transmitted to the mammalian host organism by an infected sand fly. Some *Leishmania* species, such as *Leishmania major*, remain mainly in the skin, while other species, like *Leishmania donovani chagasi*, infect visceral organs. Leishmaniasis is associated with a wide range of clinical manifestations, from self-healing skin lesions to no less than fatal visceral infections. Visceral leishmaniasis accounts for 20 000−40 000 deaths every year.[1]

Carbonic anhydrases (CAs, EC 4.2.1.1) are ubiquitous enzymes that catalyze the reversible hydration reaction of carbon dioxide as follows: $CO_2 + H_2O \leftrightarrow HCO_3^- + H^+$.[2−4] CAs are usually zinc-containing metalloenzymes, but the ζ-form use cadmium or zinc (in an interexchangeable manner),[3] as an alternative metal cofactor. γ-CAs may contain iron(II) ions within the active site, at least in some anaerobic *Archaea*.[5,6] The reaction catalyzed by CAs is essential in the regulation of acid−base balance in organisms.[2−6] Moreover, this reaction helps to remove carbon dioxide out of tissues, participates in biosynthetic reactions such as gluconeogenesis and ureagenesis, and is involved in many other physiological processes.[2]

Until now, five classes of carbonic anhydrases have been identified: α, β, γ, δ, and ζ.[7] A previously described ε-CA class[8] has been reclassified as a distinct type of β-CA on the basis of its crystallographic structure,[9] as the enzyme showed a fold almost identical to that of the archaeal cab-type[10] and plant-type[11] β-CAs. In the ζ-CA (from the marine diatom *Thalassiosira weissflogii*) the coordination of the metal ion within the active site was very similar to that of the β-CAs, with one His, two Cys, and a water molecule acting as ligands of the Cd(II) or Zn(II) ions.[3]

β-CAs appear to be the CA group with the widest distribution, as they have been described from various groups of organisms including *Archae* and *Bacteria* domains and with high probability all species of plants and fungi among *Eukarya*.[12] Additionally, our previous studies suggest the widespread occurrence of at least a single-copy β-CA gene among animal species distinct from chordates.[13] β-CAs have so far been reported from various pathogenic organisms, including the fungi/yeasts *Candida albicans*, *Candida glabrata*, *Cryptococcus neoformans*, and *Saccharomyces cerevisiae*[14−19] and bacteria *Mycobacterium tuberculosis*, *Brucella suis*, *Salmonella typhimurium*, *Helicobacter pylori*, *Streptococcus pneumoniae*, and *Haemophilus influenza*.[20−26] The inhibition profiles of these enzymes with various agents such as sulfonamides, anions, carboxylates, phenols, dithiocarbamates, and boronic acids have also been explored.[14−21,23−32] Recently, β-CAs have been reported from two invertebrate species, namely, the insect *Drosophila melanogaster* and the worm *Caenorhabditis elegans*.[13,33] β-CAs are absent from vertebrates, which may lead to the design of β-CA-specific inhibitors that could be used against the pathogenic, invertebrate organisms. However, not such inhibitors have been reported so far. Protozoa were only known to encode for α-CAs. Indeed, *Plasmodium falciparum*, the malaria producing protozoa, encodes several such enzymes,[34] and more recently, one such α-CA was also characterized from the unicellular protozoa responsible of Chagas' disease, *Trypanosoma cruzi*.[34d]

No investigations of the CAs from protozoa belonging to the genus *Leishmania* were reported so far. We performed thus sequence searches in the genomes of these pathogens and found out that *Leishmania* encodes for one α- and one β-CA. The aim of this study was to express, purify, and characterize the β-CA from *L. donovani* (subspecies *chagasi*, as there are many *L. donovani* subspecies), denominated here LdcCA, which is one of the causative agents of visceral leishmaniasis.[1] The new β-CA described here is the first such enzyme characterized from a protozoan. Kinetic and inhibition studies with a large set of inhibitors were carried out to characterize its catalytic activity and inhibition profile, whereas some of the compounds showing good in vitro activity were also tested against various *Leishmania* species in vivo. The interesting biological activity reported here allow us to propose this β-CA as a new antileishmanial drug target.

RESULTS AND DISCUSSION

Expression of LdcCA in Sf9 Insect Cells. No β-CAs were so far investigated in protozoa, although the existence of β-CA sequences has been confirmed in *Placozoa*, *Cnidaria*, *Platyhelminthes*, *Nematoda*, *Arthropoda*, and *Annelida* and also in many classes of *Deuterostomia* and *Protostomia*.[13] Using Blast searches[34f] we found that β-CAs are also present in the genus *Leishmania*, which is a subgroup of *Excavata*. As such enzymes are absent from vertebrates,[13] this opens possibilities for the development of parasite-specific β-CA inhibitors that could be used to fight this tropical disease. This was the rationale for the cloning, characterization, and inhibitor design studies of the leishmanial β-CA LdcCA reported here.

Previously, β-CAs were produced in recombinant form only in *Escherichia coli*, but here we report the use of Sf9 insect cells (an eukaryotic system, as the protozoa itself), which were transfected with the β-CA gene obtained from *L. donovani chagasi* cDNA. The expression was performed using the Bac-to-Bac baculovirus expression system. According to SDS−PAGE, the molecular mass of the enzyme was around 35 kDa before the removal of the polyhistidine tag used for its purification on a Ni-affinity column (see Experimental Protocols for details and Supplementary Figure 1 of the Supporting Information).

LdcCA Catalytic Activity. The LdcCA catalytic activity for the CO_2 hydration reaction is shown in Table 1,[35,36] where data for other CAs [such as the widespread and highly investigated human (h) isoforms hCA I and II as well as the *T. cruzi* TcCA enzyme, belonging to the α-class][34e] and β-CAs from a bacterium *Methanobacterium thermoautotrophicum* (Cab),[18] the yeast *S. cerevisiae* (SceCA),[17,19] and the plant *Flaveria bidentis* (isoform 1, FbiCA 1)[37] are included for comparison reasons. A stopped-flow CO_2 hydrase assay has been used to measure the catalytic activity of these enzymes under identical conditions.[35] It may be observed that LdcCA has kinetic parameters similar to those of the human isoform hCA I and the yeast enzyme SceCA, being slightly less effective than the human isoform hCA II, one of the catalytically most active such enzymes known to date (together with hCA IX).[36] Indeed, with a k_{cat}/K_m of 5.9×10^7 M^{-1} s^{-1}, LdcCA is a highly effective catalyst for the CO_2 hydration to bicarbonate and protons, being more effective compared to the plant enzyme FbiCA 1 or the bacterial one Cab (Table 1). However, unlike hCA II, but similar to the other protozoan enzyme investigated earlier, TcCA, LdcCA is much less sensitive to the sulfonamide inhibitor acetazolamide (5-acetamido-1,3,4-thiadiazole-2-sulfonamide, **AAZ**). Some α-CAs considered here, such as hCA II, are strongly inhibited by this sulfonamide in clinical use, with a K_I of 12 nM (Table 1). Similar to hCA I and TcCA, which are less sensitive to this sulfonamide (K_I of 61.6−250 nM), LdcCA was inhibited only with a K_I of 91.7 nM by this compound, which is thus a medium potency inhibitor. It should

dx.doi.org/10.1021/jm400939k | J. Med. Chem. 2013, 56, 7372−7381

Table 1. Kinetic Parameters for CO_2 Hydration Reaction Catalyzed by Some α-/β-CA Isozymes of Human (h) hCA I and II, the Protozoan TcCA (*T. cruzi*) and Cab (*M. thermoautotrophicum*), FbiCA (*F. bidentis* CA), and SceCA (*S. cerevisiae* enzyme) as well as LdcCA (*L. donovani chagasi*), at 20 °C and pH 7.5 (for the α-CAs) and pH 8.4 (for the β-CA), and Their Inhibition Data with Acetazolamide AAZ (5-Acetamido-1,3,4-thiadiazole-2-sulfonamide), a Clinically Used Drug

enzyme	k_{cat} (s^{-1})	K_m (M)	k_{cat}/K_m (M^{-1} s^{-1})	K_I(acetazolamide) (nM)
hCA I[a]	2.00×10^5	4.0×10^{-3}	5.00×10^7	250
hCA II[a]	1.40×10^6	9.3×10^{-3}	1.50×10^8	12
TcCA[b]	1.21×10^6	8.1×10^{-3}	1.49×10^8	61.6
Cab[c]	3.10×10^4	1.7×10^{-3}	1.82×10^7	12100
SceCA[d]	9.4×10^5	9.6×10^{-3}	9.8×10^7	82
FbiCA 1[e]	1.2×10^5	1.6×10^{-3}	7.5×10^6	27
LdcCA[f]	9.35×10^5	15.8×10^{-3}	5.9×10^7	91.7

[a]Human recombinant isozymes, stopped flow CO_2 hydrase assay method, from ref 2. [b]From ref 34e. [c]From ref 18. [d]From refs 17, 19. [e]From ref 37. [f]Recombinant enzyme, stopped flow CO_2 hydrase assay method,[35] this work.

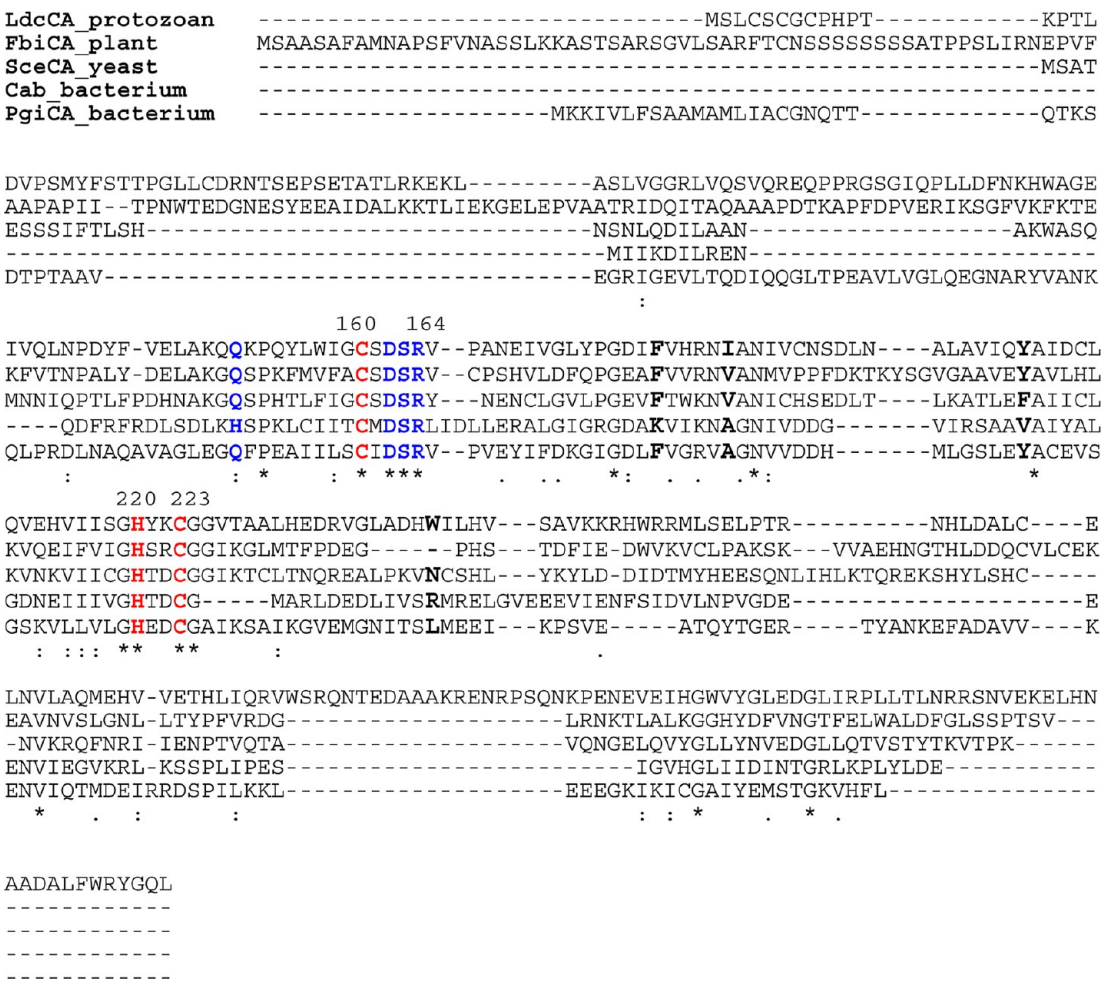

Figure 1. Alignment of the predicted amino acid sequences of selected β-CAs from protozoan, plant, yeast, and bacterial organisms. The *P. sativum* numbering system was used. Zinc ligands are indicated in red; amino acids involved in the enzyme catalytic cycle are indicated in blue; amino acids forming the continuous hydrophobic surface in the binding pocket are in bold. An asterisk (*) indicates identity at a position and a colon (:) designates conserved substitutions, while a period (.) indicates semiconserved substitutions. Multiple alignment was performed with the program Clustal W, version 2.1. Legend: LdcCA_protozoan, *L. donovani chagasi* (to be submitted); FbiCA_plant, *F. bidentis*, isoform I (accession number AAA86939.2); SceCA_yeast, *S. cerevisiae* (accession number GAA26059); Cab_bacterium, *M. thermoautotrophicum* (accession number GI: 13786688); PgiCA_bacterium, *Porphiromonas gingivalis* (accesion number YP_004510261).[11]

be also observed that some β-CAs, such as FbiCA 1, have higher affinities for this sulfonamide inhibitor and others, such as LdcCA and SceCA, have medium affinity, whereas Cab is rather insensitive to inhibition by acetzolamide (K_I of 12.1 μM).

Sequence and Phylogenetic Analyses. To rationalize the kinetic data in Table 1, an alignment of the amino acid sequence of LdcCA 1 with that of selected β-CAs from plants (FbiCA 1, from *F. bidentis*)[37] and yeasts (SceCA, from *S. cerevisiae*)[17,19] as well as the bacteria *M. thermoautotrophicum* (Cab) and *Porphiromonas gingivalis* (PgiCA) is shown Figure 1. LdcCA has all the amino acid residues involved in catalysis, as is the case for the other members of the β-CA family (Figure 1): (i) the

dx.doi.org/10.1021/jm400939k | J. Med. Chem. 2013, 56, 7372−7381

three Zn(II) ligands, Cys160, His220, and Cys223 (*Pisum sativum* CA numbering system);[11] (ii) the Asp162−Arg164 catalytic dyad, which forms a hydrogen bond network with the water coordinated to the Zn(II) ion, enhancing its nucleophilicity;[11,17−19] and (iii) a cluster of hydrophobic amino acid residues considered to be involved in the binding of the substrate (and inhibitors), including those in positions 151, 179, and 184.[11,17−19] Indeed, some of them are conserved in almost all the enzymes used in the alignment, even if they are from organisms in various life kingdoms.

As this is the first β-CA from a protozoa, we also explored its phylogenetic relationship with other members of the family belonging to bacteria, yeast, algae, and plants (Figure 2). In

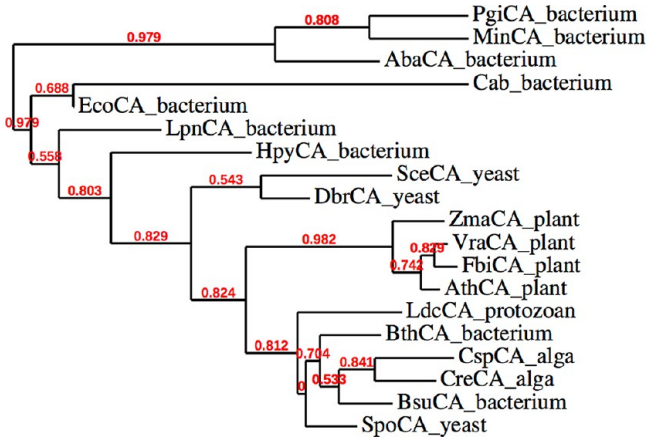

Figure 2. Phylogenetic tree of the β-CAs from prokaryotic and eukaryotic sources. The tree was constructed using the program PhyML 3.0. Branch support values are reported at branch points. Legend: PgiCA_bacterium, *P. gingivalis* (accesion number YP_004510261); MinCA_bacterium, *Myroides injenensis* M09-0166 (accession number ZP_10784819); AbaCA_bacterium, *Acinetobacter baumannii* AB307-0294 (accession number YP_002326524); Cab_bacterium, *M. thermoautotrophicum* (accession number GI: 13786688); EcoCa_bacterium, *E. coli* (accession number ACI70660); LpnCA_bacterium, *Legionella pneumophila* 2300/99 (accession number YP_003619232); HpyCA_bacterium, *Helicobacter pylori* (accession number BAF34127.1); SceCA_yeast, *S. cerevisiae* (accession number GAA26059); DbrCA_yeast, *Dekkera bruxellensis* AWRI1499 (accession number EIF49256); ZmaCA_-plant, *Zea mays* (accession number NP_001147846.1); VraCA_plant, *Vigna radiata* (accession number AAD27876); FbiCA_plant, *F. bidentis* isoform I (accession number AAA86939.2); AthCA_plant, *Arabidopsis thaliana* (accession number AAA50156); LdcCA_protozoan; *L. donovani caghasi* (to be submitted); BthCA_bacterium, *Burkholderia thailandensis* Bt4 (accession number ZP_02386321); CspCA_alga, *Coccomyxa* sp. (accession number AAC33484.1); CreCA_alga, *Chlamydomonas reinhardtii* (accession number XP_001699151.1); BsuCA_bacterium, *B. suis* 1330 (accession number NP_699962.1); SpoCA_yeast, *Schizosaccharomyces pombe* (accession number CAA21790).

Figure 2 we present a phylogenetic tree including a large number of such enzymes from diverse organisms belonging to both prokaryotes and eukaryotes. It may be observed that the protozoan enzyme LdcCA has its own branch, but it clustered not far from some bacterial, algal, and yeast β-CAs, being rather distinct from the plant type of such enzymes (which all clustered on the superior, brother branch of the one including the protozoan enzyme). However, it may be observed that the phylogeny of the β-CAs is not at all simple, with a rather intricate tree (Figure 2) even when considering a reduced number of organisms. This is probably also due to the fact that, as mentioned above, the β-CA seems to be the most widespread family of such enzymes.

LdcCA Inhibition Studies. Sulfonamides are the main class of zinc-binding CA inhibitors (CAIs),[38,39] but several other classes of inhibitors were also reported recently, such as the thiols, dithocarbamates, coumarins, and polyamines among others.[40] We have thus included a range of sulfonamides and several thiols in an initial screening program to find compounds targeting this new protozoan enzyme.

Data of Tables 2 and 3 show the LdcCA inhibition data with a range of aromatic/heterocyclic sulfonamides of types **1**−**24** (Chart 1), **AAZ** through **HCT** (Chart 2), and 1,3,4-thiadiazole-2-thiols (Chart 3),[41] shown earlier to act as effective inhibitors of the protozoan CA from *T. cruzi*.[35e] Simple aromatic and heteroaromatic sulfonamides of types **1**−**24** were among the investigated sulfonamides, as well as derivatives **AAZ** through **HCT**, which are clinically used drugs (or agents in clinical development). Acetazolamide (**AAZ**), methazolamide (**MZA**), ethoxzolamide (**EZA**), and dichlorophenamide (**DCP**) are the classical, systemically acting CAIs.[2,4] Dorzolamide (**DZA**) and brinzolamide (**BRZ**) are topically acting antiglaucoma agents,[2] benzolamide (**BZA**) is an orphan drug belonging to this class of pharmacological agents, whereas topiramate (**TPM**), zonisamide (**ZNS**), and sulthiame (**SLT**) are widely used antiepileptic drugs.[2] Sulpiride (**SLP**), indisulam (**IND**), valdecoxib (**VLX**), celecoxib (**CLX**), saccharin (**SAC**), and hydrochlorothiazide (**HCT**) were recently shown by this group to belong to this class of pharmacological agents.[2] Sulfonamides **1**−**24** and the clinically used agents investigated in this study were either commercially available or were prepared as reported earlier by our group.[42] The following should be observed from the data of Table 2, where inhibition data of hCA I and II as well as TcCA are also reported for comparison reasons:

(i) Most of the simple sulfonamides investigated here, such as compounds **1**−**17**, **19**, **DCP**, **DZA**, **BRZ**, **BZA**, **TPM**, **ZNS**, **SLP**, **IND**, **VLX**, **CLX**, **SLT**, and **SAC**, were weak or ineffective as inhibitors of LdcCA. Indeed, several such sulfonamides (and **TPM**, the only sulfamate investigated here) did not inhibit significantly LdcCA (K_I values > 100 μM; see Table 2), whereas the largest majority of these derivatives showed inhibition constants in the range of 136−9251 nM. It may be observed that they belong to rather heterogeneous classes of aromatic or heterocyclic sulfonamides, so that the structure−activity relationship (SAR) is not straightforward.

(ii) A better inhibition profile of LdcCA has been observed with the following derivatives: **18**, **20**−**24**, **AAZ**, **MZA**, **EZA**, and **HCT**, which had K_I values in the range of 50.2−95.1 nM (Table 2). Apart from the 4-carboxybenzenesulfonamide **18**, which is a simple and rather compact molecule, compounds **20**−**24** incorporate an elongated molecule of the arylsulfonylated sulfonamide type. The five-membered heterocyclic sulfonamides **AAZ** and **MZA** were also among these effective inhibitors, but they were weaker LdcCA inhibitors compared to the bicyclic **EZA** and **HCT**, which were the most potent sulfonamide inhibitors detected here, with K_I values in the range of 50.2−51.5 nM.

(iii) The inhibition profile of LdcCA with the investigated sulfonamides is very different from that of the mammalian enzymes hCA I and II (which is a positive feature if one needs to inhibit the parasite and not also the host enzymes) or the protozoan one from *T. cruzi* (Table 2).

As most of the sulfonamides were not highly effective CAIs against the protozoan enzyme reported here, we decided to investigate thiols as possible LdcCA inhibitors, it being well-documented that the mercapto moiety (in ionized, anionic form)

Table 2. Inhibition of Human Isoforms hCA I and hCA II, as Well as the Protozoan Ones from *T. cruzi* (TcCA) and *L. donovani chagasi* (LdcCA), with Sulfonamides 1−24 and the Clinically Used Agents AAZ through HCT

	K_I[a] (nM)			
inhibitor	hCA I[b]	hCA II[b]	TcCA[c]	LdcCA[d]
1	28000	300	25460	5960
2	25000	240	57300	9251
3	79[d]	8	63800	8910
4	78500	320	44200	>100000
5	25000	170	7231	>100000
6	21000	160	9238	>100000
7	8300	60	8130	15600
8	9800	110	6925	9058
9	6500	40	8520	8420
10	7300	54	9433	9135
11	5800	63	842	9083
12	8400	75	820	4819
13	8600	60	534	584
14	9300	19	652	433
15	5500	80	73880	927
16	9500	94	71850	389
17	21000	125	66750	227
18	164	46	84000	59.6
19	109	33	810	>100000
20	6	2	88.5	95.1
21	69[d]	11[d]	134	50.2
22	164	46	365	136
23	109	33	243	87.1
24	95	30	192	73.4
AAZ	250	12	61.6	91.7
MZA	50	14	74.9	87.1
EZA	25	8	88.2	51.5
DCP	1200	38	128	189
DZA	50000	9	92.9	806
BRZ	45000	3	87.3	764
BZA	15	9	93.6	236
TPM	250	10	85.5	>100000
ZNS	56	35	867	>100000
SLP	1200	40	87.9	>100000
IND	31	15	84.5	316
VLX	54000	43	82.7	338
CLX	50000	21	91.1	705
SLT	374	9	71.9	834
SAC	18540	5959	8210	>100000
HCT	328	290	134	50.2

[a]Errors in the range of 5−10% of the shown data, from three different assays. [b]Human recombinant isozymes, stopped flow CO_2 hydrase assay method, from ref 38. [c]Recombinant bacterial enzyme, stopped flow CO_2 hydrase assay method, from ref 34e. [d]Recombinant protozoan enzyme, this work.

may act as a good zinc-binding group (similar to the SO_2NH^- one) for obtaining effective CAIs.[2,35e,41] The 1,3,4-thiadiazole-5-mercapto derivatives **25**−**34** (Chart 3) were reported earlier by our group as medium potency hCA I and II inhibitors[41] and were here investigated for their interaction with LdcCA (Table 3). It may be observed that already the simple semicarbazido derivative **25** is a rather effective LdcCA inhibitor (K_I of 74.1 nM), whereas many of its Schiff's bases of types **26**−**30** and **32** are even better inhibitors of the protozoan enzyme, with inhibition constants in the range of 13.4−40.1 nM. A loss of inhibitory activity was

Table 3. hCA I, hCA II, and LdcCA Inhibition Data for Thiols 25−34 and Anti-Leishmanial in Vivo Data for Some of These Derivatives[a]

	K_I (nM)			% inhibition of growth[d]	
compd	hCA I[b]	hCA II[b]	LdcCA[c]	*L. chagasi*	*L. amazonensis*
25	7100	9200	74.1	nt	nt
26	3000	354000	27.9	36.3	45.8
27	30770	3830	33.1	18	56
28	18740	13460	18.4	51.5	62.3
29	71600	235000	13.4	100[e]	97[f]
30	8540	2670	40.1	32.2	76.4
31	144000	3890	95.3	0	7
32	8530	8850	19.5	74.8	91.9
33	7890	8360	144	0	0
34	3710	7970	152	0	0

[a]Promastigote forms of *L. chagasi* MHOM/BR/1974/PP75 and *L. amazonensis* Raimundo strains MHOM/BR/76/Ma−5 have been used for the in vivo experiments.[43,44] Concentrations of test compounds ranging from 2 to 256 μM were used. [b]From ref 41. [c]This work; nt = not tested. [d]Determined as described in ref 44, representing the percent inhibition observed at 256 μM concentration of test compound. [e]Percent inhibition at 128 μM: 30%. [f]Percent onhibition at 128 μM: 28%.

Chart 1. Sulfonamides 1−24

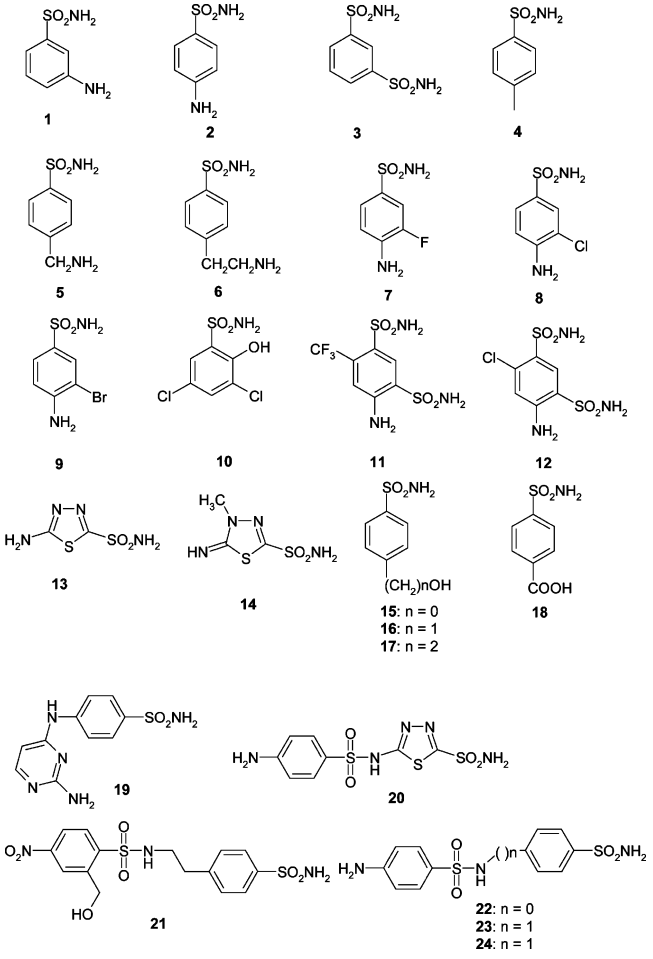

observed for compounds **31**, **33**, and **34**, which showed K_I values in the range of 95.3−152 nM (Table 3); SAR is here very interesting. Thus, the Schiff's bases of types **26**−**30** obtained

dx.doi.org/10.1021/jm400939k | J. Med. Chem. 2013, 56, 7372−7381

Chart 2. Clinically Used Agents

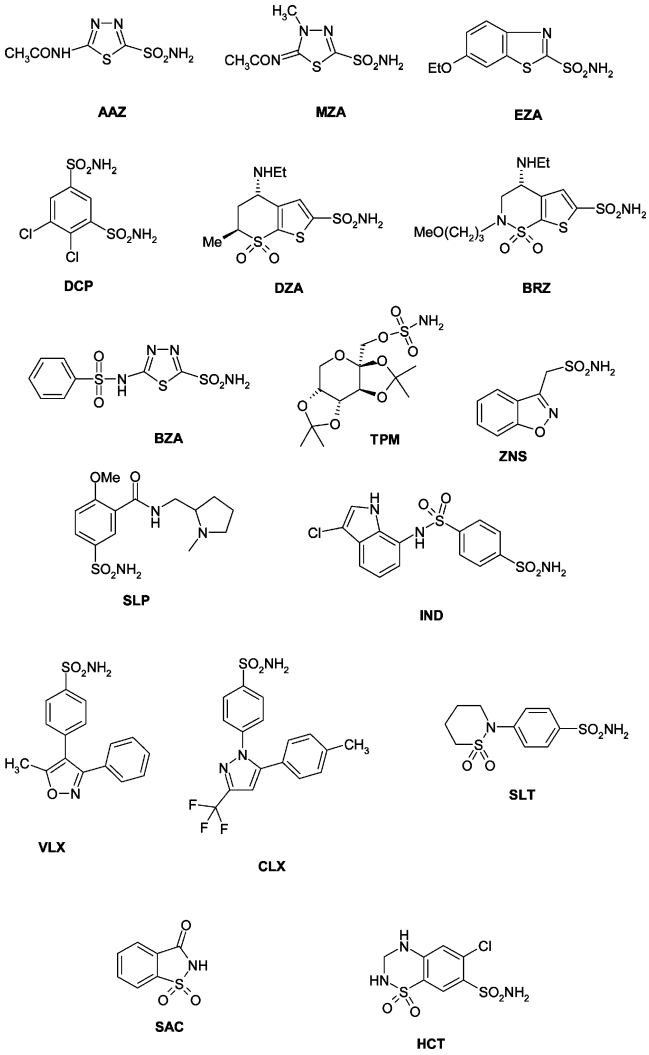

Chart 3. 1,3,4-Thiadiazole-2-thiols 25−34

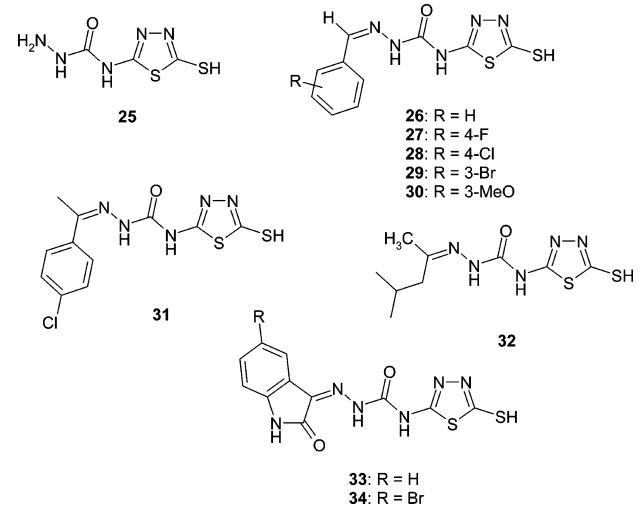

from substituted benzaldehydes showed the best LdcCA inhibitory activity, with the chloro and bromo derivatives **28** and **29** being the best inhibitors. The chloroacetophenone derivative **31**, which differs only by the presence of an extra methyl moiety compared to **28**, was 5.17 times less effective as LdcCA inhibitor compared to **28**. The bulkier derivatives **33** and **34** also led to a loss of LdcCA inhibitory power compared to the less bulky compounds **26**−**30** or the one incorporating an aliphatic side chain (**32**) (Table 3).

In Vivo Inhibition Studies. The effect of the 1,3,4-thiadiazolethiol derivatives **25**−**34** (which were among the best in vitro LdcCA inhibitors) on *Leishmania* spp. viability was assessed in vivo, too (Table 3 and Figure 3). Table 3 summarizes

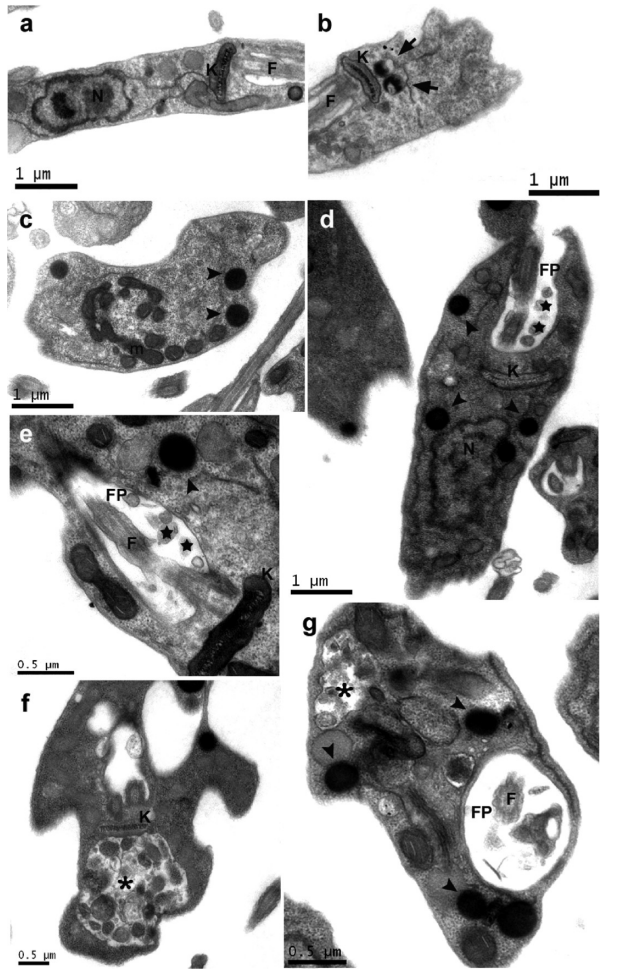

Figure 3. Ultrastructure effects of compound **29** on *L. chagasi* promastigotes after 24 h treatment. (a and b) Ultrathin sections of untreated parasites presenting typical elongated morphology with normal nucleus, kinetoplast, mitochondria, and flagellum. Note the normal aspect of the flagellar pocket. Arrows indicate acidocalcisomes (b). (c−g) Parasites treated with 253 μM of **29**, showing accumulation of intracytoplasmic electron-dense granules (arrowhead) and several alterations in flagellar pocket, such as the presence of vacuoles (stars in d and e) and marked swelling (g). An asterisk indicates autophagic vacuoles (f and g). N, nucleus; K, kinetoplast; m, mitochondria; F, flagellum; FP, flagellar pocket.

the compounds tested and their inhibitory effect on two *Leishmania* species, *L. chagasi* and *L. amazonensis* promastigotes. After 120 h treatment, compounds **26**−**30** and **32** exhibited a significant antileishmanial activity, at concentrations of 256 μM. The best results were obtained with compounds **29** and **32**, which demonstrated an inhibition of growth of both *L. chagasi* and *L. amazonensis* in the range of 74.8−100% (Table 3). Only compound **29** was able to completely abrogate *Leishmania* growth, with an MIC of 256 μM. In fact, when parasites were

dx.doi.org/10.1021/jm400939k | J. Med. Chem. 2013, 56, 7372−7381

treated with this concentration of compound **29** and were then reincubated in fresh medium, they were no longer able to grow.

Ultrastructural Analysis by Transmission Electron Microscopy. Photomicrographs of *L. chagasi* treated with compound **29** at 256 μM were obtained in order to evaluate the antileishmanial mechanism that leads to the parasite death. Figure 3 shows important ultrastructural alterations in promastigotes treated for 24 h with this LdcCA inhibitor. Figure 3a,b shows longitudinal sections of untreated parasites, displaying the nucleus and the mitochondria containing the kinetoplast. A normal aspect of the flagellar pocket and the presence of acidocalcisomes is observed in Figure 3b. After 24 h treatment with compound **29**, some alterations of the parasites were observed, such as the appearance of electron-dense granules in the cytoplasm (Figure 3c–g). Alterations in the flagellar pocket, as well as the presence of many vesicles with the same appearance of the cytoplasm (Figure 3c,d,g), and an increase in its size were also noted in most of the treated parasites (Figure 3d,g). Finally, some photomicrographs indicated that compound **29** led to a complete destruction of cytoplasm, it being possible to observe the appearance of autophagic structures (Figure 3f,g). These preliminary data prove that the LdcCA inhibitors may be used against *Leishmania* spp. and that this enzyme be considered as a new target for development of antileishmanial drugs with a novel mechanism of action.

CONCLUSIONS

We report here the identification, cloning, and characterization of a β-CA from the unicellular parasitic protozoan *L. donovani chagasi*. This enzyme showed interesting catalytic activity and was inhibited in the nanomolar range by several sulfonamides and thiols. Some of the investigated thiols efficiently inhibited the in vivo growth of *L. chagasi* and *L. amazonensis* promastigotes, by impairing the flagellar pocket and movement of the parasites, and causing their death. *Leishmania* CA may thus be a potential target for developing antileishmanial drugs with a novel mechanism of action.

EXPERIMENTAL PROTOCOLS

Chemistry. Sulfonamides **1**–**24** and **AAZ** through **HCT** were commercially available or reported earlier by us.[42] Thiols **25**–**31** were prepared as reported earlier by this group.[41] Purity of all compounds was assessed by means of HPLC and they were >98% pure.

Construction of β-CA Fusion Protein. Total RNA of *L. donovani chagasi* homogenate was isolated using RNAeasy Mini Kit (Qiagen) according to manufacturer's instructions. However, 800 μL of RLT-buffer was used instead of 600 μL. DNAase treatment was performed after the isolation. The RNA was converted to cDNA using First Strand cDNA Synthesis Kit #K1612 (Fermentas) according to the manufacturer's instructions. The β-CA gene was retrieved from NCBI protein databases using Blast[35] (http://blast.ncbi.nlm.nih.gov/Blast.cgi). In the primer design we used the sequence from *L. infantum* since the *L. donovani* sequence was not available at that time. The full length β-CA gene was identified and amplified from cDNA by PCR using Phusion Hot Start High Fidelity DNA Polymerase (Finnzymes, Espoo, Finland). Sequence-specific primers were ordered from Sigma-Aldrich (St. Louis, MO). The forward primer was 5′-ATGTCGCTGT-GCAGCTGCGGC-3′ (F1), and the reverse primer was 3′-CTACAG-CTGCCCGTAGCGCCA-5′ (R1). PCR was performed in a PTC 2000 thermal cycler (MJ Research, Waltham, MA), and the program consisted of a single 98 °C denaturation step for 3 min, followed by 35 cycles of denaturation at 98 °C for 10 s, annealing at 73 °C for 30 s, and extension at 72 °C for 30 s. A final extension was performed at 72 °C for 10 min. The PCR product band was separated from the gel and dissolved using Illustra GFX PCR DNA and GEL Band Purification Kit (GE Healthcare Life Sciences, Buckinghamshire, UK). The validity of the PCR product was verified by sequencing.

For the sequencing, the purified plasmid was used as a template. The sequencing was carried out using ABI PRISM Big Dye Terminator Cycle Sequencing Ready Reactions Kit version 3.1 (Applied Biosystems). The sequencing was performed in both directions using F1 and R1 primers described above. One microliter of purified plasmid was mixed with 4 μL of Big Dye mix, 4 μL of ddH_2O, and 1 μL of 1.6 μM primer. The reactions were performed in a PTC 2000 thermal cycler (MJ Research, Waltham, MA) according to the manufacturer's instructions. The products were purified by ethanol precipitation, resuspended in HiDi formamide (Applied Biosystems), and denatured according to the manufacturer's instructions. The sequencing was performed using an ABI PRISM Genetic Analyzer instrument 9100 (Applied Biosystems).

For recombinant protein production the β-CA gene was constructed and cloned into the pFastBac1TM vector. The forward primer used in the initial amplification of the β-CA gene was 5′-CGCGAATTCAT-GTCGCTGTGCAGCTGCGGC-3′ (F2), and the reverse primer was 5′-GCCCTCGAGTTAATGGTGGTGATGGTGGTGGGAA-CCACGGGGCACCAGCAGCTGCCCGTAGCGCCAGAA-3′ (R2). The latter primer contains nucleotide repeats to create the C-terminal polyhistidine tag of six histidines. In addition, the forward primer contained the restriction site for *Eco*RI and the reverse primer for *Xho*I. The reverse primer also contained the nucleotide sequence encoding the thrombin cleavage site. The PCR program was as follows: 98 °C for 3 min and then 35 cycles of 98 °C for 10 s, 62 °C for 15 s, and 72 °C for 30 s, and finally 72 °C for 10 min.

The PCR product was run on an agarose gel, and the obtained band was purified. pFastBac1 plasmid (Invitrogen) and the PCR product were digested at 37 °C overnight with *Eco*RI and *Xho*I restriction enzymes (New England Biolabs). The digested plasmid and PCR product containing full length recombinant β-CA gene were purified and then ligated overnight at 4 °C using T4 DNA ligase (New England Biolabs). The ligated product was transformed into TOP10 bacteria (Invitrogen). Overnight cultures (8 mL) were made from these colonies, and plasmids were purified using a QIAprep Spin Miniprep Kit (Qiagen, Hilden, Germany). The construction of baculoviral genomes encoding the recombinant proteins has been described previously.[36]

Expression and Purification of *L. donovani chagasi* β-CA. The Sf9 insect cells were grown in HyQ SFX-Insect serum-free cell culture medium (HyClone, Logan, UT) in an orbital shaker at 27 °C (125 rpm) for 3 days after infection. Protein purification was performed after centrifugation (5000*g*, 20 °C, 8 min) from the supernatant. Purification was performed using the Protino Ni-NTA agarose (Macherey-Nagel) under native binding conditions with wash and elution buffers made according to the manufacturer's instructions. The purification procedure per 400 mL of insect cell medium was as follows: 3 L of native binding buffer (50 mM NaH_2PO_4, 500 mM NaCl, pH 8.0) and 8 mL of the nickel-chelating agarose were added to the medium, and the His-tagged protein was then allowed to bind to the resin on a magnetic stirrer at 25 °C for 3 h. The resin was washed with 40 + 20 mL of washing buffer (50 mM NaH2PO4, 500 mM NaCl, 20 mM imidazole, pH 8.0). The protein was then eluted with elution buffer (50 mM NaH_2PO_4, 500 mM NaCl, 250 mM imidazole, pH 8.0).

The purified recombinant protein was transferred to a buffer of 10 mM HEPES, pH 7.5, using an Vivaspin Turbo 15 centrifugal filter device (Sartorius-Stedim) according to the manufacturer's instructions. During the purification the protein was tightly attached to the filter membrane after the His-tag removal. Because of this unwanted property of the protein, we decided to use the uncleaved β-CA protein (containing polyhistidine tag) in the kinetic measurements. Protein concentration was determined using the DC Protein Assay (Bio-Rad) with three different dilutions. Purified recombinant β-CA protein was analyzed using 10% sodium dodecyl sulfate–polyacrylamide gel electrophoresis (SDS–PAGE) under reducing conditions. The gels were stained using the Colloidal Blue Staining Kit (Invitrogen).

SDS–PAGE showed that the LdcCA appeared as three distinct bands. Therefore, an electrophoretically separated protein sample was analyzed by mass spectrophotometry at Protein Chemistry Unit of University of Helsinki, and subsequently the proteins were identified. All

three bands proved to represent LdcCA. We speculated that the appearance of three bands in the SDS−PAGE is the result of differences in protein glycosylation. The possible glycosylation sites were thus analyzed, using DictyOGlyc 1.1 (http://www.cbs.dtu.dk/services/DictyOGlyc/) and NetNGlyc 1.0 (http://www.cbs.dtu.dk/services/NetNGlyc/) softwares to test O- and N-glycosylation sites, respectively. No O-glycosylation sites were present, whereas N-glycosylation sites were found in positions 34 and 41. The presence of these two glycosylation sites would well explain the three bands seen on the gel of Supplementary Figure 1 of the Supporting Information. The lower two bands would represent the partially and fully deglycosylated forms of the enzyme.

CA Activity Measurements and Inhibition Studies. An Applied Photophysics stopped-flow instrument has been used for assaying the CA-catalyzed CO_2 hydration activity. Phenol red (at a concentration of 0.2 mM) has been used as indicator, working at the absorbance maximum of 557 nm, with 20 mM Hepes (pH 7.4) or 20 mM Tris (pH 8−4) as buffers, and 20 mM Na_2SO_4 (for maintaining constant the ionic strength), following the initial rates of the CA-catalyzed CO_2 hydration reaction for a period of 10−100 s.[35] The CO_2 concentrations ranged from 1.7 to 17 mM for the determination of the kinetic parameters and inhibition constants. For each inhibitor at least six traces of the initial 5−10% of the reaction have been used for determining the initial velocity. The uncatalyzed rates were determined in the same manner and subtracted from the total observed rates. Stock solutions of inhibitors (10 mM) were prepared in distilled−deionized water and dilutions up to 0.01 nM were done thereafter with the assay buffer. Inhibitor and enzyme solutions were preincubated together for 15 min at room temperature prior to assay, in order to allow for the formation of the E-I complex. The inhibition constants were obtained by nonlinear least-squares methods using PRISM 3, as reported earlier,[42] and represent the mean from at least three different determinations. All CA isoforms were recombinant ones obtained in house as reported earlier.[42]

In Vivo Anti-Leishmanial Activity. *Parasite Strains and Cell Cultures.* Promastigote forms of two *Leishmania* species, *L. chagasi* (MHOM/BR/1974/PP75) and *L. amazonensis* (Raimundo strain MHOM/BR/76/Ma-5), were both axenically cultured in PBHIL medium supplemented with 10% fetal bovine serum (FBS), at 26 °C as previously described.[43]

Anti-Leishmanial Activity and Minimum Inhibitory Concentration Evaluation. The assay was carried out in a 96-well microtiter plate, where compound **29** was serially diluted in duplicates to final test concentrations (2−256 μM). Then 5.0×10^5 promastigotes forms of *L. chagasi* and *L. amazonensis* were harvest at early stationary phase and added to each well, and the plate was incubated at 26 °C for 120 h. After the incubation period, resazurin solution [5 mg/100 mL of phosphate buffer saline (PBS), pH 7.2] was prepared, 25 μL added to each well, and incubation continued for a further 2−4 h as described by Rolon et al.[44] MIC was considered the lowest concentration of the compound **29** that completely prevented the growth of *Leishmania* in vitro. Alternatively, 120-h treated parasites were centrifuged, washed in PBS, and then reincubated in fresh culture medium in order to evaluate the leishmanicidal effect.

Transmission Electron Microscopy (TEM). Parasites were harvested as described above, washed twice with PBS, and incubated in the presence of compound **29** at MIC concentration for 24 h. Then the parasites were fixed in a solution containing 2.5% glutaraldehyde and 3.5% sucrose in 0.1 M sodium cacodylate buffer adjusted to pH 7.4 at 4 °C for 60 min. Next, cells were rinsed in PBS (pH 7.4) and pelleted by centrifugation, and the pellets were then postfixed in 1% osmium tetroxide and potassium ferrocyanide solution for 1 h, dehydrated sequentially in acetone, and then embedded in Epon 812. Thin sections were cut using an LKB ultramicrotome, collected on copper grids, and stained with uranyl acetate and lead citrate. Observations were performed using a JEOL JEM1011 transmission electron microscope.

■ ASSOCIATED CONTENT

Supporting Information

Supplementary Figure 1. This material is available free of charge via the Internet at http://pubs.acs.org.

■ AUTHOR INFORMATION

Corresponding Author

*L.S.: tel, +358-50-318-6251; e-mail, leo.syrjanen@uta.fi. C.T.S.: tel, +39-055-457-3005; fax, +39-055-457-3385; e-mail, claudiu.supuran@unifi.it.

Notes

The authors declare no competing financial interest.

■ ACKNOWLEDGMENTS

The work in our laboratories is supported by the competitive Research Funding of the Tampere University Hospital (Grant 9N054) and the grants from Academy of Finland, Sigrid Juselius Foundation, and Jane and Aatos Erkko Foundation. The authors wish to acknowledge the Brazilian National Council for Scientific and Technological Development (MCT-CNPq), Carlos Chagas Filho Foundation for Research Support in the State of Rio de Janeiro (FAPERJ), Coordination for the Improvement of Higher Education Personnel (CAPES). The authors thank Marianne Kuuslahti and Aulikki Lehmus for skillful technical assistance.

■ ABBREVIATIONS USED

CA, carbonic anhydrase; hCA I, human carbonic anhydrase I; hCA II, human carbonic anhydrase II; TcCA, *T. cruzi* carbonic anhydrase; LdcCA, *L. donovani chagasi* carbonic anhydrase; CAI, carbonic anhydrase inhibitors; K_I, inhibition constant.

■ REFERENCES

(1) McCall, L. I.; Zhang, W. W.; Matlashewski, G. Determinants for the development of visceral leishmaniasis disease. *PLoS Pathog.* **2013**, *9*, e1003053.

(2) (a) Aggarwal, M.; McKenna, R. Update on carbonic anhydrase inhibitors: A patent review (2008−2011). *Expert. Opin. Ther. Pat.* **2012**, *22*, 903−915. (b) Supuran, C. T. Structure-based drug discovery of carbonic anhydrase inhibitors. *J. Enzyme Inhib. Med. Chem.* **2012**, *27*, 759−772.

(3) (a) Lane, T. W.; Saito, M. A.; George, G. N.; Pickering, I. J.; Prince, R. C.; Morel, F. M. Biochemistry: A cadmium enzyme from a marine diatom. *Nature* **2005**, *435*, 42. (b) Xu, Y.; Feng, L.; Jeffrey, P. D.; Shi, Y.; Morel, F. M. Structure and metal exchange in the cadmium carbonic anhydrase of marine diatoms. *Nature* **2008**, *452*, 56−61.

(4) (a) Neri, D.; Supuran, C. T. Interfering with pH regulation in tumours as a therapeutic strategy. *Nat. Rev. Drug Discovery* **2011**, *10*, 767−777. (b) Aggarwal, M.; Boone, C. D.; Kondeti, B.; McKenna, R. Structural annotation of human carbonic anhydrases. *J. Enzyme Inhib. Med. Chem.* **2013**, *28*, 267−277.

(5) Tripp, B. C.; Bell, C. B., 3rd; Cruz, F.; Krebs, C.; Ferry, J. G. A role for iron in an ancient carbonic anhydrase. *J. Biol. Chem.* **2004**, *279*, 6683−6687.

(6) Macauley, S. R.; Zimmerman, S. A.; Apolinario, E. E.; Evilia, C.; Hou, Y. M.; Ferry, J. G.; Sowers, K. R. The archetype gamma-class carbonic anhydrase (Cam) contains iron when synthesized in vivo. *Biochemistry* **2009**, *48*, 817−819.

(7) Zimmerman, S. A.; Ferry, J. G. The beta and gamma classes of carbonic anhydrase. *Curr. Pharm. Des.* **2008**, *14*, 716−721.

(8) So, A. K.; Espie, G. S.; Williams, E. B.; Shively, J. M.; Heinhorst, S.; Cannon, G. C. A novel evolutionary lineage of carbonic anhydrase (epsilon class) is a component of the carboxysome shell. *J. Bacteriol.* **2004**, *186*, 623−630.

(9) Sawaya, M. R.; Cannon, G. C.; Heinhorst, S.; Tanaka, S.; Williams, E. B.; Yeates, T. O.; Kerfeld, C. A. The structure of beta-carbonic anhydrase from the carboxysomal shell reveals a distinct subclass with one active site for the price of two. *J. Biol. Chem.* **2006**, *281*, 7546−7555.

(10) Strop, P.; Smith, K. S.; Iverson, T. M.; Ferry, J. G.; Rees, D. C. Crystal structure of the "cab"-type beta class carbonic anhydrase from

the archaeon *Methanobacterium thermoautotrophicum*. *J. Biol. Chem.* **2001**, *276*, 10299−10305.
(11) Kimber, M. S.; Pai, E. F. The active site architecture of *Pisum sativum* beta-carbonic anhydrase is a mirror image of that of alpha-carbonic anhydrases. *EMBO J.* **2000**, *19*, 1407−1418.
(12) Hewett-Emmett, D. Evolution and distribution of the carbonic anhydrase gene families. *EXS* **2000**, *90*, 29−76.
(13) Syrjanen, L.; Tolvanen, M.; Hilvo, M.; Olatubosun, A.; Innocenti, A.; Scozzafava, A.; Leppiniemi, J.; Niederhauser, B.; Hytonen, V. P.; Gorr, T. A.; Parkkila, S.; Supuran, C. T. Characterization of the first beta-class carbonic anhydrase from an arthropod (*Drosophila melanogaster*) and phylogenetic analysis of beta-class carbonic anhydrases in invertebrates. *BMC Biochem.* **2010**, *11*, 28.
(14) Klengel, T.; Liang, W. J.; Chaloupka, J.; Ruoff, C.; Schroppel, K.; Naglik, J. R.; Eckert, S. E.; Mogensen, E. G.; Haynes, K.; Tuite, M. F.; Levin, L. R.; Buck, J.; Muhlschlegel, F. A. Fungal adenylyl cyclase integrates CO_2 sensing with cAMP signaling and virulence. *Curr. Biol.* **2005**, *15*, 2021−2026.
(15) Bahn, Y. S.; Cox, G. M.; Perfect, J. R.; Heitman, J. Carbonic anhydrase and CO_2 sensing during *Cryptococcus neoformans* growth, differentiation, and virulence. *Curr. Biol.* **2005**, *15*, 2013−2020.
(16) Innocenti, A.; Muhlschlegel, F. A.; Hall, R. A.; Steegborn, C.; Scozzafava, A.; Supuran, C. T. Carbonic anhydrase inhibitors: Inhibition of the beta-class enzymes from the fungal pathogens *Candida albicans* and *Cryptococcus neoformans* with simple anions. *Bioorg. Med. Chem. Lett.* **2008**, *18*, 5066−5070.
(17) Isik, S.; Kockar, F.; Arslan, O.; Guler, O. O.; Innocenti, A.; Supuran, C. T. Carbonic anhydrase inhibitors. Inhibition of the beta-class enzyme from the yeast *Saccharomyces cerevisiae* with anions. *Bioorg. Med. Chem. Lett.* **2008**, *18*, 6327−6331.
(18) Zimmerman, S. A.; Ferry, J. G.; Supuran, C. T. Inhibition of the archaeal beta-class (Cab) and gamma-class (Cam) carbonic anhydrases. *Curr. Top. Med. Chem.* **2007**, *7*, 901−908.
(19) Isik, S.; Kockar, F.; Aydin, M.; Arslan, O.; Guler, O. O.; Innocenti, A.; Scozzafava, A.; Supuran, C. T. Carbonic anhydrase inhibitors: Inhibition of the beta-class enzyme from the yeast *Saccharomyces cerevisiae* with sulfonamides and sulfamates. *Bioorg. Med. Chem.* **2009**, *17*, 1158−1163.
(20) Minakuchi, T.; Nishimori, I.; Vullo, D.; Scozzafava, A.; Supuran, C. T. Molecular cloning, characterization, and inhibition studies of the Rv1284 beta-carbonic anhydrase from *Mycobacterium tuberculosis* with sulfonamides and a sulfamate. *J. Med. Chem.* **2009**, *52*, 2226−2232.
(21) Nishimori, I.; Minakuchi, T.; Vullo, D.; Scozzafava, A.; Innocenti, A.; Supuran, C. T. Carbonic anhydrase inhibitors. Cloning, characterization, and inhibition studies of a new beta-carbonic anhydrase from *Mycobacterium tuberculosis*. *J. Med. Chem.* **2009**, *52*, 3116−3120.
(22) Joseph, P.; Turtaut, F.; Ouahrani-Bettache, S.; Montero, J. L.; Nishimori, I.; Minakuchi, T.; Vullo, D.; Scozzafava, A.; Kohler, S.; Winum, J. Y.; Supuran, C. T. Cloning, characterization, and inhibition studies of a beta-carbonic anhydrase from *Brucella suis*. *J. Med. Chem.* **2010**, *53*, 2277−2285.
(23) Vullo, D.; Nishimori, I.; Minakuchi, T.; Scozzafava, A.; Supuran, C. T. Inhibition studies with anions and small molecules of two novel beta-carbonic anhydrases from the bacterial pathogen *Salmonella enterica serovar Typhimurium*. *Bioorg. Med. Chem. Lett.* **2011**, *21*, 3591−3595.
(24) Nishimori, I.; Minakuchi, T.; Kohsaki, T.; Onishi, S.; Takeuchi, H.; Vullo, D.; Scozzafava, A.; Supuran, C. T. Carbonic anhydrase inhibitors: The beta-carbonic anhydrase from *Helicobacter pylori* is a new target for sulfonamide and sulfamate inhibitors. *Bioorg. Med. Chem. Lett.* **2007**, *17*, 3585−3594.
(25) Burghout, P.; Vullo, D.; Scozzafava, A.; Hermans, P. W.; Supuran, C. T. Inhibition of the beta-carbonic anhydrase from *Streptococcus pneumoniae* by inorganic anions and small molecules: Toward innovative drug design of antiinfectives? *Bioorg. Med. Chem.* **2011**, *19*, 243−248.
(26) Cronk, J. D.; Rowlett, R. S.; Zhang, K. Y.; Tu, C.; Endrizzi, J. A.; Lee, J.; Gareiss, P. C.; Preiss, J. R. Identification of a novel noncatalytic bicarbonate binding site in eubacterial beta-carbonic anhydrase. *Biochemistry* **2006**, *45*, 4351−4361.
(27) Innocenti, A.; Winum, J. Y.; Hall, R. A.; Muhlschlegel, F. A.; Scozzafava, A.; Supuran, C. T. Carbonic anhydrase inhibitors. Inhibition of the fungal beta-carbonic anhydrases from *Candida albicans* and *Cryptococcus neoformans* with boronic acids. *Bioorg. Med. Chem. Lett.* **2009**, *19*, 2642−2645.
(28) Innocenti, A.; Hall, R. A.; Schlicker, C.; Scozzafava, A.; Steegborn, C.; Muhlschlegel, F. A.; Supuran, C. T. Carbonic anhydrase inhibitors. Inhibition and homology modeling studies of the fungal beta-carbonic anhydrase from *Candida albicans* with sulfonamides. *Bioorg. Med. Chem.* **2009**, *17*, 4503−4509.
(29) Innocenti, A.; Hall, R. A.; Schlicker, C.; Muhlschlegel, F. A.; Supuran, C. T. Carbonic anhydrase inhibitors. Inhibition of the beta-class enzymes from the fungal pathogens *Candida albicans* and *Cryptococcus neoformans* with aliphatic and aromatic carboxylates. *Bioorg. Med. Chem.* **2009**, *17*, 2654−2657.
(30) Schlicker, C.; Hall, R. A.; Vullo, D.; Middelhaufe, S.; Gertz, M.; Supuran, C. T.; Muhlschlegel, F. A.; Steegborn, C. Structure and inhibition of the CO_2-sensing carbonic anhydrase Can2 from the pathogenic fungus *Cryptococcus neoformans*. *J. Mol. Biol.* **2009**, *385*, 1207−1220.
(31) Innocenti, A.; Leewattanapasuk, W.; Muhlschlegel, F. A.; Mastrolorenzo, A.; Supuran, C. T. Carbonic anhydrase inhibitors. Inhibition of the beta-class enzyme from the pathogenic yeast *Candida glabrata* with anions. *Bioorg. Med. Chem. Lett.* **2009**, *19*, 4802−4805.
(32) Nishimori, I.; Minakuchi, T.; Vullo, D.; Scozzafava, A.; Supuran, C. T. Inhibition studies of the beta-carbonic anhydrases from the bacterial pathogen *Salmonella enterica serovar Typhimurium* with sulfonamides and sulfamates. *Bioorg. Med. Chem.* **2011**, *19*, 5023−5030.
(33) Fasseas, M. K.; Tsikou, D.; Flemetakis, E.; Katinakis, P. Molecular and biochemical analysis of the beta class carbonic anhydrases in *Caenorhabditis elegans*. *Mol. Biol. Rep.* **2011**, *38*, 1777−1785.
(34) (a) Krungkrai, J.; Scozzafava, A.; Reungprapavut, S.; Krungkrai, S. R.; Rattanajak, R.; Kamchonwongpaisan, S.; Supuran, C. T. Carbonic anhydrase inhibitors. Inhibition of *Plasmodium falciparum* carbonic anhydrase with aromatic sulfonamides: Towards antimalarials with a novel mechanism of action? *Bioorg. Med. Chem.* **2005**, *13*, 483−489. (b) Krungkrai, J.; Krungkrai, S. R.; Supuran, C. T. Malarial parasite carbonic anhydrase and its inhibitors. *Curr. Top. Med. Chem.* **2007**, *7*, 909−917. (c) Krungkrai, J.; Supuran, C. T. The alpha-carbonic anhydrase from the malarial parasite and its inhibition. *Curr. Pharm. Des.* **2008**, *14*, 631−640. (d) Krungkrai, J.; Krungkrai, S. R.; Supuran, C. T. Carbonic anhydrase inhibitors. Inhibition of *Plasmodium falciparum* carbonic anhydrase with aromatic/heterocyclic sulfonamides: In vitro and in vivo studies. *Bioorg. Med. Chem. Lett.* **2008**, *18*, 5466−5471. (e) Pan, P.; Vermelho, A. B.; Capaci Rodrigues, G.; Scozzafava, A.; Tolvanen, M. E.; Parkkila, S.; Capasso, C.; Supuran, C. T. Cloning, characterization, and sulfonamide and thiol inhibition studies of an alpha-carbonic anhydrase from *Trypanosoma cruzi*, the causative agent of Chagas disease. *J. Med. Chem.* **2013**, *56*, 1761−1771. (f) Altschul, S. F.; Gish, W.; Miller, W.; Myers, E. W.; Lipman, D. J. Basic local alignment search tool. *J. Mol. Biol.* **1990**, *215*, 403−410.
(35) Khalifah, R. G. The carbon dioxide hydration activity of carbonic anhydrase. I. Stop-flow kinetic studies on the native human isoenzymes B and C. *J. Biol. Chem.* **1971**, *246*, 2561−2573.
(36) Hilvo, M.; Baranauskiene, L.; Salzano, A. M.; Scaloni, A.; Matulis, D.; Innocenti, A.; Scozzafava, A.; Monti, S. M.; Di Fiore, A.; De Simone, G.; Lindfors, M.; Janis, J.; Valjakka, J.; Pastorekova, S.; Pastorek, J.; Kulomaa, M. S.; Nordlund, H. R.; Supuran, C. T.; Parkkila, S. Biochemical characterization of CA IX, one of the most active carbonic anhydrase isozymes. *J. Biol. Chem.* **2008**, *283*, 27799−27809.
(37) Monti, S. M.; Ludwig, M.; Vullo, D.; Scozzafava, A.; Capasso, C.; Supuran, C. T. Kinetic and anion inhibition studies of a β-carbonic anhydrase (FbCA1) from the C_4 plant *Flaveria bidentis*. *Bioorg. Med. Chem. Lett.* **2013**, *23*, 1626−1630.
(38) (a) Supuran, C. T. Carbonic anhydrases: Novel therapeutic applications for inhibitors and activators. *Nat. Rev. Drug Discovery* **2008**, *7*, 168−181. (b) Supuran, C. T. Carbonic anhydrase inhibitors. *Bioorg.*

Med. Chem. Lett. **2010**, *20*, 3467−3474. (c) Alterio, V.; Di Fiore, A.; D'Ambrosio, K.; Supuran, C. T.; De Simone, G. Multiple binding modes of inhibitors to carbonic anhydrases: How to design specific drugs targeting 15 different isoforms? *Chem. Rev.* **2012**, *112*, 4421−4468.

(39) (a) Supuran, C. T. Bacterial carbonic anhydrases as drug targets: Toward novel antibiotics? *Front. Pharmacol.* **2011**, *2*, 34. (b) Supuran, C. T. Carbonic anhydrase inhibitors and activators for novel therapeutic applications. *Future Med. Chem.* **2011**, *3*, 1165−1180.

(40) (a) De Simone, G.; Alterio, V.; Supuran, C. T. Exploiting the hydrophobic and hydrophilic binding sites for designing carbonic anhydrase inhibitors. *Expert Opin. Drug Discovery* **2013**, *8*, 793−810. (b) Supuran, C. T.; Scozzafava, A.; Casini, A. Carbonic anhydrase inhibitors. *Med. Res. Rev.* **2003**, *23*, 146−189. (c) Supuran, C. T. Carbonic anhydrases: From biomedical applications of the inhibitors and activators to biotechnologic use for CO_2 capture. *J. Enzyme Inhib. Med. Chem.* **2013**, *28*, 229−230.

(41) Abdel-Hamid, M. K.; Abdel-Hafez, A. A.; El-Koussi, N. A.; Mahfoouz, N. M.; Innocenti, A.; Supuran, C. T. Design, synthesis and docking studies of new 1,3,4-thiadiazole-2-thione derivatives with carbonic anhydrase inhibitory activity. *Bioorg. Med. Chem.* **2007**, *15*, 6975−6984.

(42) (a) Scozzafava, A.; Mastrolorenzo, A.; Supuran, C. T. Modulation of carbonic anhydrase activity and its applications in therapy. *Expert Opin. Ther. Pat.* **2004**, *14*, 667−702. (b) Supuran, C. T.; Scozzafava, A.; Casini, A., Development of sulfonamide carbonic anhydrase inhibitors. In *Carbonic Anhydrase−Its Inhibitors and Activators*; Supuran, C. T., Scozzafava, A., Conway, J., Eds.; CRC Press: Boca Raton, 2004; pp 67−147. (c) Liu, F.; Martin-Mingot, A.; Lecornué, F.; Jouannetaud, M. P.; Maresca, A.; Thibaudeau, S.; Supuran, C. T. Carbonic Anhydrases inhibitory effects of new benzenesulfonamides synthesized by using superacid chemistry. *J. Enzyme Inhib. Med. Chem.* **2012**, *27*, 886−891. (d) Ozensoy, O.; Arslan, M.; Supuran, C. T. Carbonic anhydrase inhibitors: Purification and inhibition studies of pigeon (*Columba livia* var. domestica) red blood cell carbonic anhydrase with sulfonamides. *J. Enzyme Inhib. Med. Chem.* **2011**, *26*, 749−753. (e) Bootorabi, F.; Jänis, J.; Hytönen, V. P.; Valjakka, J.; Kuuslahti, M.; Vullo, D.; Niemelä, O.; Supuran, C. T.; Parkkila, S. Acetaldehyde-derived modifications on cytosolic human carbonic anhydrases. *J. Enzyme Inhib. Med. Chem.* **2011**, *26*, 862−870.

(43) Rodrigues, I. A.; da Silva, B. A.; dos Santos, A. L.; Vermelho, A. B.; Alviano, C. S.; Dutra, P. M.; Rosa, M. S. A new experimental culture medium for cultivation of *Leishmania amazonensis*: Its efficacy for the continuous in vitro growth and differentiation of infective promastigote forms. *Parasitol. Res.* **2010**, *106*, 1249−1252.

(44) Rolon, M.; Veja, C.; Escario, J. A.; Gomez-Barrio, A. Development of resazurin microtiter assay for drug sensibility testing of *Trypanosoma cruzi* epimastigotes. *Parasitol. Res.* **2006**, *99*, 103−107.

Syrjänen et al. Frontiers in Zoology (2015) 12:19
DOI 10.1186/s12983-015-0111-3

FRONTIERS IN ZOOLOGY

RESEARCH Open Access

β carbonic anhydrase is required for female fertility in *Drosophila melanogaster*

Leo Syrjänen[1,2,3†], Susanna Valanne[1*†], Marianne Kuuslahti[1,2], Tea Tuomela[1], Ashwin Sriram[1,4], Alberto Sanz[1,4], Howard T. Jacobs[1,5,6], Mika Rämet[1,7,8] and Seppo Parkkila[1,2,9]

Abstract

Background: Carbonic anhydrases (CAs, EC 4.2.1.1) are ubiquitous enzymes that catalyze the reversible hydration reaction of carbon dioxide. CAs are present as six structurally divergent enzyme families: α, β, γ, δ, ζ and η. β-CAs have a wide distribution across different species including invertebrates. Previously, we showed that *Drosophila melanogaster* β-CA is a highly active mitochondrial enzyme. In this study, we investigated the function of *Drosophila* β-CA by silencing the expression of the *β-CA* gene using UAS/GAL4-based RNA interference (RNAi) in *Drosophila* in vivo.

Results: Crossing *β-CA* RNAi lines over ubiquitous *Actin* driver flies did not produce any viable progeny, indicating that *β-CA* expression is required for fly development. RNAi silencing of *β-CA* ubiquitously in adult flies did not affect their survival rate or function of mitochondrial electron transport chain. Importantly, *β-CA* RNAi led to impaired reproduction. All β-CA knockdown females were sterile, and produced few or no eggs. Whole ovaries of knockdown females looked normal but upon cadherin staining, there was an apparent functional defect in migration of border cells, which are considered essential for normal fertilization.

Conclusions: These results indicate that although *Drosophila* β-CA is dispensable for survival of adult flies, it is essential for female fertility.

Background

Carbonic anhydrases (CAs, EC 4.2.1.1) are metalloenzymes that catalyze the reversible hydration reaction of carbon dioxide according to the following equation: $CO_2 + H_2O \leftrightarrow HCO_3^- + H^+$ [1]. This reaction catalyzed by CAs is fundamental in the regulation of acid–base balance in living organisms. In addition, this reaction is involved in many physiological processes such as gluconeogenesis and ureagenesis, and it also helps to remove carbon dioxide out of tissues [1].

To date, six different classes of CAs have been identified: α, β, γ, δ, ζ and η [2, 3]. The three major classes α, β and γ are widely distributed among living organisms. On the other hand, the ζ-CAs are found only in diatoms, and the δ-CAs in diatoms and other marine phytoplankton. The novel group of CAs, namely η-CAs, was only recently discovered from malaria causing protozoan organisms of the genus *Plasmodium*. Of different CA-classes, β-CAs seems to be the class with the widest distribution. β-class CAs have been characterized throughout the tree of life. These enzymes are found in most species belonging to the *Archaea* and *Bacteria* domains and additionally probably all species of fungi and plants among domain *Eukarya* [4]. However, β-CAs are not present in in humans or other vertebrates [5].

β-CAs were first characterized in two metazoan organisms, namely the fruit fly *Drosophila melanogaster* [5], which possesses one β-CA, CAHβ (with annotation symbol CG11967, flybase number FBgn0037646, also called DmBCA [5]) and the nematode *Caenorhabditis elegans* [6], which possesses two β-CAs, one of which seems to be inactive. There have been no studies focusing on the biological function of β-CA in *D. melanogaster*. Fasseas and coworkers found no phenotypic changes in *C. elegans* when they performed RNAi experiments by feeding [6]. Recently, another β-CA was characterized from the protozoan parasite *Leishmania* and the effects of different CA-inhibitors were tested *in vitro* and also against living

* Correspondence: susanna.valanne@uta.fi
†Equal contributors
[1]BioMediTech, University of Tampere, Tampere, Finland
Full list of author information is available at the end of the article

parasites in vivo. One of the studied compounds was a Schiff's base type bromoderivative, which was a very efficient inhibitor of β-CA both *in vitro* and in vivo. Addition of this compound into growth medium containing living *Leishmania* parasites led to intracellular damages and death of the parasites [7]. Hence, it seems that β-CA is an essential enzyme for survival of *Leishmania* parasites.

The physiological roles of β-CAs are poorly understood, especially in invertebrate animal species having this gene. However, in some organisms β-CA has a support role for enzymes that utilize or dispose of CO_2 or HCO_3^-. One example of such an enzyme is ribulose-1,5-biphosphate carboxylase (Rubisco) [8]. Even though *D. melanogaster* β-CA was characterized four years ago, the physiological significance of this enzyme has remained unclear. Here we have investigated the function of *Drosophila* β-CA utilizing RNA interference (RNAi) -mediated gene silencing in both developing and adult flies. We show that β-CA is needed for proper border cell migration in the developing egg and is therefore essential for egg fertilization.

Results

Ubiquitous silencing of *β-CA* causes lethality in *Drosophila* during development

Crossing two independent *β-CA* RNAi lines (#100233 and #38612, referred to as *β-CA* RNAi^1 and *β-CA* RNAi^2, respectively) over ubiquitous *ActGAL4*/CyOy + flies did not produce viable progeny of the phenotype indicative of *β-CA* dsRNA expression, implying that silencing of *β-CA* is lethal during fly development. In order to bypass developmental defects and to analyze the significance of *β-CA* expression for adult *Drosophila*, we used the inducible *GeneSwitch-tubulin-GAL4* (*GS-tub-GAL4*) driver line for *β-CA* silencing. The Gene Switch system allows selective expression of the hairpin construct in a chosen time of development, via addition of the inducing agent, Mifepristone (RU-486, hereafter Mif), in the fly food. Therefore, genetically identical siblings from a cross can be used as experimental flies (induction with Mif) and controls (no induction), which eliminates potential concerns regarding genetic background effects. Therefore, after eclosion, F1 progeny (*β-CA* RNAi/*GS-tub-GAL4*) flies were placed in Mif-containing food for *β-CA* silencing in the adults, and control siblings were placed in food without Mif. Firstly, the efficacy of gene silencing in *β-CA* RNAi flies crossed over *GS-tub-GAL4* and treated with Mif was analyzed using qRT-PCR. As shown in Fig. 1, both RNAi lines showed effective silencing when crossed over *GS-tub-GAL4* and induced with Mif. In *β-CA* RNAi^1/*GS-tub-GAL4* males the level of gene expression was 35 ± 6 % from that of control males without Mif induction, and in females 69 ± 16 % when compared to control females without induction. With *β-CA* RNAi^2/*GS-tub-GAL4* flies the values were 39 ± 8 % and 65 ± 4 %. These data indicate that Mif induced RNAi can be used to analyze the importance of *β-CA* expression in adult flies.

β-CA expression is required for female fertility in *Drosophila*

To evaluate whether *β-CA* expression is required for survival of adult flies, *β-CA* RNAi flies were crossed to *GS-tub-GAL4* and monitored for survival after introduction to a Mif-containing diet. During 15 days follow-up, there were no statistically significant differences in survival between *β-CA* knockdown flies and controls: 90 % of *β-CA* RNAi^1/*GS-tub-GAL4* F1 progeny flies were alive, while the percentage of live flies was 96 % in the control group. In the *β-CA* RNAi^2/*GS-tub-GAL4* group the values were 92 % and 93 %, respectively (Fig. 2). This indicates that β-CA knockdown has no effect on the fly survival during the 15 day follow-up time, but does not exclude lifespan differences that may appear during later life. However, the analysis of fertility indicated that the egg laying capacity of Mif-induced *β-CA* RNAi/*GS-tub-GAL4* females was severely reduced. In one representative experiment performed, 50 female knockdown flies were kept together with 30 control w^{1118} males, and the flies did not lay a single egg within four days. Occasionally, a very low number of eggs were seen (Additional file 1: Table S1; 0–5 daily), but the eggs did not hatch. On the contrary, eggs, larvae and adult flies were found in all other cross combinations (Additional file 1: Table S1). In vials containing control w^{1118} females and *β-CA* RNAi/*GS-tub-GAL4* males, adult flies eclosed. This result implicated that *β-CA* has an essential function for the female fertility in *Drosophila*. Of note, fertility of female flies was restored by the second day after transferring the flies onto normal food. Thus, the effect on fertility was reversible.

Mitochondrial oxygen consumption

Since we have shown earlier that β-CA is a mitochondrial protein [5], we decided to assess whether silencing of *β-CA* gene expression affects mitochondrial oxygen consumption. Upon knockdown of *β-CA* we observed a female sterile phenotype (Additional file 1: Table S1); it has been recently shown that mutations in mitochondrial proteins cause general sterility in flies by dysfunction of the electron transport chain (ETC.) [9]. Moreover, complementation of the respiratory phenotype can rescue this and other associated phenotypes [9]. Using high resolution respirometry [10] we measured if mitochondrial respiration in whole fly preparations was affected upon knockdown of the *β-CA* gene. We did not

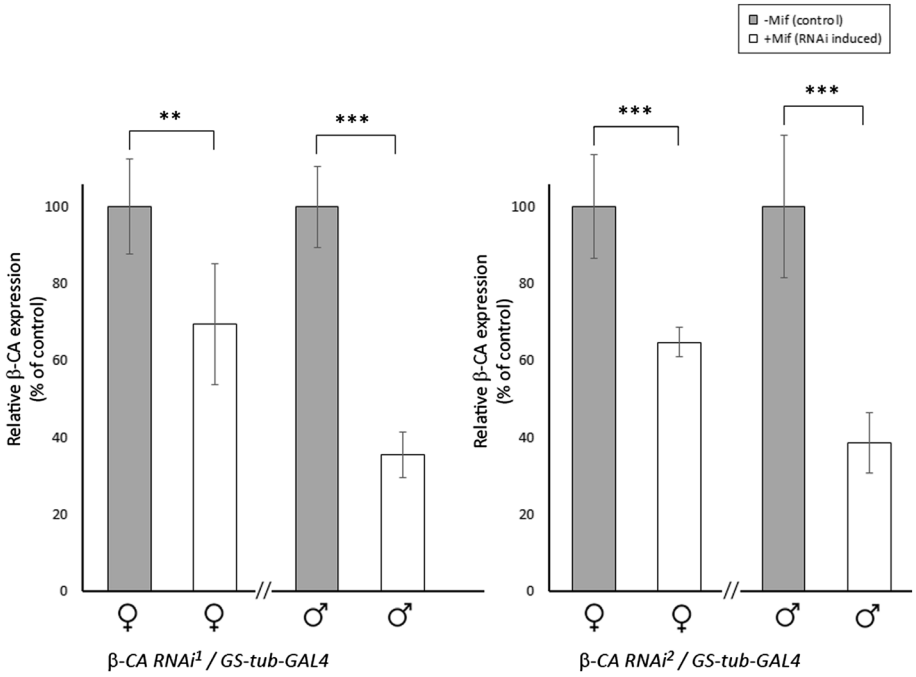

Fig. 1 *β-CA* gene expression level is reduced in RNAi knockdown flies (+Mif) compared to control flies (–Mif). *β-CA* RNAi lines were crossed over the *GS-tub-GAL4* line and the eclosed F1 generation progeny was grown for 6 days at +29 °C in food with Mif (knockdown flies, +Mif) or without Mif (control flies, –Mif). Total RNA was extracted from 3 x 3–5 females and males of the lines indicated. Results are shown as % of expression of the control lines, which were normalized to 100 % each. ** = $p < 0.01$, *** = $p < 0.001$. *β-CA* RNAi^1/*GS-tub-GAL4* females ctrl vs. RNA-induced: t stat = 3.63, df = 9; *β-CA* RNAi^1/*GS-tub-GAL4* males ctrl vs. RNA-induced: t stat = 12.15, df = 9; *β-CA* RNAi^2/*GS-tub-GAL4* females ctrl vs. RNA-induced: t stat = 6.13, df = 10; *β-CA* RNAi^1/*GS-tub-GAL4* males ctrl vs. RNA-induced: t stat = 7.48, ds = 10.

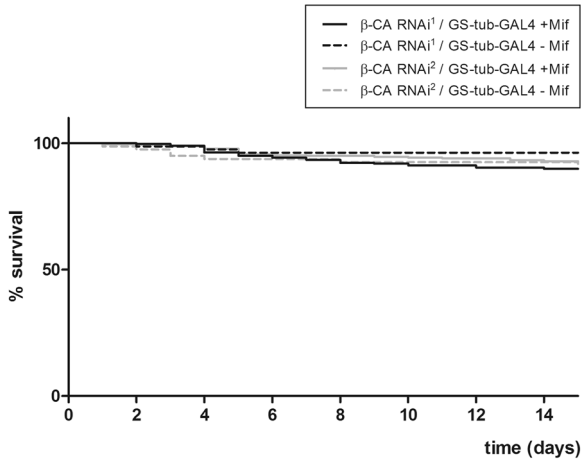

Fig. 2 Fly survival is not impaired upon knockdown of *β-CA* expression. *β-CA RNAi*^{1} and *β-CA RNAi*^{2} lines were crossed over *GS-tub-GAL4*. *β-CA RNAi*^{1}/*GS-tub-GAL4* flies ($n = 385$) and *β-CA RNAi*^{2}/*GS-tub-GAL4* flies ($n = 504$) were collected and grown in food vials containing 400 μM Mif for 15 days. Flies from the same crosses were collected and used as controls by growing them in food vials without Mif ($n = 81$ and $n = 80$, respectively). The number of dead flies was recorded daily

observe any significant differences using complex I- (pyruvate + proline), complex III- (sn-glycerol-3-phosphate) or complex IV-linked (ascorbate + TMPD) substrates in the presence of ADP (Fig. 3a). Additionally, mitochondrial density, measured by the citrate synthase assay, was not altered by *β-CA* RNAi (Fig. 3b). In conclusion, ubiquitous silencing of the *β-CA* gene in adult flies did not affect the mitochondrial oxygen consumption in whole flies.

β-CA RNAi causes delayed migration of border cells in *Drosophila* oogenesis

Because we discovered that silencing of *β-CA* causes female sterility by almost completely abolishing the egg laying capacity, we hypothesized that *β-CA* knockdown might cause a functional defect in the ovaries. To test this hypothesis, we exposed one to two-day old *β-CA* RNAi^1/*GS-tub-GAL4* and *β-CA* RNAi^2/*GS-tub-GAL4* female flies to Mif-containing diet to silence *β-CA* expression. Flies from the same crosses without Mif were used as controls. At day four, flies were exposed to males to facilitate egg production and after 6 days, ovaries from *β-CA* RNAi/*GS-tub-GAL4* knockdown and control flies were dissected. Ovaries were immunostained with DCAD2 antibody and observed under Carl Zeiss LSM

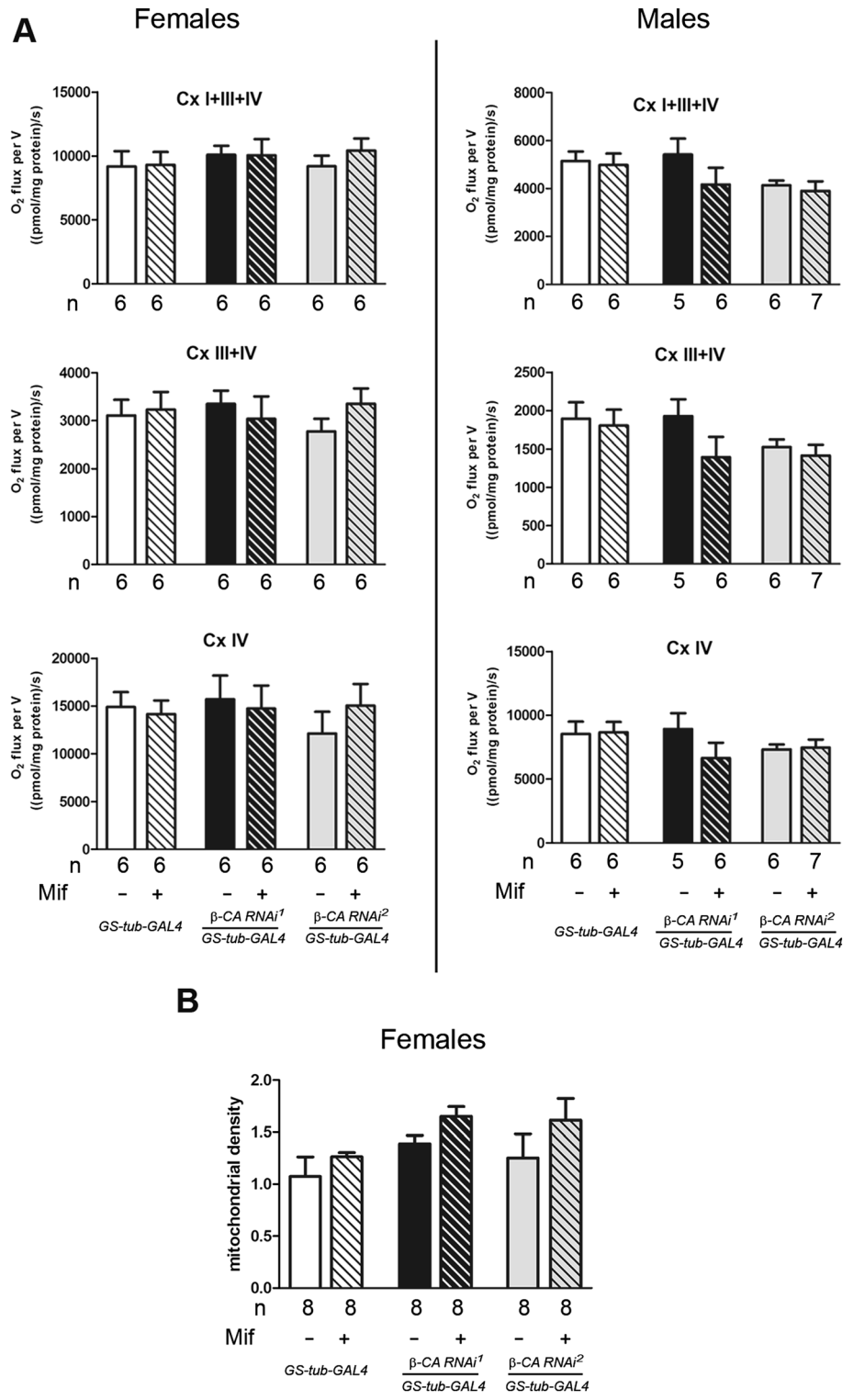

Fig. 3 *β-CA* RNAi does not alter mitochondrial function in fruit flies. **a** Mitochondrial oxygen consumption (nmol O_2/s mg protein) from female and male *Drosophila* flies using P + Pr + ADP (CI + III + IV), G3P (CIII + IV) and Ascorbate + TMPD (CIV) as substrates. Number of experiments (*n*) per group is indicated, data are shown as the mean ± SEM. **b**) Mitochondrial density measured as citrate synthase activity (UNITS mg/ml of mitochondrial protein) shown as the mean ± SEM from 8 replicate experiments. ADP - Adenosine diphosphate; G3P - Glyceraldehyde 3-phosphate; P – pyruvate; Pr – proline; TMPD - N,N,N',N'-Tetramethyl-*p*-Phenylenediamine dichloride

780 confocal microscope. DCAD2 antibody stains DE-cadherin in border cells, which are a group of somatic cells that migrate at stage 9 during *Drosophila* oogenesis. Border cells arise and detach from the monolayer follicular epithelium, and they invade and migrate between the nurse cells towards the oocyte. Border cells were so named because they end up on the border between nurse cells and oocyte at early stage 10 [11]. A cartoon of a normal, early stage 10 developing egg is shown in Fig. 4a. Representative images of early stage 10 developing oocytes in *β-CA* knockdown (+Mif) and control (−Mif) ovaries are shown in Fig. 4b (*β-CA* RNAi^{1} line) and 4c (*β-CA* RNAi^{2} line). The results clearly indicate that border cell migration was delayed in *β-CA* knockdown cells compared to controls. At early stage 10, border cells reached the border of the developing oocyte in controls, but in many of the knockdown ovaries the border cells were still under migration and located between the nurse cells. 14/36 *β-CA* RNAi^{1}/*GS-tub-GAL4* early stage 10 knockdown oocytes showed delayed border cell migration, whereas in all 18 control oocytes analyzed, the border cells had already reached the border of the developing oocyte. The phenotype was weaker but visible also with the *β-CA* RNAi^{2}/*GS-tub-GAL4* flies, where 7/27 knockdown oocytes showed delayed border cell migration compared to 26 controls, in all of which the movement of border cells was normal.

We conclude that silencing *β-CA* expression in *Drosophila* females causes delayed border cell migration during oogenesis, which contributes to the sterility of the female *β-CA* knockdown flies.

Discussion

Our results show that β-CA is essential for *D. melanogaster* reproduction. RNAi-mediated silencing of the *β-CA* gene caused sterility of females. When *Drosophila* ovaries were examined from both control and RNAi flies, it was found that RNAi flies had disturbances in border cell migration during oogenesis. Previously it has been shown that defective border cell migration leads to sterility of female flies due to impaired formation of the micropyle which is needed in fertilization [12, 13]. Additionally, even mature virgin *Drosophila* females should spontaneously ovulate at low rate (~1 egg/day) [14], but the knockdown flies typically did not lay any eggs in our study (Additional file 1: Table S1). The mechanism by which oocytes are released from the *Drosophila* ovary is unknown. The absence of β-CA possibly affects the physiological conditions of the ovulatory tract so that ovulation does not occur. Expression of *β-CA* has been studied in a publicly available DNA microarray dataset: in FlyAtlas (http://flyatlas.org/atlas.cgi?name=CG11967-RA website, [15]) *β-CA* expression levels are provided for 17 adult and 8 larval *D. melanogaster* tissues. The highest upregulated *β-CA* expression levels in adult flies are found in spermatheca (female), fat body, and heart. The spermatheca is a sperm storage organ, and it is possible that, in addition to disturbances in border cell migration and to the possible effect on ovulation, female sterility upon *β-CA* knockdown is related to the function of spermatheca. Also, it is interesting that the reduced fertility of *β-CA* knockdown flies is reversible once *β-CA* gene expression is no longer silenced. This may be related to the fact that RNAi does not fully remove gene function but drastically lowers the *β-CA* expression dose, which is sufficient to cause the phenotype, but is reversible once normal gene expression is restored.

Although phenotypes caused by *β-CA* silencing (lethality during development and sterility in adult flies) are reminiscent of the ones caused by mitochondrial dysfunction [9], we did not detect alterations in electron transport chain (ETC.) functions. In the past, we have found that reduction in mitochondria respiration causes sterility, whereas complementation of the respiratory defect rescues it [9, 10, 16]. Here, the sterile phenotype was not associated with a reduction in respiration indicating a more subtle alteration in mitochondrial function.

Human isozymes CA IX and XII have been linked to tumor invasiveness and migration [17, 18]. It has been suggested that CAs facilitate cell migration by low pH-induced activation of matrix metalloproteinases [19]. Notably, these CA enzymes are membrane-bound, whereas β-CA is mitochondrial. Because HCO_3^- does not readily diffuse across the mitochondrial membrane, the impaired movement of border cells probably results from disturbances in biosynthetic pathways. Interestingly, a mitochondrial β-CA has been shown to be important in the sexual reproduction of filamentous ascomycete *Sordaria macrospore* [20]. In the presence of *β-CA* gene mutation *cas2,* vegetative growth, fruiting-body development and ascospore germination were affected, and the double mutant strain *cas1/2* was completely sterile. In *S. macrospore*, *cas2* was shown to be mitochondrial while other two β-CAs *cas1* and *cas3* were cytoplasmic. Defects caused by the lack of *cas2* could be partially compensated by elevated carbon dioxide levels in addition to overexpression of *cas1*, *cas3*, or a non-mitochondrial *cas2* variant. It was depicted that there may be a functional connection between β-CAs and adenylyl cyclase. In this way, the cAMP signaling may be affected. However, this is related to carbon dioxide and bicarbonate sensing in fungi and therefore cannot be directly related to signaling pathways in animals.

The effect of mitochondrial CA function has been tested in mammals. In a recent study, the roles of CA VA and VB were examined in mice with targeted mutagenesis [21]. During the study it was found CA VA null mice were smaller than wild-type mice and bred

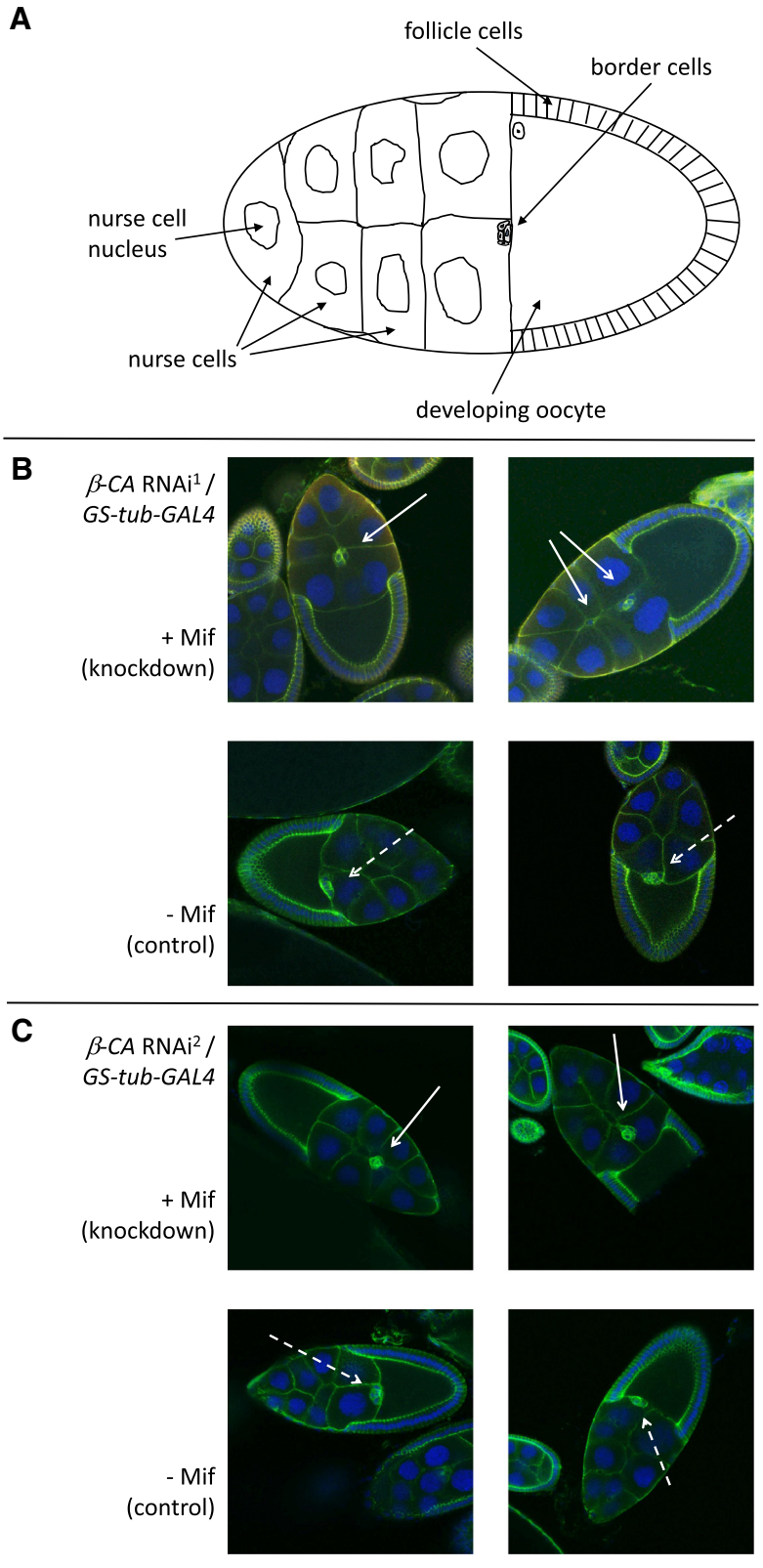

Fig. 4 (See legend on next page.)

(See figure on previous page.)
Fig. 4 RNAi-mediated silencing of β-CA expression causes delayed border cell migration in *Drosophila* oogenesis. **a** A cartoon naming the cells involved in the development of an early stage 10 egg. **b** & **c**) Migration of DCAD2-labeled border cells towards the developing oocyte is delayed in *β-CA* knockdown early stage 10 eggs (white arrows) compared to controls (dashed white arrows). **b**) Developing eggs from *β-CA RNAi*^{1}*/GS-tub-GAL4* control and knockdown flies, **c**) Developing eggs from *β-CA RNAi*^{2}*/GS-tub-GAL4* control and knockdown flies

poorly. However, when sodium-potassium citrate-supplemented water was given, the production of offspring was normal. Blood ammonia concentrations of CA VA null mice were elevated, but fasting blood sugar levels were normal. On the other hand, CA VB null mice showed normal growth, normal blood ammonia levels as well as normal fasting blood sugar levels. CA VA/B double-knockout (DKO) mice showed additional abnormalities. Impairment of growth and hyperammonemia were more severe than for CA VA null mice. DKO animals reproduced less than predicted despite of supplemented sodium-potassium citrate in their drinking water. Additionally, survival after weaning was reduced, especially for males. Moreover, fasting blood glucose levels for DKO mice were significantly lower compared to controls. Clearly, these enzyme deficiencies in mice (and probably other vertebrates) are not lethal but cause significant metabolic problems and also have effects on breeding.

Fasseas and coworkers performed CA RNAi studies with *C. elegans* [6]. Two *β-CA* genes were found: *bca-1* and *y116a8c.28*. Of these, the latter was shown to encode for an active enzyme. In normal conditions, the authors found some phenotypes, like slow growth rates, but they were unable to consistently reproduce the effects, and the conclusion was that visible phenotype was not found. The level of gene silencing was not reported; it is possible that the level of silencing was not sufficient. On the other hand, it is possible that some other CA might compensate the loss of β-CA function. In addition to the results of this study, our recent findings on *Leishmania* parasites indicate that the enzyme is essential for invertebrates and protozoans [7].

D. melanogaster β-CA is a mitochondrial enzyme as are most of the other *Dipteran* β-CAs [22]. It is plausible that findings in *D. melanogaster* can be generalized also to the other *Dipteran* species which act commonly as disease vectors. These species include the malaria mosquito *Anopheles* and the yellow fever mosquito *Aedes.* In light of this, inhibitors against these enzymes could also be used to restrict the spread of various diseases.

Conclusions

Thus far the physiological role of invertebrate β-CAs has been unclear. Our study indicates that the β-CA function is not vitally important for adult *D. melanogaster* since *β-CA* RNAi had no effect on survival, although the enzyme was required during development. However, β-CA is essential for reproduction. Our study suggests that disturbance of β-CA function leads to abnormal border cell migration during *Drosophila* oogenesis. Previously it has been shown that defective border cell migration leads to sterility of female flies due to impaired formation of micropyle which is needed in fertilization. Vertebrates do not possess β-class CAs, but these enzymes are widespread throughout the phylogeny of life on Earth. This makes them exciting new targets for parasitic drug development. Indeed, β-CAs are found in many pathogenic organisms and pathogen vectors of the animal kingdom and protozoans, including the *Leishmania* parasites, the malaria mosquito *Anopheles*, and the yellow fever mosquito *Aedes*. Our study shows that invertebrate β-CAs are indeed important enzymes, which encourages further studies on anti-parasitic drug development. Since interference of β-CA function seems to cause sterility of female flies, this feature could be used in controlling the amount of insects that cause or distribute harmful diseases.

Methods

Generation of β-CA knockdown flies

Two different *β-CA* RNAi lines were obtained from Vienna *Drosophila* RNAi Center (VDRC) from KK and GD collections with the following IDs: #100233 (hereafter referred to as *β-CA RNAi*^{1}*)* and #38612 (hereafter referred to as *β-CA RNAi*^{2}*)* [23]. These stocks have been generated to overexpress a dsRNA hairpin construct, specific to the *β-CA* gene under *upstream activation sequence* (*UAS*) control. When these flies are crossed over a GAL4 activator protein expressing line, *β-CA* gene is silenced in the tissue where GAL4 protein is expressed [24]. For ubiquitous RNAi-mediated silencing, β-CA RNAi lines were crossed over the *Actin-GAL4* line or a Mifepristone-inducible *Geneswitch-tub5-GAL4* line [25].

RNA extraction

β-CA RNAi lines were crossed over the *GS-tub-GAL4* line and the eclosed F1 generation progeny were grown for 6 days at +29 °C in food with 400 μM Mif (knockdown flies) or without Mif (control flies). The flies were transferred into new food vials once during the period. RNA extractions were made as triplicates for both sexes: for each line, 3 x 3–5 females and males were used.

RNA extraction was done using TRI Reagent® Solution (Ambion), according to manufacturer's instructions.

Quantitative reverse transcriptase PCR (qRT-PCR)

qRT-PCR was performed with the above mentioned extracted total RNAs to quantify the level of gene silencing. Also RNA extracted from the *GS-tub-GAL4* line was tested by qRT-PCR to identify possible leakiness of the tubulin driver. PCR reactions were performed in MicroAmp optical 96-well reaction plates using a SYBR-Green PCR master mix kit (Applied Biosystems), according to the manufacturer's instructions. Primers for qRT-PCR were designed using Primer Express Software v2.0 (Applied Biosystems). The forward primer used in the reaction for β-CA gene expression was 5'-GACAAGGGAGCAAATGGTCAA-3' and the reverse primer was 5'-TCTACTGTCCATGCAGGTGAAGAA-3'. The β-CA amplicon size was 88 bp. The reaction was carried out in an ABI PRISM 7000 Detection System (Applied Biosystems). The data were analyzed with ABI PRISM 7000 SDS software and normalized to the RpL32 housekeeping gene. The forward primer used for RpL32 was 5'-GGTTACGGATCGAACAAGCG-3' and the reverse primer was 5'-TTCTGCATGAGCAGGA CCTC-3'. The RpL32 amplicon size was 101 bp. The final results were expressed as % of expression of the control lines, which were normalized to 100 % each, as described in [26].

Survival study

To study the effect of the *β-CA* gene knockdown on the survival rate of flies, the *β-CA RNAi*^{1} and *β-CA RNAi*^{2} lines were crossed over *GS-tub-GAL4*. Eclosed, one day old *β-CA RNAi*^{1}/*GS-tub-GAL4* flies and *β-CA RNAi*^{2}/*GS-tub-GAL4* flies were collected and grown in mixed-sex groups in food vials containing 400 μM Mif for 15 days. Flies from the same crosses were collected and used as controls by growing them in food vials without Mif. The number of dead flies was recorded daily.

Fly fertility

To study the fertility of *D. melanogaster* β-CA knockdown flies, the *β-CA RNAi*^{1}/*GS-tub-GAL4* and *β-CA RNAi*^{2}/*GS-tub-GAL4* eclosed flies were collected and placed at +29 °C in normal food (control) or food containing 400 μM Mif (*β-CA RNAi* induced) for six days. w^{1118} control flies were kept in the same conditions. Thereafter the flies were mated with flies from the same cross or with w^{1118} control flies, in different combinations (Additional file 1: Table S1). Fertility was followed up to 15 days.

Additionally, the possible reversibility of fly fertility was studied by providing normal food to the previously mentioned flies after 6 days. The flies were put into new vials daily to find out when their fertility was restored.

Measurement of mitochondrial oxygen consumption by high-resolution respirometry

Whole fly homogenates from *β-CA RNAi*^{1}/*GS-tub-GAL4* and *β-CA RNAi*^{2}/*GS-tub-GAL4*, grown with or without Mif for six days, were used for respirometry measurements. Twenty flies were homogenized in MIB (250 mM sucrose, 2 mM EGTA, 5 mM Tris–HCl pH 7.4) and filtered before immediately being used in an OROBOROS O2k oxygraph (Oroboros Instruments, Innsbruck, Austria). Homogenates were incubated in assay buffer (120 mM KCl, 5 mM KH2PO4, 3 mM Hepes, 1 mM EGTA, 1 mM MgCl2, 0.2 % BSA, pH 7.2) at 25 °C. Experiments were performed according to the previously described protocol [10]. Values were normalized to protein concentration as calculated by the Bradford method.

Mitochondrial density measurements via the citrate synthase assay

Approximately 40–60 flies were immobilised on ice and then transferred to a chilled mortar. The flies were homogenised in 500 μl of ice-cold mitochondria isolation medium (250 mM sucrose, 5 mM Tris–HCl, 2 mM EGTA), and the homogenate was filtered through cheesecloth. Then, an additional 500 μl of the mitochondria isolation medium containing 1 mM DTT was added, and the samples were frozen at −80 °C overnight. Next, the samples were defrosted, and 50 μl of the sample was diluted 1:5 in mitochondria isolation medium containing 1 mM PMSF. The remainder of the sample was used to isolate mitochondria as described elsewhere [27]. The mitochondria were subsequently diluted 1:4 in mitochondria isolation buffer containing 1 mM PMSF. Measurements were performed in a 96-well plate, in which 182 μl of fresh reaction buffer (100 mM Tris–HCl (pH 7.5) and 2.5 mM EDTA), 2 μl of 30 mM acetyl-CoA and 2 μl of 10 mM DTNB were added to each well. Finally, the samples (either the whole homogenate or isolated mitochondria) were added. The reaction was initiated by adding 10 μl of 10 mM oxaloacetate (OAA), and the linear increase in absorbance at 412 nm was followed for 3–4 min using a PerkinElmer EnVision 2104 plate reader. Blanks were made from the same samples without the addition of OAA and then measured. Mitochondrial density was calculated by dividing the specific citrate synthase activity measured in the whole-fly homogenates by the specific citrate synthase activity measured in isolated mitochondria.

Dissection, staining and examination of ovaries

One to two-day old female *β-CA RNAi*^{1}/*GS-tub-GAL4* and *β-CA RNAi*^{2}/*GS-tub-GAL4* flies were placed at +29 °C in normal food (control) or food containing 400 μM Mif (*β-CA RNAi* induced) for six days. Flies were moved to fresh food with or without Mif every two days. On day four, male *Oregon R* flies were added to induce egg production of the females. On the 6th day, the knockdown and control females were anesthetized on a CO_2 pad and the ovaries were dissected.

The dissected ovaries were transferred in 0.5 ml tubes containing phosphate-buffered saline (PBS), fixed using 4 % paraformaldehyde (PFA) for 20 min at +4 °C and rinsed 2x with PBS 0.3 % Triton (PBT). Ovaries were washed 2x 15 min in PBT containing 0.5 % bovine serum albumin (BSA), incubated overnight with the DCAD2 primary antibody (Developmental Studies Hybridoma Bank, Iowa, USA, 1:20) in PBT-BSA, rinsed 2x with PBT and washed again 2 x 15 min in PBT-BSA. Incubation with the secondary Goat anti-rat antibody (AlexaFluor 488 conjugate, Life Technologies, 1:1000) in PBT-BSA was carried out for 2 h at RT. Ovaries were rinsed again 2x in PBT and washed 3x 15 min in PBT. DAPI (final conc. 1 μg/ml, Sigma) was added to the second last wash. After the final wash, ovaries were placed in 70 % glycerol for at least 30 min at +4 °C, and then transferred in Vectashield Mounting medium (Vector Laboratories).

Prior to microscopy, the ovaries were put on microscope slides, the egg chambers separated using a sharpened wire and the samples mounted and sealed using cover slips and nail varnish. Ovaries were examined and imaged using the Zeiss LSM 780 confocal microscope with 20x objective. Early stage 10 developing eggs were distinguished from earlier developmental stages based on the shape of the follicle cells surrounding the developing oocyte (see Fig. 4a and [28] Fig. 1b). Images are snap-shots of the focal plane of each developing oocyte where border cells are visible.

Statistical analyses

Statistical analysis of *β-CA* gene expression in control and knockdown flies by qRT-PCR was carried out using Student's *t*-test for two samples assuming equal variances. Statistical analysis of fly survival experiments was carried out in Prism 6 (GraphPad) using the log-rank (Mantel-Cox) test. High resolution respirometry data were analyzed with Prism 6 (GraphPad) using the unpaired Student's *T*-test. The level of statistical significance was established as $p < 0.05$.

Additional file

Additional file 1: Table S1. Fly fertility is severely reduced in crosses where *β-CA* is knocked down in females.

Competing interests

The authors declare that they have no competing interests.

Authors' contributions

LS and SV drafted the manuscript, performed survival and fertility studies, and participated in examination of fly ovaries. Also MK was involved in survival and fertility studies and examination of fly ovaries. LS and MK performed RNA extraction and qRT-PCR. SV performed statistical analysis. TT participated in examination of fly ovaries. A. Sanz and A. Sriram performed mitochondrial oxygen consumption studies. MR, HJT and SP were involved in conduction of the study and helped to draft the manuscript. All authors read and approved the final manuscript.

Acknowledgements

We thank the Vienna *Drosophila* Resource Center (VDRC, http://stockcenter.vdrc.at) for providing the *β-CA* RNAi lines. *Drosophila GS-tub-GAL4* line was a kind gift from Dr Scott Pletcher. The DCAD2 polyclonal antibody developed by Tadashi Uemura was obtained from the Developmental Studies Hybridoma Bank, created by the NICHD of the NIH and maintained at the University of Iowa, USA. We thank Professor Sarah Bray in the University of Cambridge, UK, for ovary dissection and staining methods.

Funding

This study has been supported by funds from The Academy of Finland (MR, SP, HTJ and A. Sanz), European Research Council (A. Sanz), Jane & Aatos Erkko Foundation (MR and SP), Sigrid Juselius Foundation (MR and SP) and FinMIT Centre of Exellence and Academy professorship funding (HTJ). This study was also supported by the Competitive State Research Financing of the Expert Responsibility Area of Tampere University Hospital (MR and HTJ), Competitive State Research Financing of the Expert Responsibility area of Oulu University Hospital (MR) and the Tampere Tuberculosis Foundation (MR).

Author details

[1]BioMediTech, University of Tampere, Tampere, Finland. [2]School of Medicine, University of Tampere and Tampere University Hospital, Tampere, Finland. [3]Department of Otorhinolaryngology, Central Finland Central Hospital, Jyväskylä, Finland. [4]Institute for Cell and Molecular Biosciences and Newcastle University Institute for Ageing Health, Newcastle University, Newcastle upon Tyne, UK. [5]Institute of Biotechnology, University of Helsinki, Helsinki, Finland. [6]Tampere University Hospital, Tampere, Finland. [7]Department of Pediatrics, Tampere University Hospital, Tampere, Finland. [8]PEDEGO Research Center, Medical Research Center Oulu, and Department of Children and Adolescents, Oulu University Hospital, Oulu, Finland. [9]Fimlab Laboratories Ltd, Tampere, Finland.

Received: 17 June 2015 Accepted: 12 August 2015
Published online: 22 August 2015

References

1. Sly WS, Hu PY. Human carbonic anhydrases and carbonic anhydrase deficiencies. Annu Rev Biochem. 1995;64:375–401.
2. Zimmerman SA, Ferry JG. The beta and gamma classes of carbonic anhydrase. Curr Pharm Des. 2008;14:716–21.
3. Del Prete S, Vullo D, Fisher GM, Andrews KT, Poulsen SA, Capasso C, et al. Discovery of a new family of carbonic anhydrases in the malaria pathogen *Plasmodium falciparum*–the eta-carbonic anhydrases. Bioorg Med Chem Lett. 2014;24:4389–96.
4. Hewett-Emmett D. Evolution and distribution of the carbonic anhydrase gene families. EXS. 2000;90:29–76.
5. Syrjänen L, Tolvanen M, Hilvo M, Olatubosun A, Innocenti A, Scozzafava A, et al. Characterization of the first beta-class carbonic anhydrase from an arthropod (*Drosophila melanogaster*) and phylogenetic analysis of beta-class carbonic anhydrases in invertebrates. BMC Biochem. 2010;11:28.

6. Fasseas MK, Tsikou D, Flemetakis E, Katinakis P. Molecular and biochemical analysis of the beta class carbonic anhydrases in *Caenorhabditis elegans*. Mol Biol Rep. 2009;38:1777–85.
7. Syrjänen L, Vermelho AB, de Almeida RI, Corte-Real S, Salonen T, Pan P, et al. Cloning, characterization and inhibition studies of a beta carbonic anhydrase from *Leishmania donovani chagasi*, the protozoan parasite responsible of leishmaniasis. J Med Chem. 2013;56:7372–81.
8. Majeau N, Coleman JR. Effect of CO2 Concentration on Carbonic Anhydrase and Ribulose-1,5-Bisphosphate Carboxylase/Oxygenase Expression in Pea. Plant Physiol. 1996;112:569–74.
9. Vartiainen S, Chen S, George J, Tuomela T, Luoto KR, O'Dell KM, et al. Phenotypic rescue of a *Drosophila* model of mitochondrial ANT1 disease. Dis Model Mech. 2014;7:635–48.
10. Kemppainen KK, Rinne J, Sriram A, Lakanmaa M, Zeb A, Tuomela T, et al. Expression of alternative oxidase in *Drosophila* ameliorates diverse phenotypes due to cytochrome oxidase deficiency. Hum Mol Genet. 2014;23:2078–93.
11. Rorth P. Initiating and guiding migration: lessons from border cells. Trends Cell Biol. 2002;12:325–31.
12. Montell DJ. Border-cell migration: the race is on. Nat Rev Mol Cell Biol. 2003;4:13–24.
13. Montell DJ, Rorth P, Spradling AC. slow border cells, a locus required for a developmentally regulated cell migration during oogenesis, encodes *Drosophila* C/EBP. Cell. 1992;71:51–62.
14. Heifetz Y, Lung O, Frongillo Jr EA, Wolfner MF. The *Drosophila* seminal fluid protein Acp26Aa stimulates release of oocytes by the ovary. Curr Biol. 2000;10:99–102.
15. Chintapalli VR, Wang J, Dow JA. Using FlyAtlas to identify better *Drosophila melanogaster* models of human disease. Nat Genet. 2007;39:715–20.
16. Chen S, Oliveira MT, Sanz A, Kemppainen E, Fukuoh A, Schlicht B, et al. A cytoplasmic suppressor of a nuclear mutation affecting mitochondrial functions in *Drosophila*. Genetics. 2012;192:483–93.
17. Svastova E, Hulikova A, Rafajova M, Zat'ovicova M, Gibadulinova A, Casini A, et al. Hypoxia activates the capacity of tumor-associated carbonic anhydrase IX to acidify extracellular pH. FEBS Lett. 2004;577:439–45.
18. Parkkila S, Rajaniemi H, Parkkila AK, Kivela J, Waheed A, Pastorekova S, et al. Carbonic anhydrase inhibitor suppresses invasion of renal cancer cells *in vitro*. Proc Natl Acad Sci U S A. 2000;97:2220–4.
19. Martinez-Zaguilan R, Seftor EA, Seftor RE, Chu YW, Gillies RJ, Hendrix MJ. Acidic pH enhances the invasive behavior of human melanoma cells. Clin Exp Metastasis. 1996;14:176–86.
20. Elleuche S, Poggeler S. Beta-carbonic anhydrases play a role in fruiting body development and ascospore germination in the filamentous fungus *Sordaria macrospora*. PLoS One. 2009;4, e5177.
21. Shah GN, Rubbelke TS, Hendin J, Nguyen H, Waheed A, Shoemaker JD, et al. Targeted mutagenesis of mitochondrial carbonic anhydrases VA and VB implicates both enzymes in ammonia detoxification and glucose metabolism. Proc Natl Acad Sci U S A. 2013;110:7423–8.
22. Zolfaghari Emameh R, Barker H, Tolvanen ME, Ortutay C, Parkkila S. Bioinformatic analysis of beta carbonic anhydrase sequences from protozoans and metazoans. Parasit Vectors. 2014;7:38.
23. Dietzl G, Chen D, Schnorrer F, Su KC, Barinova Y, Fellner M, et al. A genome-wide transgenic RNAi library for conditional gene inactivation in *Drosophila*. Nature. 2007;448:151–6.
24. Brand AH, Perrimon N. Targeted gene expression as a means of altering cell fates and generating dominant phenotypes. Development. 1993;118:401–15.
25. Fernandez-Ayala DJ, Sanz A, Vartiainen S, Kemppainen KK, Babusiak M, Mustalahti E, et al. Expression of the Ciona intestinalis alternative oxidase (AOX) in *Drosophila* complements defects in mitochondrial oxidative phosphorylation. Cell Metab. 2009;9:449–60.
26. Pfaffl MW. A new mathematical model for relative quantification in real-time RT-PCR. Nucleic Acids Res. 2001;29, e45.
27. Sanz A, Soikkeli M, Portero-Otin M, Wilson A, Kemppainen E, McIlroy G, et al. Expression of the yeast NADH dehydrogenase Ndi1 in *Drosophila* confers increased lifespan independently of dietary restriction. Proc Natl Acad Sci U S A. 2010;107:9105–10.
28. Schonbaum CP, Perrino JJ, Mahowald AP. Regulation of the vitellogenin receptor during *Drosophila melanogaster* oogenesis. Mol Biol Cell. 2000;11:511–21.